BNL 52185
UC-414 (High Energy Physics-
DOE/OSTI-4500 — Interim 3)

BNL--52185

DE89 008843

Proceedings of the Third Workshop on Experiments and Detectors for a Relativistic Heavy Ion Collider (RHIC)

JULY 18-22, 1988

Edited by B. Shivakumar and P. Vincent

BROOKHAVEN NATIONAL LABORATORY
ASSOCIATED UNIVERSITIES, INC.
UPTON, LONG ISLAND, NEW YORK 11973

UNDER CONTRACT NO. DE-AC02-76CH00016 WITH THE

UNITED STATES DEPARTMENT OF ENERGY

Printed in the United States of America
Available from
National Technical Information Service
U.S. Department of Commerce
5285 Port Royal Road
Springfield, VA 22161

NTIS price codes:
Printed Copy: A10; Microfiche Copy: A01

PREFACE

A summer school and workshop were held in July of 1988 at the Brookhaven National Laboratory. The summer school was attended by about 150 participants, several of them students and young physicists. They were provided with an environment wherein they could discuss the physics of relativistic heavy ions with some of the leading scientists in the field. The school format provided for formal lectures focussing on experimental techniques and theory. At the conclusion of the summer school, many of the students stayed on to participate in a workshop on relativistic heavy ion physics.

This was the third in a series of workshops, following the ones held at Brookhaven in 1986, and Berkeley in 1987. The focus in the first two workshops was on the physics and detectors of a relativistic heavy ion collider (RHIC). Here, it was on detector techniques. The format included two classifications of working groups, those that focussed on detector systems and those that focussed on detector techniques. The groups and their convenors are listed in the table below. The detector techniques working groups met in the early part of the day, and reconvened as detector systems groups on the afternoons. The first day of the meeting included an overview of the RHIC project, and status reports on RHIC detector studies. The primary thrust on the succeeding three days was on studies of detector techniques. These were interrupted by plenary sessions where lectures on topics of general interest were presented. In the afternoons, time was allocated to the groups working on detector systems. The convenors of the different working groups presented their summaries on the fifth and final day.

Working Groups on Detector Systems	
Di-Muon Spectrometer	G.Young (ORNL)
4-Π Calorimeter	H.Gordon (BNL) D.Lissauer (BNL)
Large Solid Angle Tracking	H.Gutbrod (GSI)
Electron Pair Spectrometer	H.-G.Ritter (LBL)
4-Π Tracking Magnetic Spectrometer	S.Lindenbaum (BNL/CCNY)
B-Meson Detector for p-p collisions	N.Lockyer (Penn)

Working Group on detector techniques	
Readout Electronics	W.Cleland (Pittsburgh)
Calorimetry	S.Aronson (BNL)
Particle ID and Tracking	S.Nagamiya (Columbia)
Detector Simulation	B.Shivakumar (Yale)
Data Acquisition	M.Levine (BNL)

The charge to the working groups, as described in a handout, was as follows:

1.) What are the essential techniques for RHIC? (As determined by physics goals, machine parameters, past detector studies, etc.).
2.) What are the R&D requirements and priorities? To what extent are the necessary development projects unique to RHIC? Are some being addressed elsewhere as well?
3.) Estimate the appropriate time scales, and the levels of manpower and funding required.
4.) What test beam facilities are required?
5.) Identify university and laboratory groups interested in and capable of doing the work.

In the following document, the convenors of the working groups on detector techniques summarize the views of their groups on the topics outlined above.

We would like to thank Tom Ludlam and Ronnie Rau, the conference organizers, Lori Bennett, Colette Cadwell, Barbara Trojanowski, and Pat Tuttle the conference secretaries, without whose support the conference would not have been possible.

B.Shivakumar and P.Vincent

TABLE OF CONTENTS

Tracking and Particle identification related contributions

Read Out Electronics

Data Acquisition

Detector Simulation

B-Physics at RHIC

BROOKHAVEN NATIONAL LABORATORY

SUMMER INSTITUTE
on
RELATIVISTIC HEAVY IONS

The Workshop

July 18-22, 1988

FINAL AGENDA

Monday, July 18: *Physics Dept., Bldg. 510A, Seminar Room*

9:00	Welcome	N. P. Samios
9:20	Workshop Organization	R. R. Rau
9:40	RHIC Project: Overview and Status	H. Hahn
10:15	BREAK	
10:30	RHIC Detector R&D	T. Ludlam
10:45	The D.O.E. Perspective	D. Hendrie
	Update on RHIC Detector Studies:	
11:15	Dimuons	G. Young
11:45	Electron Pairs	H. -G. Ritter
12:15	LUNCH	
2:00	Large Solid-Angle Tracking	H. Gutbrod
2:30	4π Calorimeter	D. Lissauer
3:00	4π Tracking Spectrometer	S. Lindenbaum
3:30	B-Meson Spectrometer	N. Lockyer
4:00	BREAK	
4:15	Organize Working Groups	

Tuesday, July 19 to Thursday, July 21: *Collider Center, Bldg. 1005, 3rd floor*

9:00 - 10:15	Plenary Session
10:30 - 3:30	Working Groups on Detector Techniques
4:00 - 6:00	Working Groups on Detector Systems/ Plenary Sessions

(Tuesday 6:00 p.m.: Clambake at Brookhaven Center)

Friday, July 22: *Physics Dept. Bldg. 510A, Seminar Room*

Summaries of Working Groups on Detector Techniques (and B's)

9:00	Readout Electronics	W. Cleland
9:30	Calorimetry	S. Aronson
10:00	Tracking and Particle ID	S. Nagamiya
10:30	BREAK	
10:45	Detector Simulation	B. Shivakumar
11:15	Data Acquisition	M. Levine
11:45	B-Physics Detector	N. Lockyer
12:15	End of Workshop Presentations	

Friday Afternoon: Planning meetings of Detector Systems Groups

SCHEDULE FOR PLENARY SESSIONS

Tuesday, July 19:

9:00 - 9:45	B-Meson Physics	T. Sanda

Wednesday, July 20:

9:00 - 9:20	J/ψ Suppression	H. Satz
9:20 - 9:40	J/ψ measurement in heavy ion collisions at CERN	C. Lourenco
9:40 - 10:00	J/ψ signal in hadron-nucleus collisions at Fermilab	C. Hojvat

Wednesday, July 20:

4:00 - 4:20	The LAA R&D program at CERN	H. Gutbrod
4:20 - 4:40	The SSC detector R&D program	V. Radeka

LIST OF PARTICIPANTS

Name	Affiliation
Akiba, Y	University of Tokyo
Aronson, S	Brookhaven National Laboratory
Berger, FH	University of Muenster
Bonner, BE	Rice University
Braun-Munzinger, P	SUNY at Stony Brook
Carroll, J	Univ. of California at Los Angeles
Chasman, C	Brookhaven National Laboratory
Cleland, WE	Univ. of Pittsburgh
Cole, JD	Idaho Nat'l. Engineering Lab.
Debbe, R	Brookhaven National Laboratory
Dhawan, S	Yale University
Dietzsch, O	U.S.P., Brazil
Drigert, MW	Idaho Nat'l. Engineering Lab.
Duek, E	Brookhaven National Laboratory
Eiseman, SE	Brookhaven National Laboratory
Engelage, J	Lawrence Livermore National Laboratory
Erlandsson, B	University of Stockholm
Erskine, JR	U.S. Department of Energy
Etkin, A	Brookhaven National Laboratory
Fatyga, M	Brookhaven National Laboratory
Felgeyrolles, X	Universite de Clermont
Findeisen, C	Univ. of Wisconsin
Florkowski, W	Jagellonian University
Foley, KJ	Brookhaven National Laboratory
Franz, A	Lawrence Berkeley Laboratory
Fuchs, M	Univ. of Illinois, Urbana
Fung, S-Y	Univ. of California-Riverside
Gavron, A	Los Alamos National Laboratory
Gordon, H	Brookhaven National Laboratory
Greene, SV	Yale University
Guryn, W	Brookhaven National Laboratory
Gutbrod, HH	CERN/GSI
Hackenburg, RW	Brookhaven National Laboratory
Hahn, RL	Brookhaven National Laboratory
Hahn, H	Brookhaven National Laboratory
Hall, JR	University of New Mexico
Hallman, TJ	Johns Hopkins University
Hamagaki, H	Univ. of Tokyo
Hansen, O	Brookhaven National Laboratory
Hendrie, D	U.S. Department of Energy
Herrmann, NW	SUNY at Stony Brook
Hojvat, C	Fermi National Accelerator Laboratory
Huang, HZ	Massachusetts Institute of Technology
Humanic, TJ	GSI/Pittsburgh
Jacobs, PM	Lawrence Berkeley Laboratory
Jayananda, K	Univ. of Pittsburgh
Johnson, R	Univ. of Cincinnati
Juricic, I	Nevis Laboratories
Kadija, K	Max Planck Institute, Munich

Name	Affiliation
Kahn, SA	Brookhaven National Laboratory
Knapp, B	Nevis Laboratories
Kohlmeyer, B	University of Marburg
Kowalski, L	Montclair State College
Kramer, M	City College of New York
Kreutz, P	GSI Darmstadt
LeDoux, RJ	Massachusetts Institute of Technology
Lee, SY	Brookhaven National Laboratory
Leipuner, L	Brookhaven National Laboratory
LeVine, MJ	Brookhaven National Laboratory
Lindenbaum, SJ	Brookhaven National Laboratory
Lissauer, D	Brookhaven National Laboratory
Llope, WJ	SUNY at Stony Brook
Lockyer, N	Univ. of Pennsylvania
Longacre, RS	Brookhaven National Laboratory
Lourenco, C	LIP- Lisbon
Love, WA	Brookhaven National Laboratory
Ludlam, TW	Brookhaven National Laboratory
Madansky, L	Johns Hopkins University
Mannelli, M	Yale University
Mannelli, EB	Yale University
Margetis, S	CERN
Matsui, T	Mass. Institute of Technology
Merino, C	University of Santiago
Miake, Y	Brookhaven National Laboratory
Mitchell, JT	Yale University
Morris, TW	Brookhaven National Laboratory
Morse, W	Brookhaven National Laboratory
Mueller, C	University of Marburg
Nagae, T	Institute for Nuclear Study, Tanashi
Nagamiya, S	Nevis Laboratories
Newcomer, M	Univ. of Pennsylvania
Peitzmann, T	CERN
Persson, BAS	Lund University
Plasil, F	Oak Ridge National Laboratory
Platner, E	Brookhaven National Laboratory
Pless, IA	Massachusetts Institute of Technology
Polychronakos, VA	Brookhaven National Laboratory
Protopopescu, S	Brookhaven National Laboratory
Purschke, ML	University of Muenster
Radeka, V	Brookhaven National Laboratory
Rau, RR	Brookhaven National Laboratory
Rehak, P	Brookhaven National Laboratory
Rescia, S	Brookhaven National Laboratory
Rhoades-Brown, MJ	Brookhaven National Laboratory
Ritter, HG	Lawrence Berkeley Laboratory
Samios, NP	Brookhaven National Laboratory
Sanda, T	Rockefeller University
Satz, H	Univ. of Bielefeld/BNL
Saulys, AC	Brockhaven National Laboratory
Scharnberg, R	Purdue University
Schicker, RM	Lawrence Berkeley Laboratory

Name	Affiliation
Schroeder, L	U.S. Dept. of Energy
Schulz, W	University of Marburg
Shivakumar, B	Yale University
Shor, A	Brookhaven National Laboratory
Sidwell, R	Ohio State University
Sippach, W	Nevis Laboratories
Sorensen, S	Oak Ridge National Laboratory
Stachel, J	SUNY at Stony Brook
Steadman, SG	Massachusetts Institute of Technology
Steiner, V	Weizmann Institute
Sugitate, T	Hiroshima University
Sunier, JW	Los Alamos National Laboratory
Takai, H	Univ. of Pittsburgh
Tannenbaum, MJ	Brookhaven National Laboratory
Thomas, JH	Calif. Inst. of Technology
Thompson, PA	Brookhaven National Laboratory
Tran Thanh Van, J	Univ. of Paris Sud
VanBerg, R	Univ. of Pennsylvania
VanDijk, JH	Brookhaven National Laboratory
Vient, MA	Univ. of California - Riverside
Vincent, PJ	Brookhaven National Laboratory
Wadsworth, B	Mass. Institute of Technology
Waters, LS	SUNY at Stony Brook
Watson, WA	Brookhaven National Laboratory
Werner, K	Brookhaven National Laboratory
Wolf, K	Texas A&M Univ./LANL
Wosiek, B	Inst. of Nuclear Physics, Krakow
Young, GR	Oak Ridge National Laboratory
Yu, B	Univ. of Pittsburgh
Zajc, W	Nevis Laboratories

INTRODUCTION

This workshop represents the third in a series of studies of detectors for RHIC. The most significant development in the field of relativistic heavy ion physics affecting this workshop and distinguishing it qualitatively from previous ones, is the recent availability of new experimental results from the CERN-SPS for 60 and 200 A GeV Oxygen and Sulfur beams and from the BNL Tandem- AGS for 14.5 A GeV Oxygen and Silicon projectiles [1,2]. These experiments have established that states of compressed nuclear matter can be created and studied under laboratory conditions in which extreme values of energy density are achieved. The new data reflect an environment of high baryon density, at energies near the maximum for nuclear stopping. The general characteristics of these events bear out the early expectations for large thermal energy deposition in violent nuclear collisions, and they point the way for extending further the range of thermodynamic conditions over which to study new forms of dense hadronic matter. The most exciting results are the several indications that, indeed, when these extreme conditions are reached, there are new physical phenomena to be explained. Some examples which have emerged from the early experiments are:

- Large amounts of nuclear stopping with the associated generation of high energy densities.
- The observation of J/Ψ suppression.
- Enhanced production of strangeness.
- Large source sizes measured via interferometry.

With the realization of RHIC, nuclear physics will have a dedicated facility which will reach energies high enough to ensure a baryon-free central region in collisions between the heaviest nuclei; incorporate the flexibility to study collisions between all nuclei from the lightest to the heaviest; and allow experiments to be carried out over the full range of energies, from a few GeV/amu. in the center of mass up to the top collider energy, with no inaccessible gaps, and with adequate intensity for sensitive experiments.

The planning and execution of RHIC experiments requires long lead times for the design and construction of detectors. Recognizing this, workshops have been organized at BNL [3] and LBL [4] to discuss the kinds of detector systems one would like to build at RHIC. In this, the third in a series of such workshops, the focus has been on detector techniques. The instrumental issues raised by the experimental results described above point to areas of research and development shared both by experiments at the SSC and at RHIC. Areas of particular importance to heavy ions are:

1. Soft calorimetry.

2. High multiplicity tracking and particle identification (PID).

3. High density electronics with local digitization of detector signals and/or trigger decision capability.

4. Data acquisition systems tailored to RHIC detector and read-out electronics.

The following articles summarize the issues relevant to the detector techniques that will be in use at RHIC experiments. Some of the ideas presented herein expand on the work done in the previous two workshops, in the light of recent developments in instrumentation. Others are discussed here for the first time.

The proceedings are organized in the following sections:

1. Machine performance

2. Calorimetry

3. Particle identification and tracking

4. Read-out electronics

5. Data acquisition

6. Detector Simulation

7. B-Physics

The last item is a new initiative, deriving from RHIC being uniquely capable of high precision experiments in the 10 GeV mass range, and a prolific source of B-quarks. This last section, therefore, discusses both physics and detector issues.

We would like to thank Tom Ludlam, Ronnie Rau, and the Brookhaven National Laboratory for hosting this workshop and the summer school that preceeded it. Our own efforts were supported in part by the department of energy though contracts DE-AC0276-ER03074 with Yale University, and DE-AC02-76CH00016 with the Brookhaven National Laboratory.

B.Shivakumar and P.Vincent

References

[1] M.Gyulassy, Z. Phys. C38, 361 (1988).

[2] Proceedings of *Quark Matter '88*, P.Braun-Munzinger, editor, in press.

[3] Proceedings of the workshop on *Experiments for a Relativistic Heavy Ion Collider*, P.E.Haustein and C.L.Woody, editors, BNL-51921, 1985.

[4] Proceedings of the workshop on *Experiments and Detectors for a Relativistic Heavy Ion Collider*, H.G.Ritter, A.Shor, editors, LBL-24604, 1987.

The RHIC Project: Overview and Status

THE RHIC PROJECT: OVERVIEW AND STATUS*

H. Hahn
Brookhaven National Laboratory
Upton, New York 11973

Introduction

The Relativistic Heavy Ion Collider at Brookhaven will extend the present heavy ion capabilities of the AGS into an energy domain not available at any other laboratory within the foreseeable future. The Brookhaven site map in Fig. 1 shows the accelerators and connecting beam tunnels involved in the heavy ion program, i.e. the Tandem Van de Graaff, the Heavy Ion Transfer Line, the AGS, the booster synchrotron presently under construction, and the existing ring tunnel for the proposed collider. Operation of the AGS for heavy ion experiments started in October 1986 with the delivery of O^{8+} beams. Subsequently, the mass range was extended with the AGS delivering typically 2×10^8 Si^{14+} ions/pulse at a kinetic energy of 13.8 GeV/u.[1] Completion of the AGS booster synchrotron in 1991 will extend the mass range to the heaviest ions, typically ^{179}Au, with ^{238}U a definite possibility.

The acceleration of heavy ions to very high energies at Brookhaven was already considered for the ISABELLE/CBA project.[2] After its cancellation, the realization of a dedicated heavy ion collider in the vacant tunnel became feasible and the design objectives were defined in 1983 by a Task Force on Relativistic Heavy Ion Physics.[3] The study of such a heavy ion accelerator/collider was initially supported by generic R&D funds and later on as part of the Brookhaven Exploratory Research Program. The results of this multi-year R&D effort were presented in the May 1986 Conceptual Design Report (CDR).[4] This document remains valid in most respects but progress resulting from two years of intensive R&D work, now supported with direct DOE funds, in the areas of accelerator physics and superconducting magnet technology resulted in a few design improvements. The present paper summarizes the major features of the RHIC design with emphasis on those aspects of particular interest to the future user and it concludes with a short discussion of the superconducting magnet R&D program.

*Work performed under the auspices of the US Department of Energy.

[1] R.K. Reece et al., Proc. 1987 IEEE Particle Accelerator Conference, Washington, DC, p. 1600.
[2] M.Q. Barton, Proc. 1982 Bielefeld Workshop on Quark Matter Formation and Heavy Ion Collisions, p. 237; and IEEE Trans. **NS 30**, 2020 (1983).
[3] T. Ludlam and A. Schwarzschild, Nucl. Phys. **A418**, 657c (1984).
[4] "*Conceptual Design of the Relativistic Heavy Ion Collider RHIC*", BNL Report 51932 (1986).

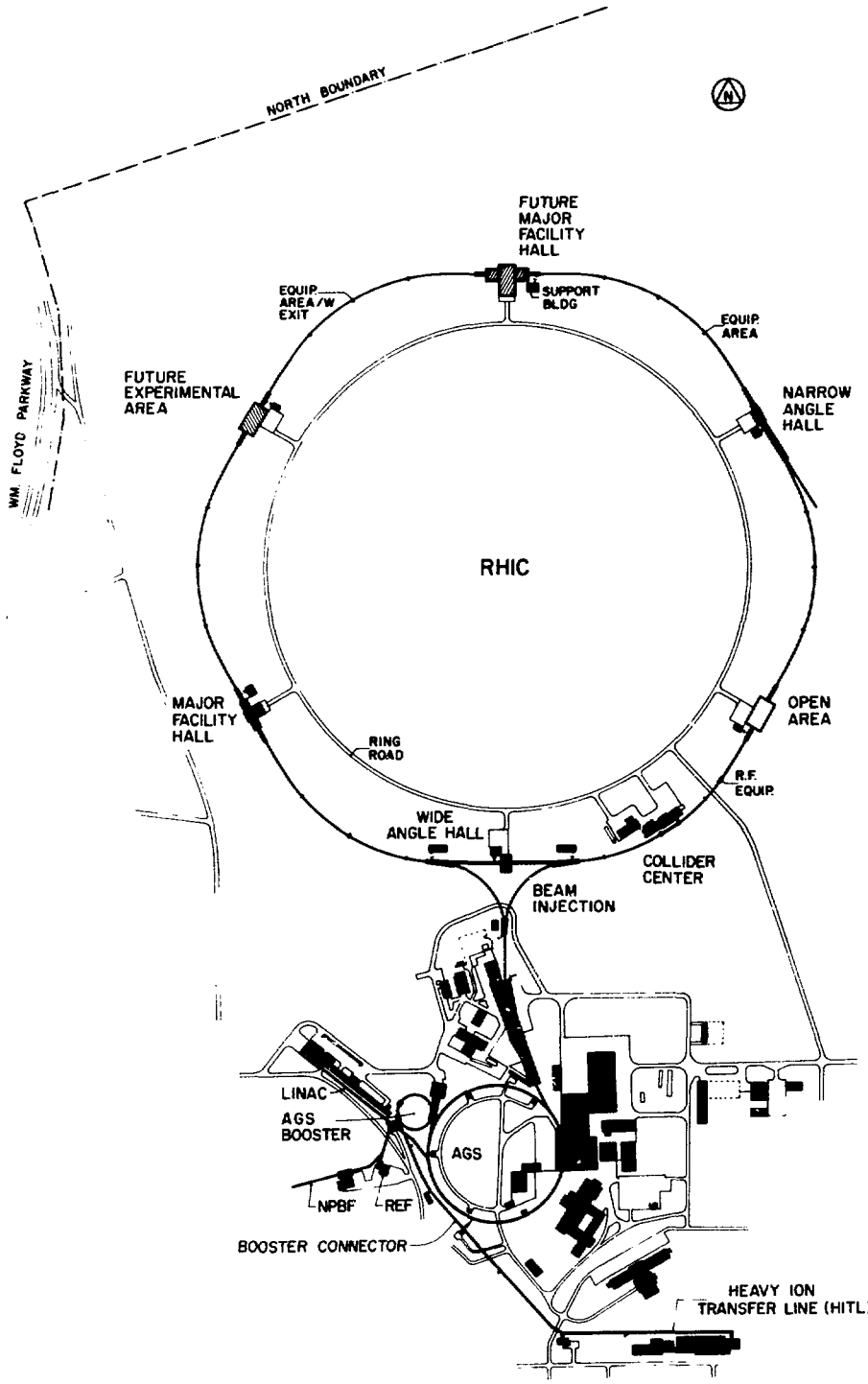

Fig. 1. Site map of accelerators at Brookhaven.

The RHIC Scenario and Major Parameters

The existence at Brookhaven of the AGS/Tandem Van de Graaff complex and the availability of the vacant ring tunnel provide a unique opportunity to construct the Relativistic Heavy Ion Collider at minimal cost. The layout of the two intersecting magnet rings in the tunnel is shown schematically in Fig. 2. Each ring consists of six arcs providing most of the bending and six insertions where the two rings intersect and the beams can be brought into collision. Of the six crossing regions built into the RHIC rings, those at the 2, 6, and 8 o'clock positions have completed experimental halls, including support buildings and crane coverage. The 4 o'clock region is an "open area" which allows considerable flexibility in the detector configuration. The magnets of each ring are cryogenically and electrically separate; they are located in the tunnel side-by-side with a 90-cm horizontal spacing as shown in Fig. 3.

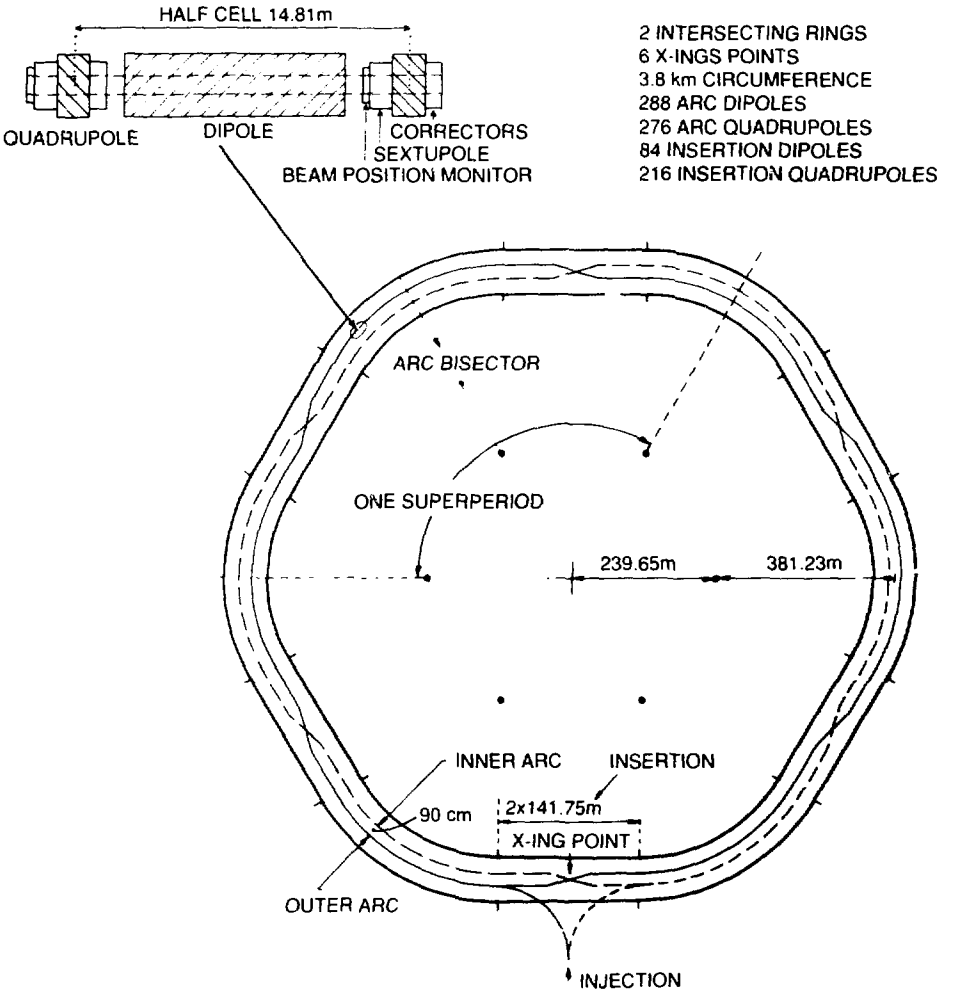

Fig. 2. Layout of the RHIC rings.

The RHIC design desiderata can be achieved in different ways. An important choice in the RHIC design was the utilization of short bunches colliding head-on to enhance the luminosity while keeping the average current and stored beam energy low. It was found that intrabeam scattering is one of the dominant design considerations in heavy ion machines, which require stronger focusing lattices and higher rf voltages then corresponding proton machines.

Given that the machine will be built in the existing 3.8-km long tunnel, a cost optimization is achieved by filling the circumference with relatively low-field magnets. The maximum energy for gold ions of 100 GeV/u is reached with a magnetic field of 3.45 T. The major parameters of the RHIC systems are listed in Table I.

The RHIC related R&D efforts have been concentrated on accelerator physics questions affecting performance and the construction of superconducting arc magnets. Other systems have received sufficient attention to come up with a conceptual design. In view of their status only a few general comments need be made here.

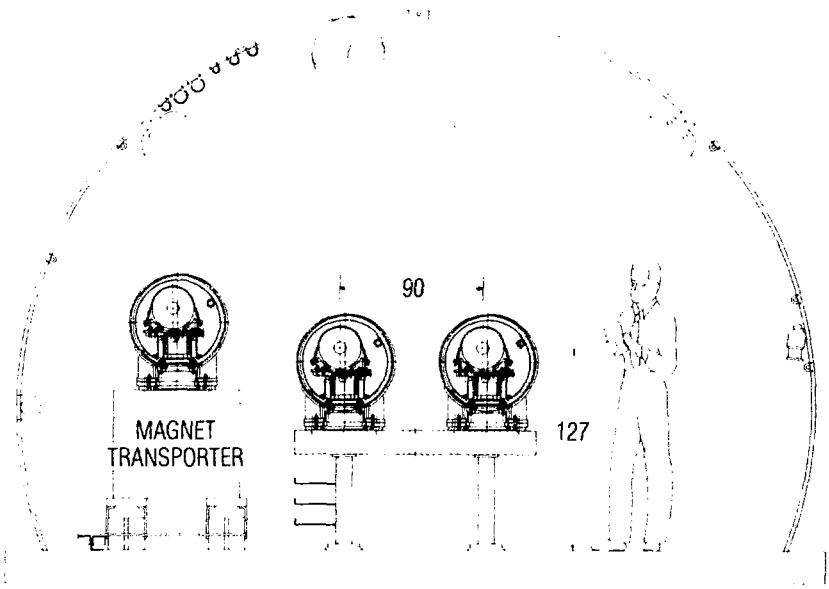

Fig. 3. RHIC tunnel cross section.

Table I. Major Parameters of RHIC Systems

Circumference, 4-3/4 C_{AGS}	3.834	km
No of dipoles (180/ring + 12 common)	372	
No. of quadrupoles (276 arc + 216 insertion)	492	
Dipole field @ 100 GeV/u, Au	3.45	T
Dipole magnetic length	9.46	m
Dipole yoke length	9.7	m
Coil i.d. arc magnets	8	cm
Beam tube i.d.	7.29	cm
Operating current	5	kA
Quadrupole gradient	72	T·m
Magnetic rigidity, $B\rho$: @ injection	96.7	T·m
@ top energy	839.5	T·m
No. of bunches/ring	57	
No. of Au-ions/bunch	1×10^9	
Filling time (each ring)	~1	min
Injection kicker rise time, 0.13 T·m	80	nsec
Stored energy, each beam	300	kJ
Beam dump kicker rise time, 1.7 T·m	~1	μsec
Acceleration rf, 26.7 MHz	400	kV
Storage rf, 160 MHz	11.4 (4.3)	MV
Acceleration time	1	min

Injector

The Tandem-Booster-AGS combination represents a very good injector for RHIC, capable of satisfying the beam parameters assumed for the collider design, e.g., Au bunches with 1×10^9 ions with normalized emittances of 10π mm·mrad and a bunch area of 0.3 eV·sec. The AGS will deliver a single bunch to RHIC, where nominally 57 bunches are accumulated in boxcar fashion. The AGS beam is transferred to RHIC and is vertically injected by a sequence of septum and kicker magnets as shown in Fig. 4. The requirements for the injection kickers listed in Table I will allow injection of 114 bunches. The intensity of Au beams is source-limited. The May-86 CDR assumed acceleration of fully stripped ions in the AGS. Higher intensities can be obtained by omitting one stripping foil after the Tandem and accelerating partially stripped ions, Au^{77+}, in the AGS. It was decided to take advantage of this possibility in order to allow the booster operation with the presently planned h=3 rf system which is simpler but provides only 10^9 Au-ions per bunch for injection into RHIC. Adding a h=1 rf system in the booster represents a future option to increase the number of ions per bunch.

Beam Extraction

The stored energy per beam is about 300 kJ which should allow an internal beam dump. The configuration of beam extraction equipment is shown in Fig. 4 and the beam dump kicker requirements are given in Table I. A 1-μsec gap in the bunch sequence, 13 μsec long, will be provided to minimize uncontrolled beam spill. Although acceptable at the design intensity, the internal beam dump may have to be replaced in the future by a beam extraction system in order to remove the constraints on beam intensity. Adding a septum magnet at the location of the beam dump would allow beam extraction, without requiring other changes to the ring.

rf Systems

The beam will be accelerated with an 26.7 MHz rf system operating on the $h = 6 \times 57$ harmonic. A voltage of about 400 kV is required. The choice of this frequency accommodates the bunch length of the injected beam as well as passage through transition. The acceleration time of 1 min is relatively slow and provisions for a fast transition jump will be made.

To limit the bunch length and thus the diamond length, a second 160 MHz storage rf system will be installed. The momentum spread of the beam grows in time due to intrabeam scattering; the rf voltage has to follow in order to keep the bunch length constant. The voltage requirements of the 160 MHz rf system for gold and proton beams are shown in Fig. 5 as function of storage time assuming a bucket half height Δ_B equal to twice the rms energy spread δ_E. The bucket half height is related to the voltage V by

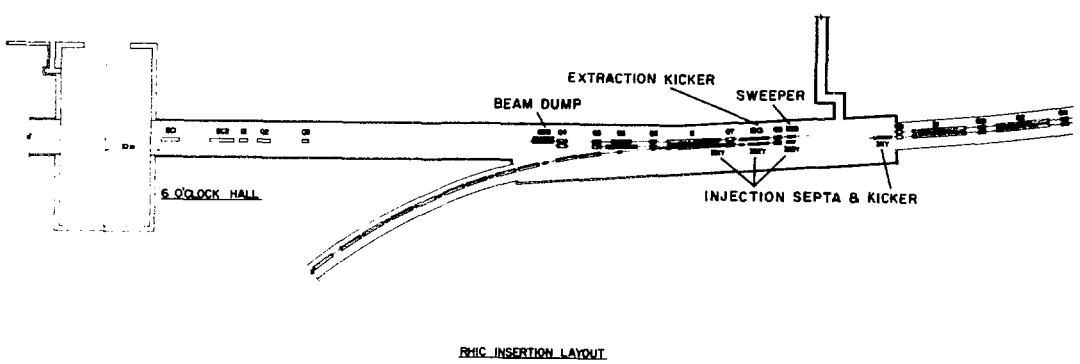

Fig. 4. Six o'clock insertion with injection and beam dump.

$$\Delta_B = \left(\frac{\Delta E}{E}\right)_B = \left(\frac{2}{\pi} \frac{\beta^2 \, e \, V}{h \, |\eta| \, \gamma \, E_o} \frac{Q}{A}\right)^{1/2}$$

with $\eta = \gamma_{tr}^{-2} - \gamma^{-2}$ and A the atomic mass unit, Q the charge state and h the rf harmonic (h = 2052 for 160 MHz). The energy spread of gold beams with 10^9 ions/bunch is computed to grow from $\delta_E = 0.25 \times 10^{-3}$ to 1.14×10^{-3} rms during the 10 h storage time. By continuously changing the rf voltage during this time, the rms bunch length remains constant at 31 cm. The minimal rf voltage at 100 GeV/u is then 11.4 MV, which requires a 160 MHz rf system with 16 cavities per ring.

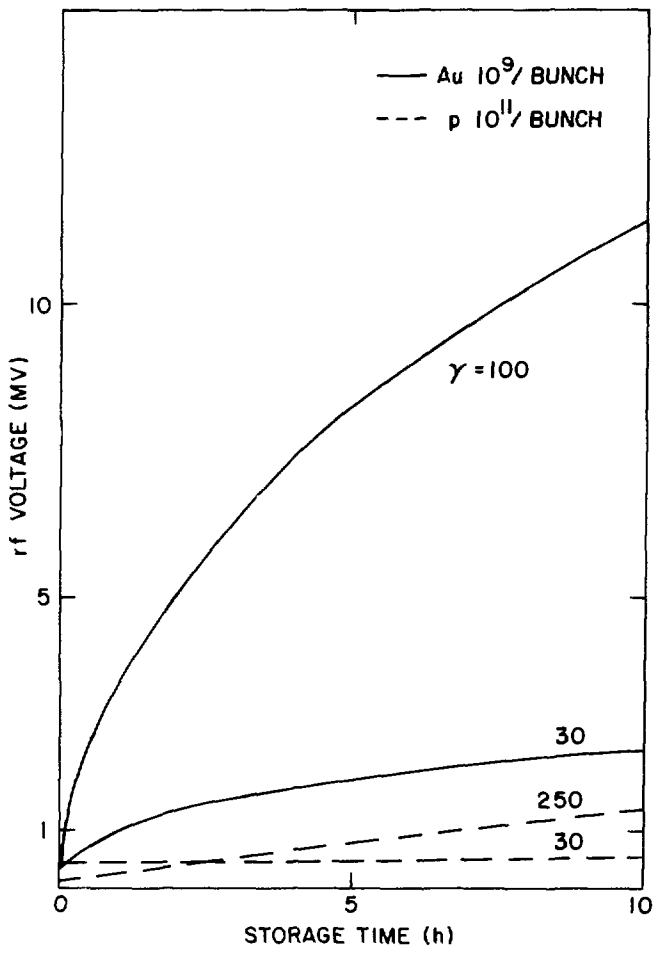

Fig. 5. Voltage requirements of storage rf system for nominal design parameters.

Intrabeam Scattering

The design and the performance of a heavy ion collider is strongly influenced by the beam growth due to intrabeam scattering. The choice of the arc-magnet aperture and of the voltage for the 160 MHz storage rf system depends directly on results from intrabeam scattering computations.[5]

The time dependence of the rms energy spread δ_E and of the transverse rms beam size σ is obtained by integrating the coupled intrabeam scattering differential equations, valid above transition and assuming full coupling ($\varepsilon_H = \varepsilon_V$)

$$\tau_E^{-1} = \frac{1}{\delta_E}\frac{d\delta_E}{dt} = \frac{27\pi}{2} L_g r_p^2 E_o \frac{\langle X_p\rangle}{<\beta>} \frac{\left[\frac{<\sigma>}{\langle X_p\rangle \delta_E}\right]^2}{\left[1+\left[\frac{<\sigma>}{\langle X_p\rangle \delta_E}\right]^2\right]^{1/2}} \frac{N_B}{S\,\varepsilon_N^2}\left[\frac{Q^2}{A}\right]^2$$

and

$$\tau_H^{-1} = \frac{1}{\sigma}\frac{d\sigma}{dt} = \frac{1}{2}\left[\frac{<\sigma>}{\langle X_p\rangle\ \delta_E}\right]^{-2} \tau_E^{-1}$$

with the longitudinal bunch area

$$S = 6\pi\ \sigma_\ell\ \delta_E\ \gamma\ E_o/c$$

the normalized 95% transverse emittance

$$\varepsilon_N = 6\pi\ (\beta\gamma)\ <\sigma>^2\ /\ <\beta>$$

and

$$L_g \approx 20$$

where r_p is the classical proton radius, $<X_p>$ the averaged dispersion and $<\beta>$ the averaged betatron function.

[5] G.Parzen, Nucl. Instr. Meth., **A251**, 220 (1986) and **A256**, 231 (1987).

For typical RHIC parameters, intrabeam scattering evolves as follows: Within the first few minutes, the energy spread increases rapidly until equipartition is reached, i.e.,

$$\langle X_p \rangle \, \delta_E \approx \langle \sigma_H \rangle$$

Transverse beam size and beam size due to the energy spread then grow together. Since the bunch length is kept constant by the rf system, the appropriate scaling law is

$$\tau_E^{-1} = \tau_H^{-1} \propto \frac{N_B}{\langle \sigma \rangle^5} \left(\frac{Q^2}{A} \right)^2$$

It follows that the aperture requirements depend only weakly on the number of particles/ bunch,

$$\langle \sigma \rangle \propto (N_B)^{1/5} \left(\frac{Q^2}{A} \right)^{2/5}$$

and the voltage requirements follow as

$$V \propto (N_B)^{2/5} \left(\frac{Q^2}{A} \right)^{4/5}$$

The differential equations governing intrabeam scattering are believed to be well-understood and reliable. There are, however, uncertainties resulting from the lack of knowledge as to the beam parameters in RHIC after injection and acceleration through transition. In view of these uncertainties which mostly impact the rf voltage requirements and the substantial cost attached to the high-frequency rf system, installation of a lower voltage rf system on day-one would seem advisable.

The impact of operating with an initial emittance larger than the nominal $\varepsilon_N = 10\pi$ mm·rad in order to reduce the rf voltage requirements were studied by Parzen.[6] The results are shown in Fig. 6 from which we conclude that a reduction of the rf voltage from 11.4 to 4.3 MV (6 instead of 16 cavities) is possible by intentionally increasing the initial emittances to 60π mm·mrad which would result in a luminosity reduction by a factor 2÷3 while maintaining the bunch length and the 10-hour lifetime.

[6] G. Parzen, private communication.

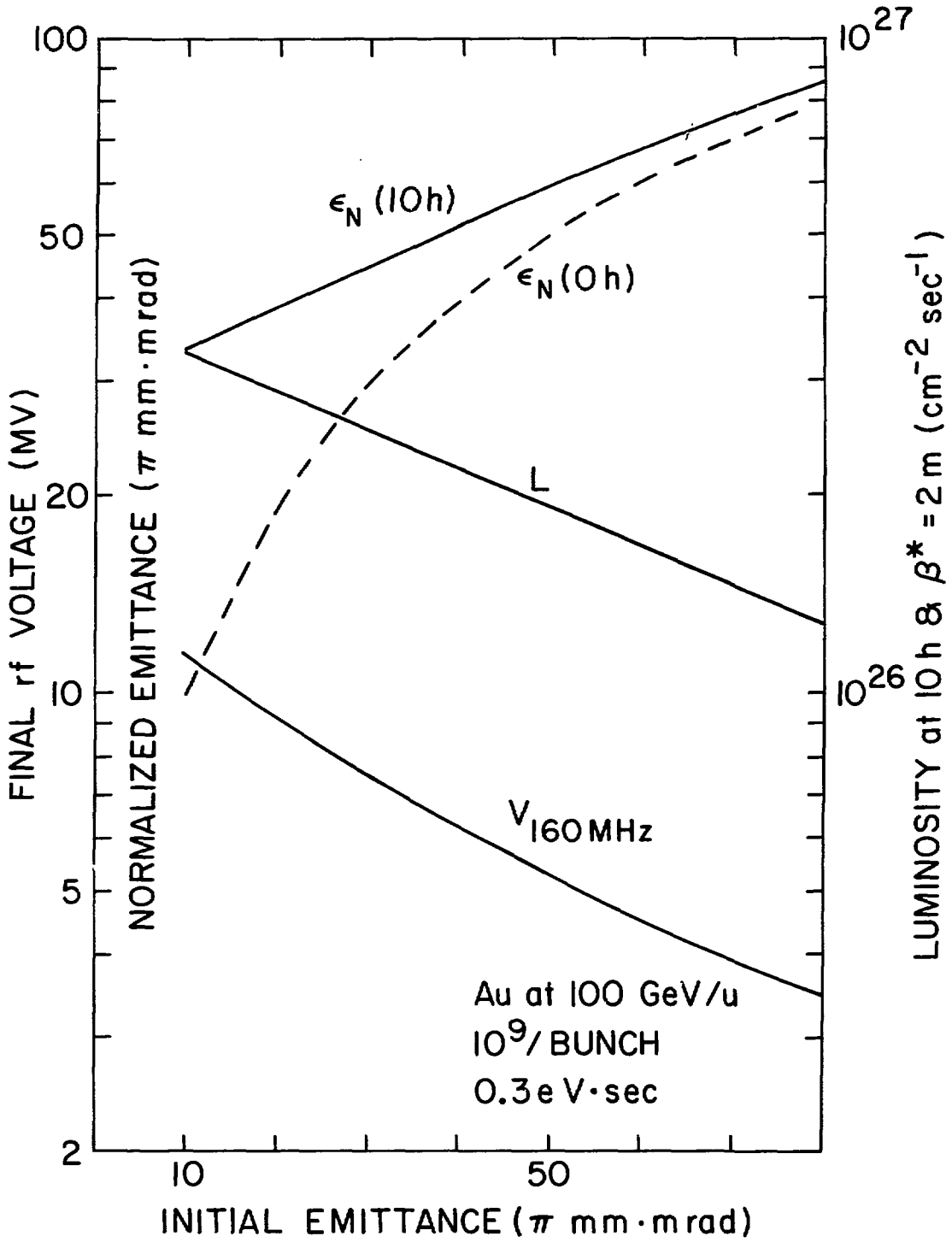

Fig. 6. Dependence of luminosity and rf voltage requirement on initial emittance.

Performance Estimates

The performance objectives for RHIC were first spelled out by a Task Force for Relativistic Heavy Ion Physics in a report[3] dated August 1983. The design requirements can be summarized in the following points.

Energy

Top energy will be about 100 × 100 GeV/u for heavy ions and 250 GeV for protons. This represents an order of magnitude increase over the SPS fixed target capabilities. It was pointed out that the collider should span a wide range of energies, down to 7 × 7 GeV/u and lower. The lower energies will be covered by internal target operation. In order to limit magnet aperture requirements, and thus cost, full luminosity requirements are limited to energies above 30 × 30 GeV/u.

The quench field of the arc dipoles is about 4.6 T which is 30% higher than the 3.45 T required at the design energy of 100 GeV/u and higher operating energies should be achievable. However, the dipole configuration at the crossing point (Fig. 7) is field limited, BC1 to ~4.7 T, and head-on collisions cannot be obtained above design energy.

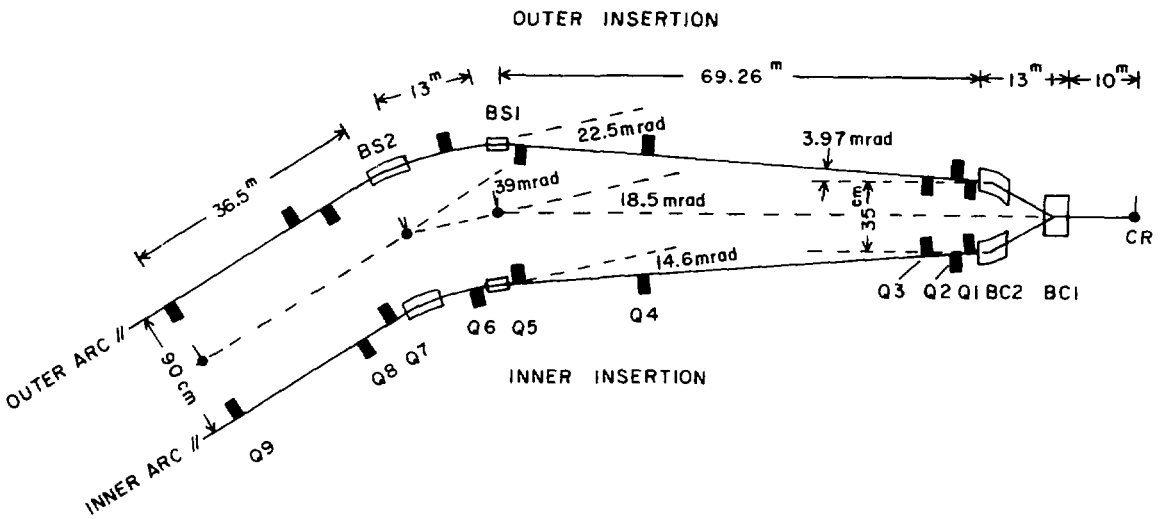

Fig. 7. Insertion magnet layout.

Range of Ion Masses

The expectations for interesting physics phenomena require a broad range of nuclei, from the heaviest (e.g., Au, U) to the lightest, including protons. Asymmetric operation, with heavy ions on protons, is considered to be crucial.

Head-on collisions of Au-p are possible as shown in Fig. 8. Operation with unequal species requires synchronization between the two beams, i.e., equal velocity and the operating field in the proton ring is lowered by the ratio $A/Q \approx 2.5$ for gold. The field in the common dipole BC1 is also lowered resulting in a change of the beam direction at the intersection point by about 3.4 mrad.

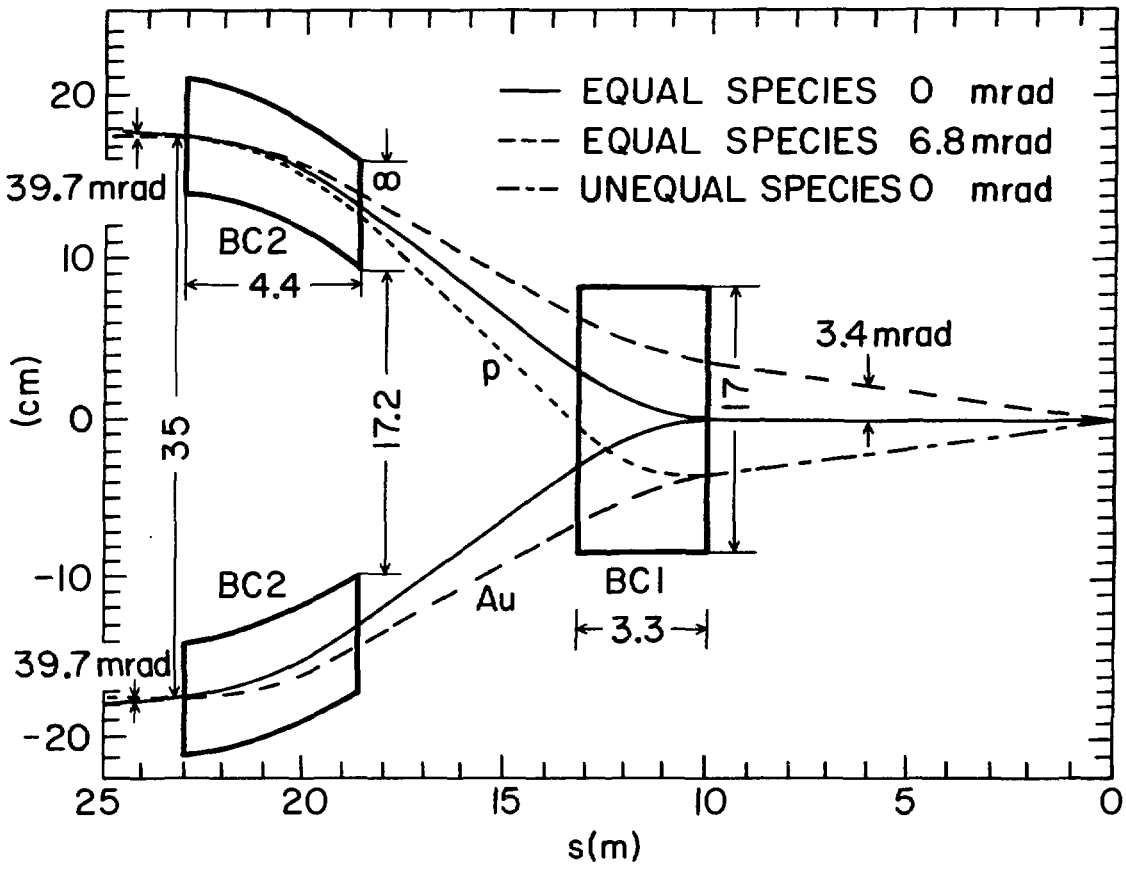

Fig. 8. Beam path at crossing point for Au-Au and Au-p collisions.

Luminosity

The luminosity requirements for initial experiments are rather modest, about 10^{25} cm^{-2} sec^{-1}. The machine is designed for Au-Au collisions with a luminosity of 3×10^{26} cm^{-2} sec^{-1} at top energy while maintaining the option for future upgrades to 2×10^{27} cm^{-2} sec^{-1}.

The maximum luminosity is obtained with head-on collisions of very short bunches, for which one has

$$L_o = \frac{3}{2} f_{rev} B \frac{(\beta\gamma) N_B^2}{\varepsilon_N \beta^*}$$

where N_B is the number of particles per bunch, B the numbers of bunches per beam, f_{rev} the revolution frequency, ε_N the invariant transverse 95% emittance, and β^* the beta-function at the crossing point. The design performance parameters for RHIC are given in Table II.

Taking into account a finite bunch length σ_ℓ and crossing angle α, the luminosity is given by

$$L = L_o/\sqrt{1+q^2}$$

with

$$q^2 = \left(\frac{1}{2}\frac{\alpha\ \sigma_\ell}{\sigma_H^*}\right)^2 + \left(\frac{\sigma_\ell}{\beta^*}\right)^2$$

where the horizontal rms beam size at the crossing point

$$\sigma_H^* = \left(\frac{\varepsilon_N}{6\pi\ (\beta\gamma)}\ \beta^*\right)^{1/2}$$

The ultimate performance of hadron colliders is limited by beam-beam effects. The experience from the CERN $Sp\bar{p}S$ suggests that the important parameter for long-term stability is the beam-beam tune spread which is given by the sum of the beam-beam tune shifts per crossing

$$\Delta\nu_{BB} = \sum_i \frac{3}{2} r_p \frac{N_B}{\varepsilon_N} \frac{Q^2}{A}$$

with the quantities as previously defined. The observational limit is $\Delta\nu_{BB} < 0.02$, which is not exceeded for the nominal RHIC design.

The beam-beam tune shift is independent of the number of bunches stored as well as of the β^* at the crossing point. Increasing the number of bunches and lowering β^* yields higher luminosities without exceeding the beam-beam limit.

Table II. RHIC Performance Parameters

Revolution frequency	78.2		kHz
No bunches	57		
Bunch spacing	224		nsec
	Au	p	
β^* @ top energy	2	2	m
No particles/bunch	1×10^{9}	1×10^{11}	
Top momentum, $\beta\gamma$	108	268	
Emittance, initial	10	20	π mm·mrad
@ 10 h	34	24	π mm·mrad
Luminosity, initial	11×10^{26}	1.4×10^{31}	cm^{-2} sec^{-1}
@ 10 h	$\sim3\times10^{26}$	$\sim10^{31}$	cm^{-2} sec^{-1}
Beam-Beam tune spread, max	0.014	0.02	
Luminosity expectation†	2×10^{27}	3×10^{32}	

†B = 114, $N_B(Au) = 2\times10^{9}$; $N_B(p) = 2\times10^{11}$, $\beta^*(p) = 0.5$ m

Doubling the number of bunches from 57 to 114 requires faster injection kickers, and is an obvious future improvement. Tripling the number of bunches, on the other hand, is incompatible with zero-angle crossing if the present free space from crossing point to BC1 is retained; furthermore, the collision frequency would require improved detector capabilities and this option is not under consideration at present.[7]

Lowering β^* is limited by the aperture of the low-beta quadrupoles. The limit is found from the following approximation

$$\beta^* > (2\ \text{m}) \left(\frac{\varepsilon_N}{34\pi\ \text{mm·mrad}}\right)\left(\frac{100}{\gamma}\right)$$

For gold beams at top energy, $\beta^* \approx 2$ m represents the minimum with the present insertion configuration. For protons at top energy, β^* could be lowered to about $\beta^* \approx 0.5$ m resulting in a luminosity gain of a factor 4 over the nominal design. This upgrade involves new power supplies for the insertion quadrupoles and, possibily, new cryogenic current leads. A further reduction of β^* has little merit due to the $\beta^* > \sigma_\ell$ limit.

By installing additional quadrupoles, common to both rings, a mini-beta insertion with $\beta^* = 1$ m for gold beams could be created.[8] However, the free space available for detectors is reduced to ±5 m and the use of common quadrupoles prevents operation with unequal species. Furthermore, the quadrupoles require larger apertures and higher

[7]W. Willis and T. Ludlam, Proc. Workshop on RHIC Performance, March 88, BNL 41604, p. 239.
[8]S.Y. Lee, "*Mini-Beta Insertion for the RHIC Lattice*", RHIC Technical Note, RHIC-34.

gradients for which no conceptual design has been developed so far. A reduction of the beam life time due to the desired beam-beam nuclear reaction also sets a lower limit on $\beta^* > 1.9$ m.[9] Clearly the mini-beta insertion represents no option for day-one.

The most direct method of increasing the luminosity above the nominal design valve is by way of a larger number of particles per bunch. The beam-beam limit is avoided by reducing the number of collision points used. The maximum N_B is probably limited by collective instabilities, with the transverse single-bunch mode-coupling instability imposing the most severe constraint.[10] Increasing the number of ions/bunch by a factor 2 is quite realistic. Higher intensities impact the accelerator system requirements, in particular the rf system and the beam dump, but are well within the range of available technical solutions.

In summary, one can expect luminosities higher than the design by a factor of

$$2 \times 2^2 \times 4 = 32 \text{ for protons}$$
$$2 \times 2^2 = 8 \text{ for gold–ions.}$$

By using other techniques to improve performance, in particular stochastic cooling, even higher luminosities are possible, but obviously quite uncertain.

Intersection Regions

A minimum of 3 intersection regions is assumed and development of all available six regions is expected in the future. A free space at the crossing point of ±10 m is required. A number of experiments call for a diamond length of ≤20 cm rms. Furthermore, flexibility in adjusting the crossing angle should be possible.

The rms diamond length σ_I is determined by the rms bunch length σ_ℓ to be for head-on collisions

$$\sigma_I = \sigma_\ell / \sqrt{2}$$

In order to obtain $\sigma_I \leq 20$ cm, a bunch length of $\sigma_\ell \approx 28$ cm is required. The rms length of the bunches injected from the AGS is about 98 cm for gold and 72 cm for protons. At the end of the acceleration cycle to top energy and transfer into the storage rf system, the rms bunch length is 31 cm for Au and 24 cm for protons. Due to intrabeam scattering the bunch length tends to grow. The bunch length is kept constant by appropriate growth of the rf voltage. The maximum bunch length, which the bunch can assume, depends on the bucket length which is set by the rf frequency. Very short bunches are possible, but a practical limit is given by the voltage requirement and thus

[9] G. Young, Proc. Workshop on RHIC Performance, March 1988, BNL 41604, p. 255.
[10] M.S. Zisman, Proc. Workshop on RHIC Performance, March 1988, BNL 46104, p. 371.

by the cost of the rf system. The choice of a 160 MHz (h = 2052) storage rf system, in addition to the 26.7 MHz (h = 342) acceleration rf system, assures an rms bunch length of

$$\sigma_\ell = \frac{2\,R}{h} \arcsin \frac{\delta_E}{\Delta_B}$$

where R = average machine radius, h = rf harmonic, δ_E = rms energy spread, and Δ_B = bucket height. For the design value of $\delta_E/\Delta_B = 0.5$, follows $\sigma_\ell = 31$ cm.

Operation with a finite crossing angle, α, further reduces the diamond length

$$\sigma_I = \frac{\sigma_\ell}{\sqrt{2}\,(1+q^2)^{1/2}}$$

with q as defined above.

However, it may well be that operation with large, finite crossing angles is prohibited by beam-beam excited synchro-betatron resonances if[11]

$$\alpha > \alpha_{SB} = 2\,\sigma_H^* / \sigma_\ell$$

The maximum acceptable crossing angle is encountered at 30 GeV/u for gold where one finds $\alpha_{SB} \approx 6.8$ mrad. The diamond length at the synchro-betatron limit is $\sigma_I = \sigma_\ell / 2 \approx$ 15 cm rms. In order to provide such a short diamond length, the common dipole BC1 must have an aperture of at least 17 cm. By coincidence, this is also the aperture required for operation of unequal species.

A cost-efficient detector design requires the luminosity in a short diamond length, i.e. a large luminosity density

$$L / \sigma_I \propto L_o / \sigma_\ell$$

which is independent of the crossing angle but which can be enhanced by reducing the bunch length. In other words, it is more desireable to reduce the diamond length by shortening the bunch length than by adjusting the crossing angle.

[11] A. Piwinski, CERN Accelerator School, Oxford, England, 1985, CERN report 87-03, p. 187.

Superconducting Magnet System

The superconducting magnet system for RHIC is the one hardware system for which the R&D efforts have advanced beyond the conceptual design stage. The superconducting arc magnets, dipoles, quadrupoles, sextupoles and corrector units have been designed. The R&D work on these magnets is well along, and it is planned that a significant fraction of the magnets for the RHIC machine will be industrially fabricated. Four full-length, field-quality dipole magnets were built in 1986. Three of these magnets were assembled by an industrial firm using coils wound at BNL. The first of the full-length magnets, assembled at BNL, has been successfully tested in February, 1987. Subsequently the remaining, industrially built magnets in this series have been tested. Two each dipoles (#5 & 6) and quadrupoles were built in 1987/88, of which one dipole and both quadrupoles have been tested individually. Preparations for the in-house construction of two dipoles (#7 & 8) with their folded-post cryostats are in progress. They will then be combined with the existing quadrupoles for a full-cell system test in FY 1989. Preparations for a series of six industrial prototype dipoles are in progress. The major items in the ongoing magnet R&D effort are summarized in Table III.

The first four full-size R&D magnets have been tested in horizontal dewars. All of these magnets reached fields of approximately 4.6 T, or 35% higher than the operating field for RHIC, with virtually no training. Measurement of field quality indicated adequate rms errors, but the need for adjustment of systematic harmonics. Dipole #5 & 6 were built with a new coil geometry, increased yoke-coil gap to reduce saturation b_4, and with a ratio of Cu:SC = 2.25 in the superconductor to improve the quench behavior. The quench curve of dipole #5 is shown in Fig. 9. The quench data for the first quadrupole is shown in Fig. 10.

The choice of the RHIC magnets was preceded by a detailed cost-benefit analysis comparing superconducting magnets of different configurations (e.g. large-aperture CBA, 3-inch FNAL, 2-in-1, window frame) as well as superferric magnets. The existence of the RHIC tunnel, of course, had a profound impact on the cost optimization, leading to the selection of single-layer, cold-iron, cold-bore arc magnets. The coil aperture of 8 cm i.d. (7.29 cm beam tube i.d.) accommodates the size of gold beams at 30 GeV/u after 10 h due to intrabeam scattering. The dipoles are bent to reduce the aperture requirements (4.8 cm sagitta). The beam tube in the dipoles is copper plated to limit beam heating. The dipole cross section is shown in Fig. 11. The quadrupoles design concepts follow directly the dipole solution as shown in Figure 12. The cross section of the sextupole and trim/corrector magnet models are shown in Figures 13 and 14. Insertion magnets may have special requirements as to aperture and field or gradient, which led to different solutions.

Table III. RHIC Superconducting Magnet R&D

- 4 Full-size arc dipole models with HERA-type cryostats
  DRA001 – DRA004: Tested in FY 87
- 2 Arc dipoles with post-type cryostats
  DRB005: Tested in June 88;
  DRB006: Test in Nov. 88
- 2 Full-size quadrupoles with cryostats
  QRA001: Tested in June 88
  QRA002: Tested in Sept. 88
- 2 Sextupoles: First test in July 88
- 2 Correctors: Test in Nov. 88
- Preparations for 2 prototype dipoles (#7 & 8) with improved post-type cryostat
  Test in Apr. 89 / June 89
- Full-cell system test
  (FY 89)
- Preparations for 6 industrial arc dipole prototypes
  (FY 89 & 90)

The major arc magnet parameters are listed in Table I. The design energy of 100 GeV/u is obtained with the relatively low field of 3.45 T. The quench field of these dipoles is expected to be about 4.6 T, providing ample safety margin and the possibility of higher operating fields. The cost analysis showed that lowering the design energy yields only minimal cost reduction due to the large fraction of field-insensitive items. Also, to minimize cost, the 9.7-m dipole length was the longest compatible with the lattice, i.e. one dipole per half cell.

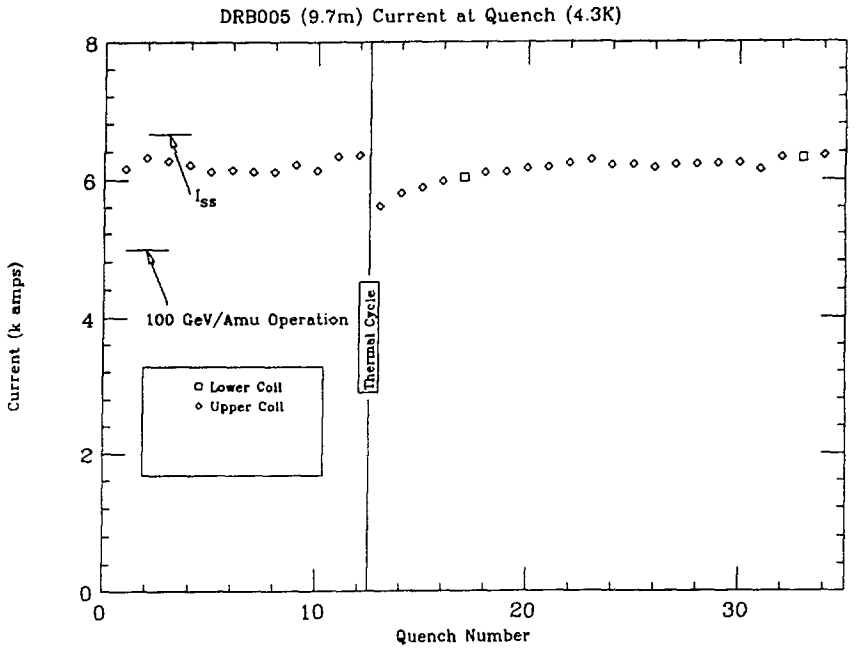

Fig. 9. Quench curve of RHIC dipole prototype.

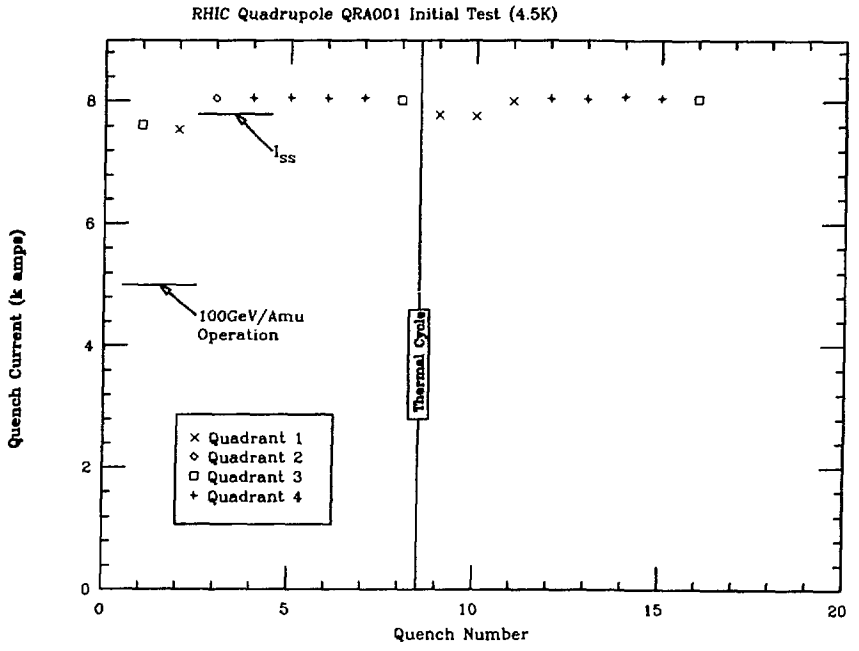

Fig. 10. Quench curve of RHIC arc quadrupole.

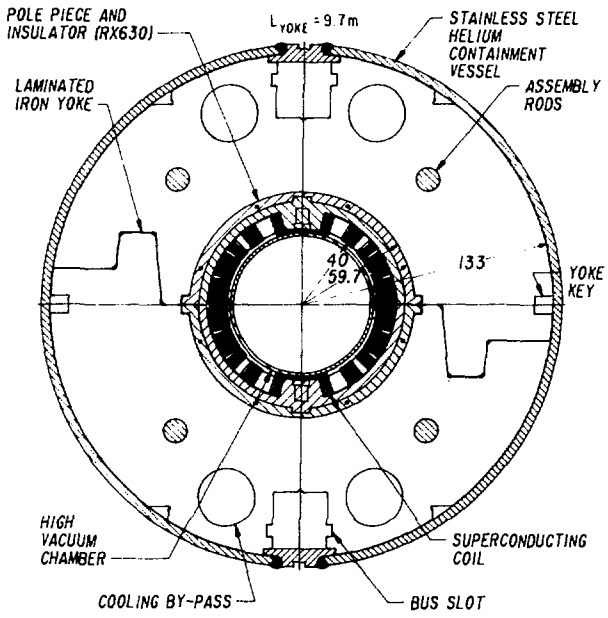

Fig. 11. RHIC arc dipole cross section.

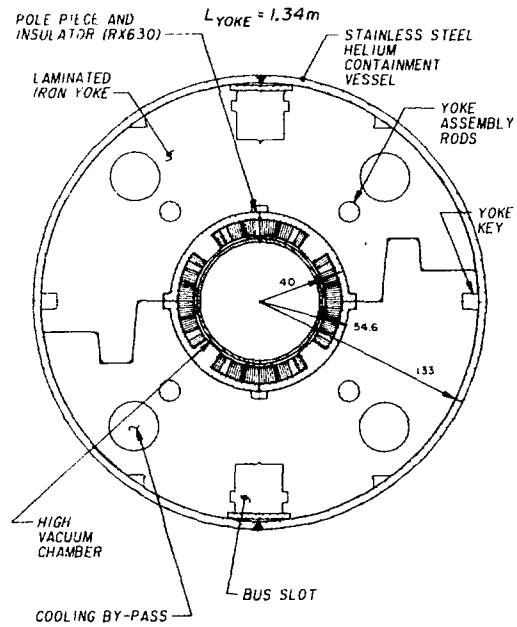

Fig. 12. RHIC arc quadrupole cross section.

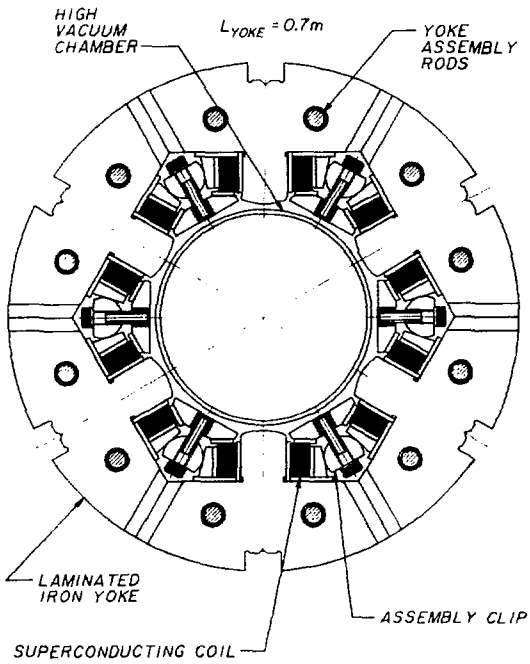

Fig. 13. RHIC arc sextupole cross section.

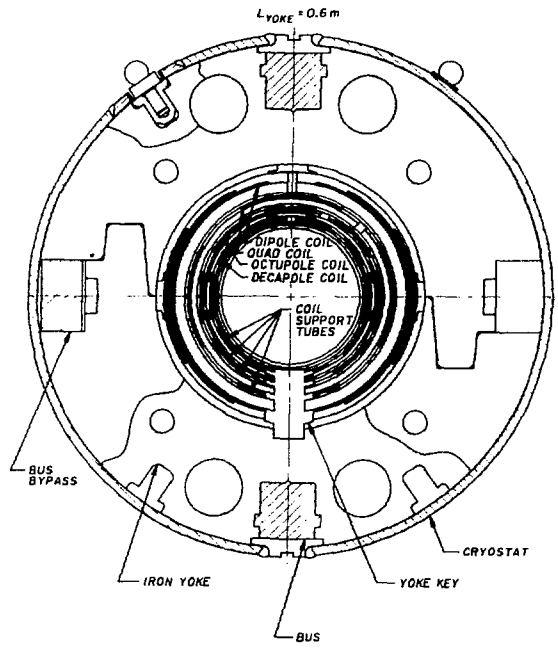

Fig. 14. RHIC arc corrector cross section.

The cross section of the RHIC dipole cryostat is shown in Fig. 15. The design follows largely the concepts developed for SSC cryostats, in particular in the use of a folded-post support. It is, however, simpler because of the need for only a single 55 K heat shield. The main advantage of this cryostat design is derived from the possibility of 1) insulating the cold mass outside of the vacuum vessel, and 2) referencing the magnet center to the ground plate prior to assembly.

The magnets of one ring are cryogenically in series. Supercritical helium at 5 atm arrives from the refrigerator at a temperature of 4.3 K, traverses the magnets of one ring and then returns. In order to keep the temperature below 4.6 K, recooler units are installed in each sextant. The total estimated heat load is about 10 kW, which is sufficiently lower than the 25 kW @ 4.3 K capability of the operational CBA refrigerator.

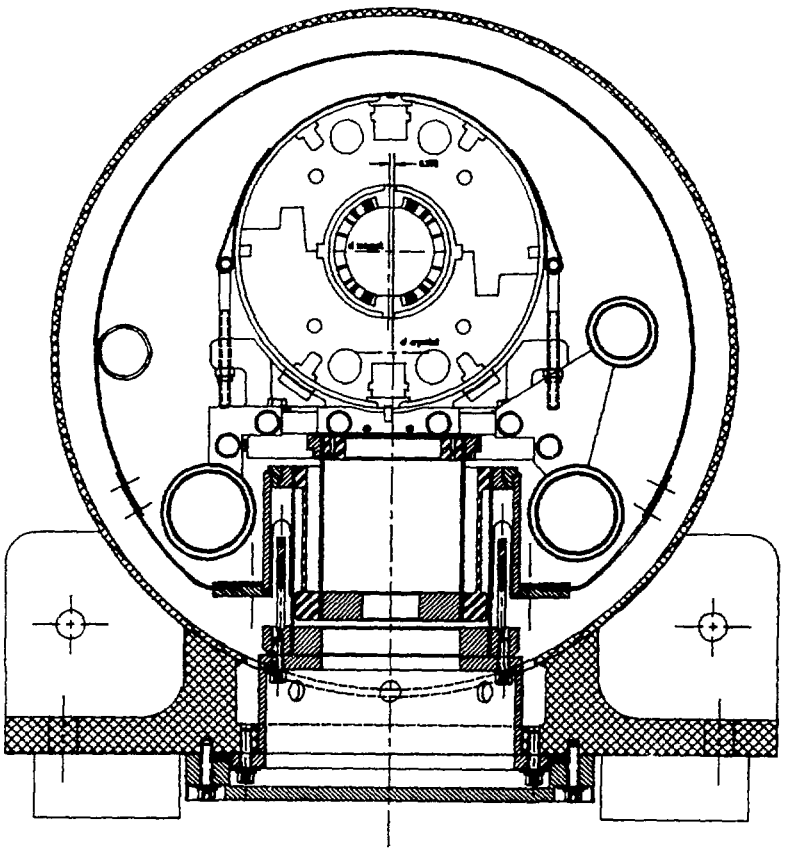

Fig. 15. RHIC dipole cryostat.

The Present Status

As noted above, a large fraction of the RHIC facility already exist. For the injector complex, the Tandem Van de Graaff, AGS, and Heavy Ion Transfer Line are already operational; the Booster Synchrotron is under construction. Most of the conventional construction for the collider is complete, including the ring tunnel, main service building and experimental halls for four of the six intersection regions. In addition, the liquid helium refrigerator, capable of cooling all of the superconducting magnets in the collider has been completed (as part of the CBA project) and successfully tested; the magnets for the AGS-to-RHIC beam transfer line are available. The superconducting magnets for RHIC have been designed, and preparations for a series of six industrial prototype dipoles are in progress. The project has been reviewed and validated by the U.S. Department of Energy. The construction of this accelerator/collider which is planned to start in Fiscal Year 1990 would take about six years and allow the start of an experimental program in 1996.

Acknowledgements

This paper summarizes the work of many in the BNL Accelerator Development and AGS Departments. Their contributions are gratefully acknowledged.

Calorimetry Related Contributions

SUMMARY OF THE WORKING GROUP ON CALORIMETRY

S. Aronson[a], M. Fatyga[a], X. Felgeyrolles[b], A. Franz[c], H. Gordon[a], W. Guryn[a], S. Kahn[a], D. Lissauer[a], W. Llope[d], S. Margetis[e], S. Persson[f], F. Plasil[g], P. Thompson[a], L. Waters[d], K. Wolf[h]

a Brookhaven National Laboratory
b Clermont Univ.
c Lawrence Berkeley National Laboratory
d SUNY – Stony Brook
e CERN/Heidelberg
f Lund Univ.
g Oak Ridge National Laboratory
h Texas A&M University

INTRODUCTION

Calorimetry will be an important aspect of essentially all experiments at RHIC. A review of prototype detectors[1] indicates several basic functions which calorimeters can be expected to perform:

1. Global event characterization – energy flow, transverse energy, fluctuations, etc. This is important both at the trigger level and in later analysis.
2. Jet detector – collimated hadronic energy.
3. Muon filter – active, segmented hadron absorber to provide a clean environment for triggering on and measuring muons.
4. Electromagnetic energy identifier – precision measurements on electrons, photons, neutral pions.

These functional characteristics are listed again in Table I, along with the technical features required for each function.

Table I. Functional Characteristics of RHIC Calorimeters

Function	*Granularity* ($\Delta\eta \times \Delta\phi$)	*Depth Segmentation*	*Total Thickness*	*Coverage* ($\Delta\eta \times \Delta\phi$)	*Energy Resolution*	*Comments*
global evt. character	0.1×0.1	"several" ($n \leq n_{D0}$)	$4 - 5\lambda_{int}$	$\pm 1 \times 2\pi$	"good" (sampling)	big systems (≥ 4000 channels)
jet detector	0.1×0.1	"several"	$> 5\lambda_{int}$	$\pm 1 \times 2\pi$	"good"	pp capability
μ filter	—	—	$5 - 10\lambda_{int}$	$\pm 3 (or 2-4) \times 2\pi$	—	minimize λ_{int}/X_0
e ident.	$\ll 0.1 \times 0.1$	several in 1st few X_0	$\geq 20X_0$ $+ few\lambda_{int}$	$\sim 1 \times 1$	very good (EM)	crystals ($$)
γ, π^0 ident.	$\ll 0.1 \times 0.1$	several in 1st few X_0	$\geq 20X_0$	$\sim 1 \times 1$	very good (EM)	need best spatial resol.

In developing calorimeter technologies to perform these functions in the RHIC environment, it is important to keep the following points in mind:

•The timescale for R&D is relatively short. It must start very soon and finish in three years or less to permit design and construction of detectors for "day-one" operation at RHIC in 1995. Research on exotic approaches to calorimetry should therefore be aimed at relatively small- scale, special- purpose devices, while large calorimeters ought to be based on technologies which, if not "proven," are at least well along in their R&D now.

•Although the center-of-mass energy of a gold-gold central collision at RHIC is equivalent to an SSC collision, there are significant differences in the final states, and hence some differences in the calorimeter requirements. Some examples below highlight the similarities and the differences:

i) Granularity. The desire to see fluctuations in the energy flow at RHIC can be satisfied with towers of $\Delta\eta \times \Delta\phi \simeq 0.1 \times 0.1$. This is not too different from SSC requirements. The track density in SSC jets is roughly comparable to the overall track density in RHIC central collisions. If electrons are to be identified at RHIC and SSC, the required segmentation of EM calorimeters will be about the same.

ii) Energy per particle. The spectrum of secondaries at RHIC is quite soft, so calorimeters can be much thinner than at SSC. Different choices of sampling media and sampling fraction may be required to optimize energy resolution.

iii) Coverage and hermeticity. Missing p_T will be a very powerful calorimeter trigger for SSC physics. This requires deep 4π calorimeters. A calorimeter trigger of comparable importance at RHIC is "centrality." This can be accomplished with partial coverage and much less depth. For this reason, some technologies may be suitable for RHIC that are not useful at the SSC.

iv) Speed. The total interaction rate is 1 MHz or less at RHIC and 50-100 MHz at SSC. The intrinsic speed of some calorimeter media may therefore be relatively

straightforward at RHIC and impossible at SSC. The same applies to methods for front-end electronics.

In the following sections of this summary we discuss the applications and R & D questions identified for various homogeneous and sampling calorimeters discussed in the Working Group. In the course of our work we identified certain needs for test beam time to develope many of these ideas; the test beam requirements are summarized in the final section.

HOMOGENEOUS CALORIMETERS

Totally active, transparent media have long been used for high-precision EM calorimetry. Table II, largely taken over from B. Pope's 1983 summary,[2] lists many of the most widely used materials.

Table II. Properties of Homogeneous Calorimeter Media

Property	*Pb Glass (SF5)*	*Scint. Glass (SCG1-C)*	*BGO*	*NaI*	*BaF_2*	*Undoped CsI*
Energy Res.	$0.045/\sqrt{E}$	$0.011/\sqrt{E}$	$0.01/\sqrt{E}$	$0.01/E^{1/4}$	$0.018/E^{0.35}$	$0.02/E^{0.4}$
Typical Int. Time	40ns	100ns	300ns	250ns	625ns(slow)	100ns
Minimum Int. Time	<10ns				<1ns(fast)	
Rad. Length	2.5cm	4.35cm	1.12cm	2.5cm	2.1^{+}cm	1.86cm
Abs. Length	42cm	45cm	23cm	41cm	30cm	
Light Output (rel. to SF5)	1	5.1	10^3	10^4	2×10^3 (fast+slow)	2×10^3
Rad. Damage (10% loss)	2500rad	$\sim 10^5 rad$	$10^2 rad$	$10^2 rad$	$> 10^7 rad$	?
Photodiode?	no	yes	yes	yes	yes	yes
No. cells/m^2 ($2X_0 \times 2X_0$)	400	130	2000	400	570	700
Problems, comments	Rad. Damage	Long Rad. Length	Cost, Temp.Dep.	Hygro-scopic	Cost, avail-ability quartz optics	Slightly hygro-scopic, needs R&D, quartz optics

A fundamental question which relates to the use of all types of EM calorimetry is whether at the low particle energies typical of RHIC collisions one can distinguish photons from neutral hadrons. This is primarily an experimental question to be answered in test beam studies.

An R & D question pertinent to homogeneous calorimeters (and all calorimeter which measure energy through light output) is the applicability of PIN diodes as readout elements. PIN diodes with local preamps offer the possibility of compact, low-cost, magnetic field-tolerant readout. The feasibility of this approach needs study; intrinsic noise may limit their utility with media having low light output.

Of the media tabulated above, undoped CsI looks very promising.[3] It is fast, rugged, has a short radiation length, has good light output, and should be cheaper and more readily available than, say, BaF_2. However, the applicability of CsI to RHIC calorimetry needs study. Radiation hardness, resolution at low energy, appropriate readout techniques all need to be explored.

SAMPLING CALORIMETERS

Any large-coverage hadronic calorimeter system will perforce employ sampling techniques. The main choice of technology (aside from high-priced, long-leadtime exotica) is between liquid ionization chamber sampling and scintillator:

•Liquid Ionization Chamber Sampling. There does not seem to be an immediate need for R & D here. In the case of liquid argon one has a mature technology; calorimeter system design could start immediately. In the case of room temperature liquids (such as TMP) one should watch the UA1 upgrade effort to judge the applicability of warm liquids to large systems.

The cryostats associated with liquid argon have often compromised the hermeticity. For RHIC, however, hermetic calorimetry is not likely to be crucial, so liquid argon systems merit serious attention, especially for calorimeters with very high channel-count.

•Scintillator-based Sampling. Several scintillator schemes were discussed in the Working Group; R & D should be pursued here:

o"Pasta" Calorimeters. These use some form of scintillating fibers as the readout medium. The so-called "spaghetti" calorimeter of Wigmans [4] has received considerable attention and is the subject of an R & D program at CERN. Individual scintillating fibers are imbedded in a passive absorber, such as *Pb* in the spaghetti calorimeter.

A variant, dubbed the "lasagna" calorimeter, uses flat ribbons of many very fine fibers as the active element. We discussed the work of Bross and collaborators [5] at Fermilab; they use scintillating fiber ribbons perpendicular to the incident particle direction (i.e., as a replacement for the sheets of scintillator in a typical calorimeter) to achieve a very high effective density. A variant suggested by F. Plasil in our working group would arrange the ribbons within a few degrees of the incident direction, as in the spaghetti calorimeter. Such a device would have its readout elements (hopefully PIN diodes) at the rear, making multi-module arrays more practical. The uniformity of response of such an arrangement would need to be studied in a comprehensive calorimeter R & D program.

oWave Shifter Fiber Readout (WSFR) Calorimeters. Here the active element is in the form of scintillator sheets interleaved with absorber plates in the standard way. The coupling to the photosensitive device is via wave shifters in the form of fibers. One version, studied at DESY,[6] uses wave shifter fibers strung through holes which penetrate the stack. Another approach, employed by BNL Experiment 814 and described by K. Wolf in our group has the fibers located in a groove in the edge of each scintillator plate and then gathered together onto the PMT or photodiode. With good coupling between the scintillator and the fiber one can imagine an EM calorimeter whose calculated resolution, based on test measurements is

$$\sigma(E)/E \simeq 0.048/\sqrt{E}$$

The question of the practicality of multi-module arrays comes up again here; the E-814 calorimeter has wave shifter fibers emerging from the edges of a module and they have to be bent toward the back with rather small radius if several modules are to sit adjacent to one another.

One needs to explore the parameter spaces of these several types of scintillator-based systems to determine their usefulness in large systems. The ratio of scintillator-to-absorber, the scintillator orientation and insertion, the appropriate readout device, the uniformity and resolution all need study. Some of this can be accomplished with simulations but test beam studies are of primary importance.

TEST BEAMS

The Calorimeter Working Group calls for the systematic study of all potential RHIC calorimeters in fairly low momentum ($200 MeV/c \leq p \leq 2000 MeV/c$) test beams with particle identification. The following performance features of these detectors should be studied:

- electron/hadron relative response
- differences in response to low-energy π, p, n and light nuclei
- e,γ,h shower profiles, position resolution and energy resolution
- uniformity and angular dependence of of response
- albedo, hadron punch-through

The test beam needs of RHIC detector R & D probably would be served at a number of labs, but it is clear that BNL will have to be a major provider of such facilities.

REFERENCES

1. Cf. *Proceedings of the Second Workshop on Experiments and Detectors for a Relativistic Heavy Ion Collider (RHIC),* Lawrence Berkeley Laboratory, May 25-29, 1987. LBL-24604/CONF-870543.
2. B. Pope, *Calorimetry Working Group Summary Report*, Proceedings of the 1983 DPF Workshop on Collider Detectors: Present Capabilities and Future Possibilities, Feb. 28 - March 4, 1983, LBL-15973.
3. C. Woody, private communication.
4. P. Jenni,*et al.*, *Construction of a Scintillating Fiber Calorimeter*, LAA Project Report (unpublished).
5. A. Bross, private communication.
6. B. Loehr,*et al.*, Nucl. Instr. & Meth.**A254** 26 (1987).

J/Ψ MEASUREMENT IN HEAVY ION COLLISIONS AT CERN

Presented by C. Lourenço (LIP, Lisbon, Portugal)
at the Workshop on Relativistic Heavy Ion Physics, BNL, July 18-22, 1988

NA38 Collaboration

M. C. Abreu[5], M. Alimi[6], C. Baglin[1], A. Baldit[3], M. Bedjidian[6], P. Bordalo[5], S. Borenstein[4], J. Britz[6], A. Bussière[1], P. Busson[4], R. Cases[9], J. Castor[3], C. Charlot[4], B. Chaurand[4], D. Contardo[6], O. Drapier[6], E. Decroix[6], A. Devaux[3], J. Fargeix[3], X. Felgeyrolles[3], A. Ferraz[5], R. Ferreira[5], P. Force[3], L. Fredj[3], C. Gerschel[7], Ph. Gorodetzky[8], J. Y. Grossiord[6], A. Guichard[6], J. P. Guillaud[1], R. Haroutunian[6], L. Kluberg[4], G. Landaud[3], C. Lourenço[5], L. Peralta[5], M. Pimenta[5], J. R. Pizzi[6], C. Racca[8], S. Ramos[5], A. Romana[4], R. Salmeron[4], A. Sinquin[7], P. Sonderegger[2], F. Staley[1] and J. Varela[5]

1 LAPP, CNRS-IN2P3, Annecy-le-Vieux, France.
2 CERN, Geneva, Switzerland.
3 LPC, Univ. de Clermont-Ferrand and CNRS-IN2P3, France.
4 LPNHE, Ecole Polytechnique and CNRS-IN2P3, Palaiseau, France.
5 LIP, Lisbon, Portugal.
6 IPN, Univ. de Lyon and CNRS-IN2P3, Villeurbanne, France.
7 IPN, Univ. de Paris-Sud and CNRS-IN2P3, Orsay, France.
8 CRN, CNRS-IN2P3 and Univ. Louis Pasteur, Strasbourg, France.
9 IFIC, Burjasot, Valencia, Spain.

1. INTRODUCTION

The NA38 experiment measures the characteristics of the muon pairs produced in relativistic ion collisions. The signals which we hope to observe as possible indications of the quark gluon plasma formation are the production of thermal dimuons and the J/Ψ suppression. Thermal dimuons will not be dealt with here.

2. THE EXPERIMENT

To cope with the rather small cross section for the production of dimuons we work with a very intense beam (around 5×10^7 ions per burst), a multiple target with 20% of an interaction length and in a rapidity domain ($2.8 < y < 4.0$) which covers mid rapidity (for incident beams of 200 GeV/c).

The NA38 apparatus is mainly composed of a dimuon spectrometer, an electromagnetic calorimeter, an active target and some beam counters.

The dimuon spectrometer [fig. 1a] starts with a hadron absorber, close to the target in order to minimize π and K decays, and whose length of 5 m of Carbon (11 L_{int}) is a compromise beetween maximizing the hadron absorption and minimizing the multiple scattering suffered by the muons. It has a toroidal magnet of hexagonal symmetry which is operated at 4000 A (producing a field of 0.22 T at a radius of one meter), 8 multiwire proportional chambers and 4 trigger hodoscopes of plastic scintillator (of 2 ns time resolution). It has a mass resolution of 5% at the J/Ψ and an acceptance which starts around 0.5 GeV/c^2 and grows up to 7% at the J/Ψ .

The electromagnetic calorimeter [fig. 1b], by measuring the transverse energy, gives us information on the energy density and on the centrality of the event. It is made of lead and scintillating fibers assembled in a very compact way (12 cm long, 12 cm outer radius) being placed right after the target to figth π and K decays. It has a very good resistance to radiation (around 1 Mrad in 10 days) and an energy resolution of 0.25 $E^{-1/2}$. Its acceptance is $1.95 < \eta < 4.15$, which covers the dimuon rapidity acceptance. By analysing its pulse shape in 4 gates of 20 ns we can use it in the rejection of pile-up events.

The active target [fig. 1b] is composed of 10 subtargets of 2% of an interaction length each, surrounded by 24 ring scintillators. It allows the identification of the subtarget where the interaction took place and the rejection of events with a reinteraction in a following subtarget.

A beam hodoscope, composed of 30 scintillators disposed in 2 planes, is placed 33 m upsteam of the target where the beam spot is large enough to allow the individual incoming ions to be counted. If a second ion is counted within a 20 ns gate the event is rejected. The active target is placed beetween a "beam in" and a "beam out" quartz cerenkov counters, immune to the high radiation level and divided into four quadrants, to allow beam centering.

3. THE DATA

From the collected data we have selected those events which verify the following conditions :

- 2 and only 2 tracks are reconstructed in the multiwire proportional chambers and in such a way that the corresponding hodoscope counters were fired and satisfy the trigger.
- those 2 tracks are in two different air sectors of the magnet.
- the active target algorithm identifies one and only one subtarget where the interaction took place.
- the beam hodoscope detects one and only one incident ion within the 20 ns gate.

In 1986 we had a 10 day run at 5×10^7 Oxygen ions per burst on Uranium and Copper targets, in 1987 we took Sulphur on Uranium data at 1-2 $\times$ 10^7 ions per burst and we also have reference data with proton beams.The number of collected

J/Ψ events (events with the mass of the dimuon beetween 2.7 and 3.5 GeV/c²) are 4.9K, 7.2K and 12.8K for the p-U, O-U and S-U systems, respectively.

The reduction of the Oxygen-Uranium data can be summarized as follows. From the 3.6 million triggers, 2.25 million muon pairs were reconstructed (1300 K opposite-sign pairs and 950 K same-sign pairs). The number of events is further reduced to 79% by demanding the identification of the interacting sub-target, to 62% by rejecting events with reinteractions, to 38% when we reject events with pile-up and to 30% after geometrical cuts. In the end we have 390 K opposite-sign pairs and 285 K same-sign pairs, from which we get 106 K prompt dimuons using the formula :

$$Signal = N^{+-} - 2\sqrt{N^{++} \times N^{--}} \qquad (1)$$

We assume that the opposite-sign muon pairs are originated by several "signal" processes like the production of resonances (ρ, ϕ, J/Ψ , ...) and the Drell-Yan mechanism but also by the decay of π's, K's, D's and $\overline{D}$'s. The same-sign muon pairs are mainly the result of the decay of the π and K mesons, allowing us to estimate through a combinatorial argument the contribution of this process to the opposite-sign set of events. As one can see from fig. 2a the background is fairly large in the low mass region of the spectra but constitutes a small fraction of the events in the J/Ψ region. In fact, fig. 2b shows a clear J/Ψ peak standing on a steeply decreasing (mainly Drell-Yan) continuum. The dimuon measurements were always made in correlation with the transverse energy deposited in the electromagnetic calorimeter [fig. 3]. We stress that the energy measured is actually the neutral energy plus a fraction (15 to 25% depending on E_T) of the hadronic charged energy.

4. ANALYSIS AND RESULTS

The dimuon mass spectrum was fitted, for masses above 1.7 GeV/c², with two gaussians superimposed on a Drell-Yan continuum :

$$\frac{dN}{dM} = \frac{N_0}{M^3}\, e^{-M/M_C} + N_1\, e^{-(M-M_{J/\Psi})^2/2\sigma^2_{J/\Psi}} + N_2\, e^{-(M-M_{\Psi'})^2/2\sigma^2_{\Psi'}} \qquad (2)$$

where the free parameters are the normalization constants (N_0, N_1 and N_2) and the parameter M_C, which is related to the shape of the continuum curve.

From the results of the fit we can compute the number of J/Ψ events, $N_{J/\Psi}$, and the number of continuum events in the J/Ψ mass range, N_C, whose ratio, S, expresses the importance of the J/Ψ relative to the continuum :

$$S = \frac{N_{J/\Psi}}{N_C} = \frac{N_1}{N_0} \frac{\int_{2.7}^{3.5} e^{-(M-M_{J/\Psi})^2/2\sigma^2_{J/\Psi}}\, dM}{\int_{2.7}^{3.5} \frac{1}{M^3}\, e^{-M/M_C}\, dM} \qquad (3)$$

In order to see how this J/Ψ relative suppression depends on E_T, the events were divided into six E_T bins (equally populated) to each of which this fitting procedure

was applied. Fig. 4 shows the fitted mass spectra for the extreme E_T bins of the O-U sample. The ratio S clearly decreases with increasing E_T [fig. 5a] while the M_C parameter stays constant within errors [fig. 5b]. By scaling E_T with $A_p^{2/3}$ we can compare directly the J/Ψ relative suppression in the various combinations of projectiles and targets studied [fig. 6]. The p-U sample, represented by an horizontal strip since it is not clear what value of A_p to apply, does not show any E_T dependence.

To investigate the p_T dependence of this suppression we compare, in fig. 7, the p_T distributions of the dimuons with masses beetween 2.7 and 3.5 GeV/c², for the low and high E_T samples. Fig. 8 shows a quantitative comparision, done through the ratio

$$R(p_T) = \frac{\frac{1}{C_H}\frac{dN^{J/\Psi}}{dp_T}(HighE_T)}{\frac{1}{C_L}\frac{dN^{J/\Psi}}{dp_T}(LowE_T)} \qquad (4)$$

where C_H (C_L) is the total number of events with $1.7 < M < 2.6$ GeV/c² and in the high (low) E_T sample. It is clear that the low p_T J/Ψ 's are the more suppressed ones.

5. CONCLUSIONS

Up to now we have observed that :

* The production of J/Ψ 's is suppressed relatively to the production of "continuum" dimuons in the events of larger energy densities;

* Low p_T J/Ψ's are more suppressed than high p_T ones;

* The mass spectra of the continuum does not seem to change its shape with E_T;

* No suppression is seen in proton-Uranium collisions.

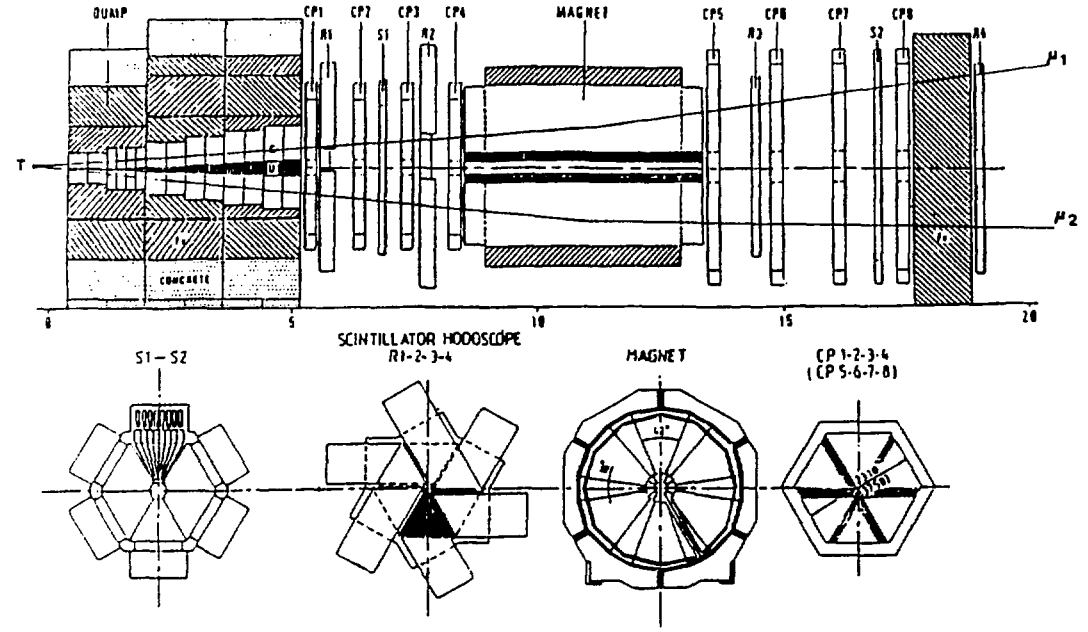

a

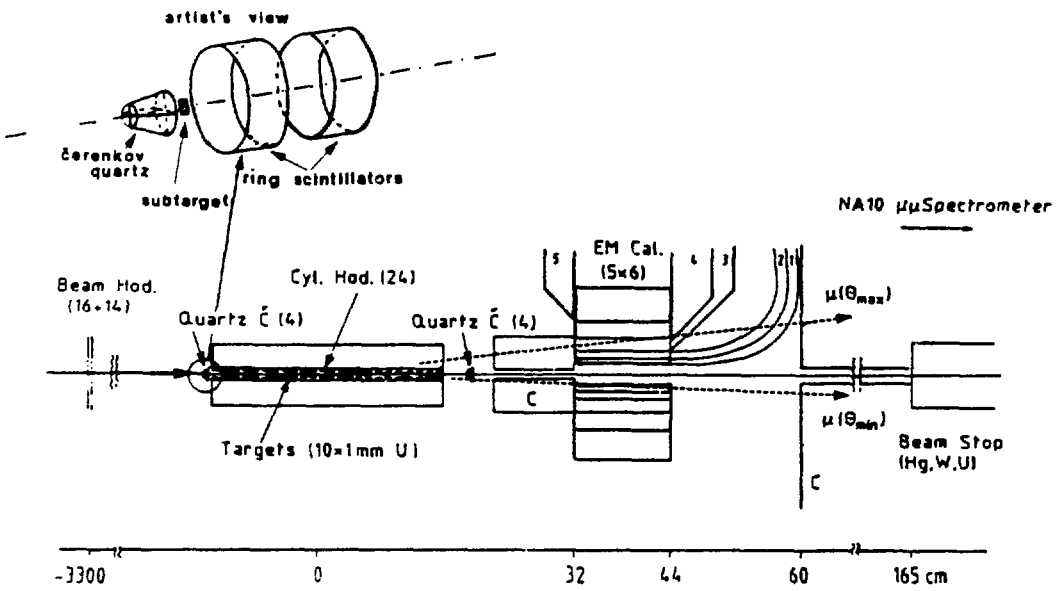

b

Figure 1. The NA38 detector. a) The muon spectrometer. b) The electromagnetic calorimeter, the multiple active target and the beam detectors.

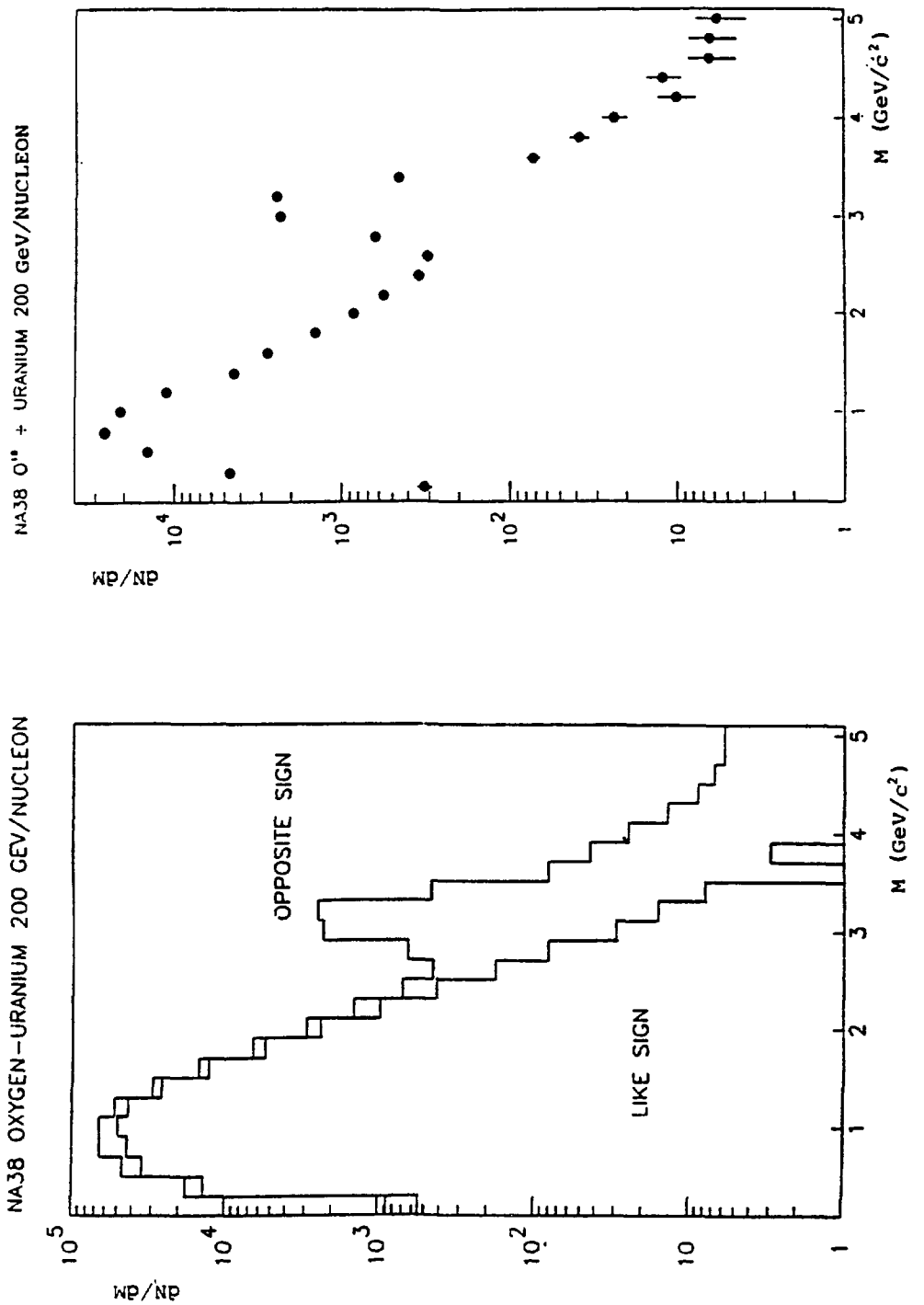

Figure 2. The mass spectra of the opposite-sign and same-sign muon pairs (a) and of the dimuon signal.

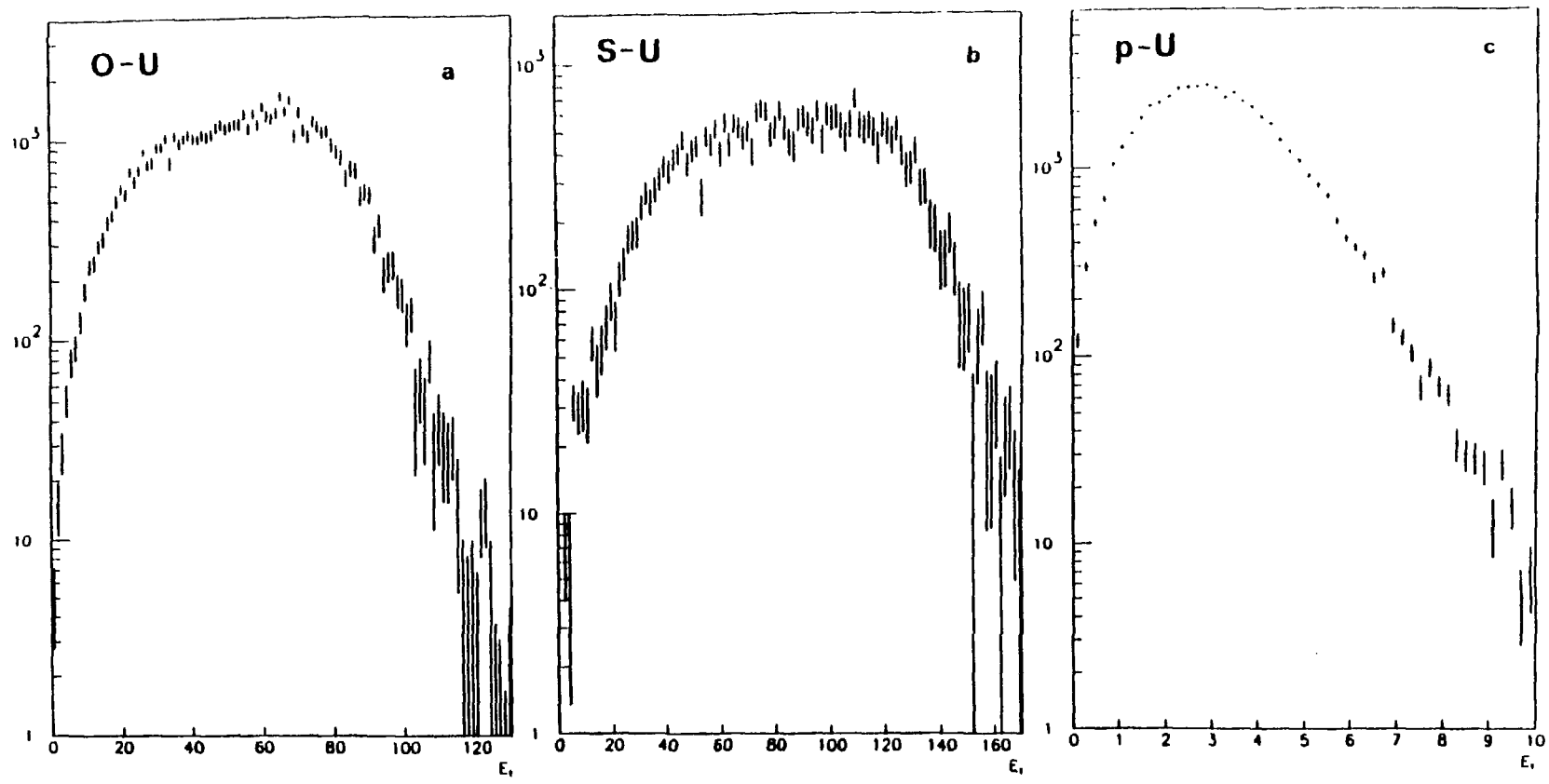

Figure 3. The E_T distributions for the a) O-U, b) S-U and c) p-U collisions.

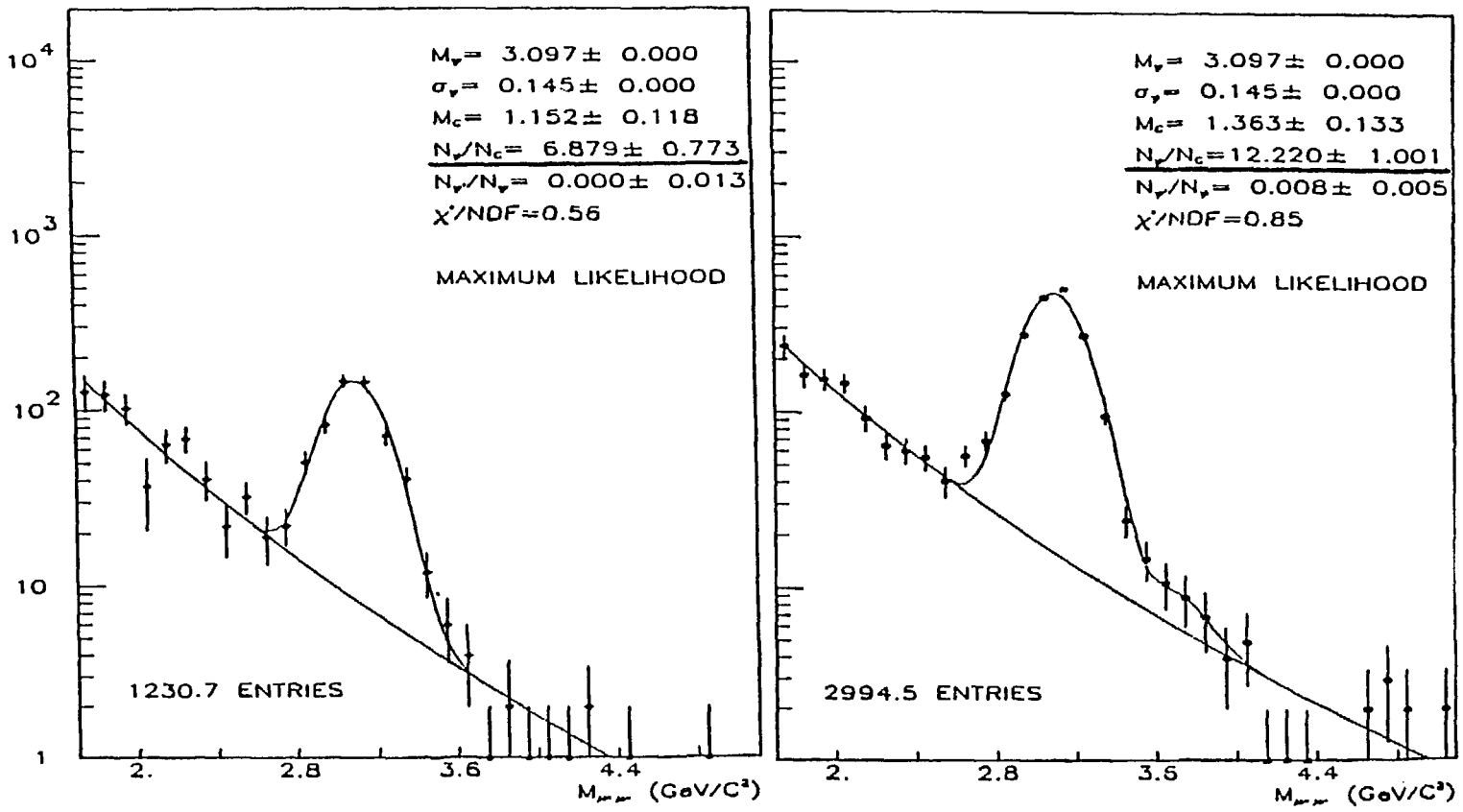

Figure 4. The fitted mass spectra for the low (a) and high (b) transverse energy bins.

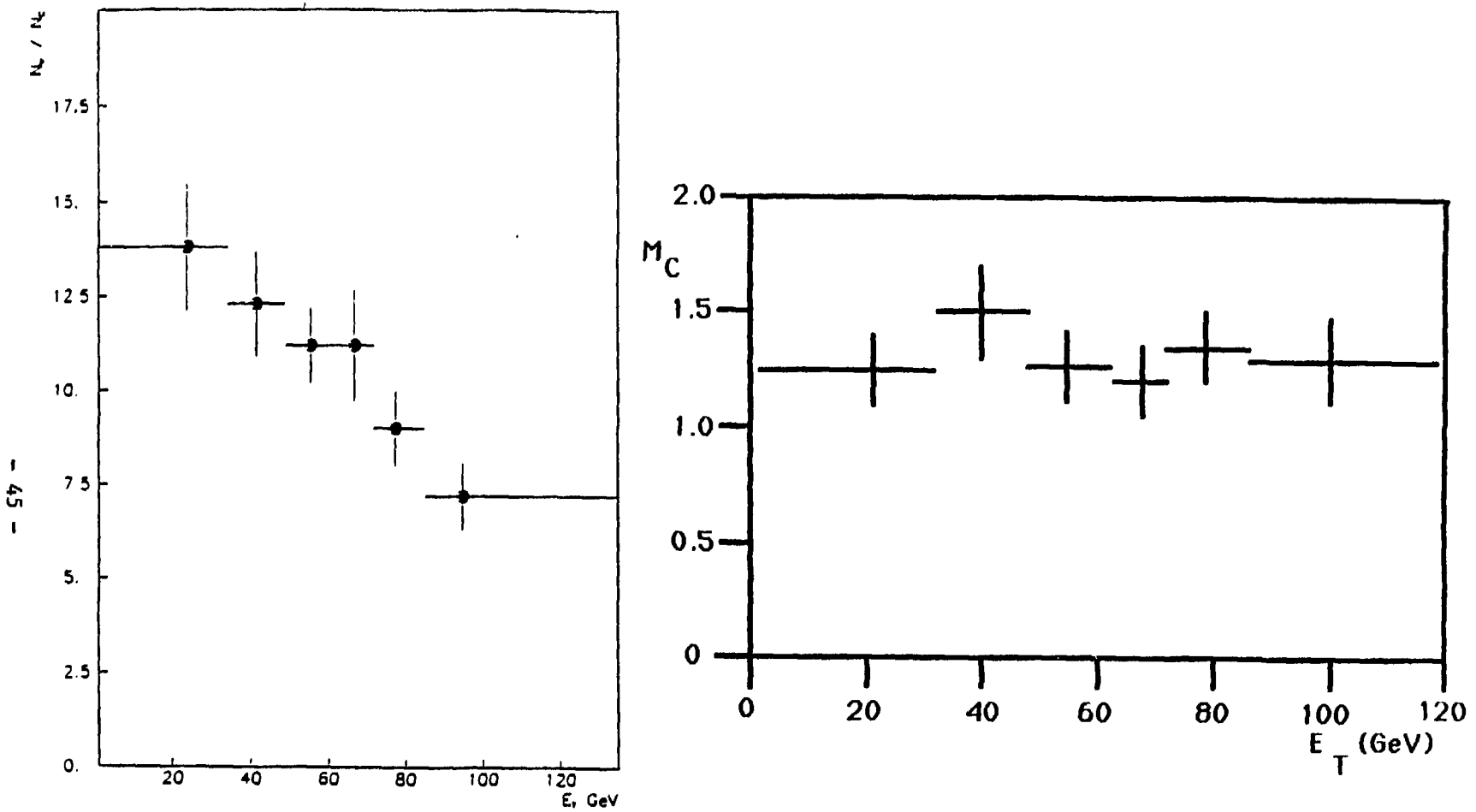

Figure 5. The E_T dependence a) of the ratio $\frac{N_{J/\Psi}}{N_c}$ and b) of the continuum parameter M_c

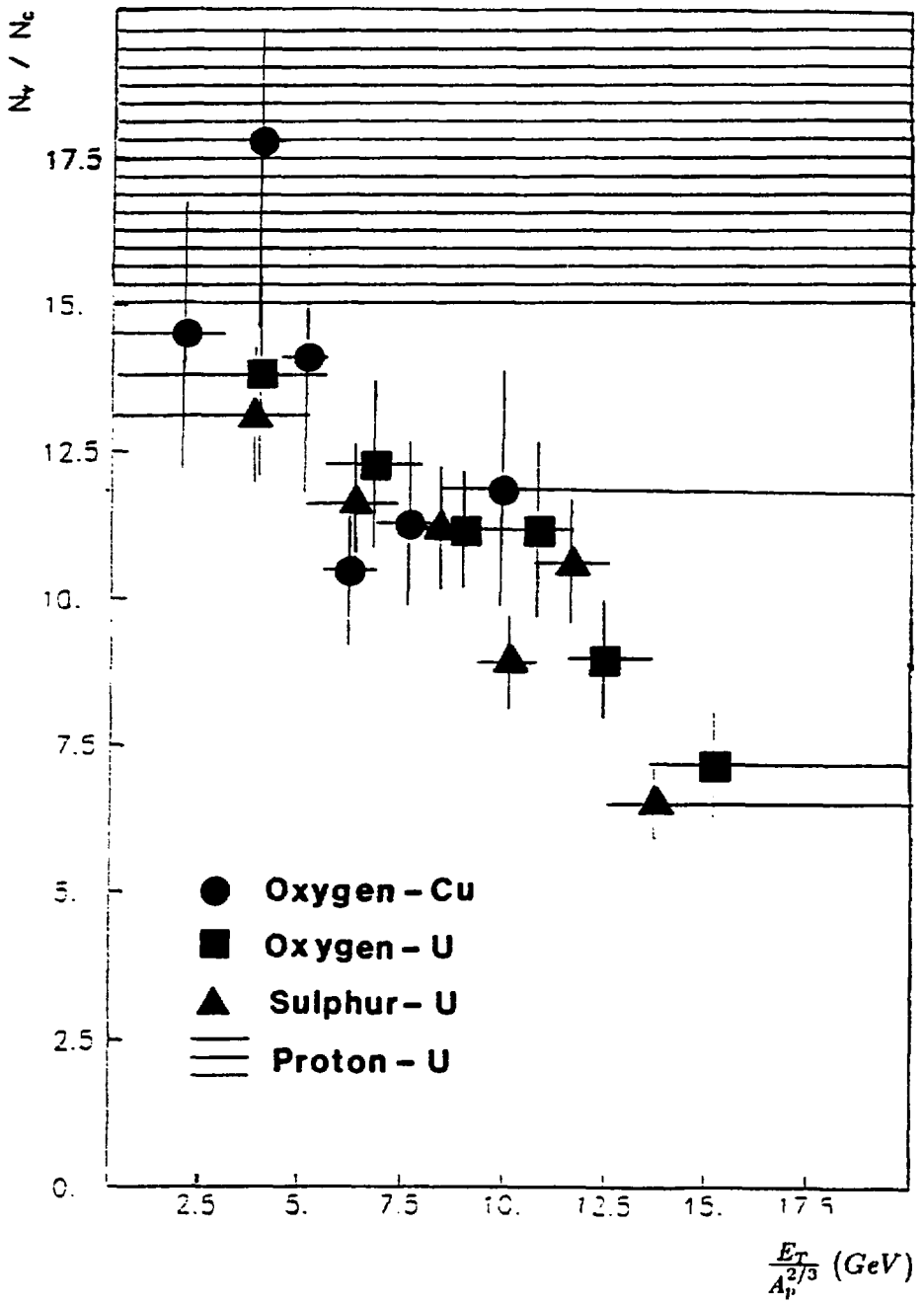

Figure 6. The ratio $\frac{N_{J/\Psi}}{N_c}$ as a function of the "energy density", estimated by $\frac{E_T}{A_p^{2/3}}$, for the several types of studied collisions.

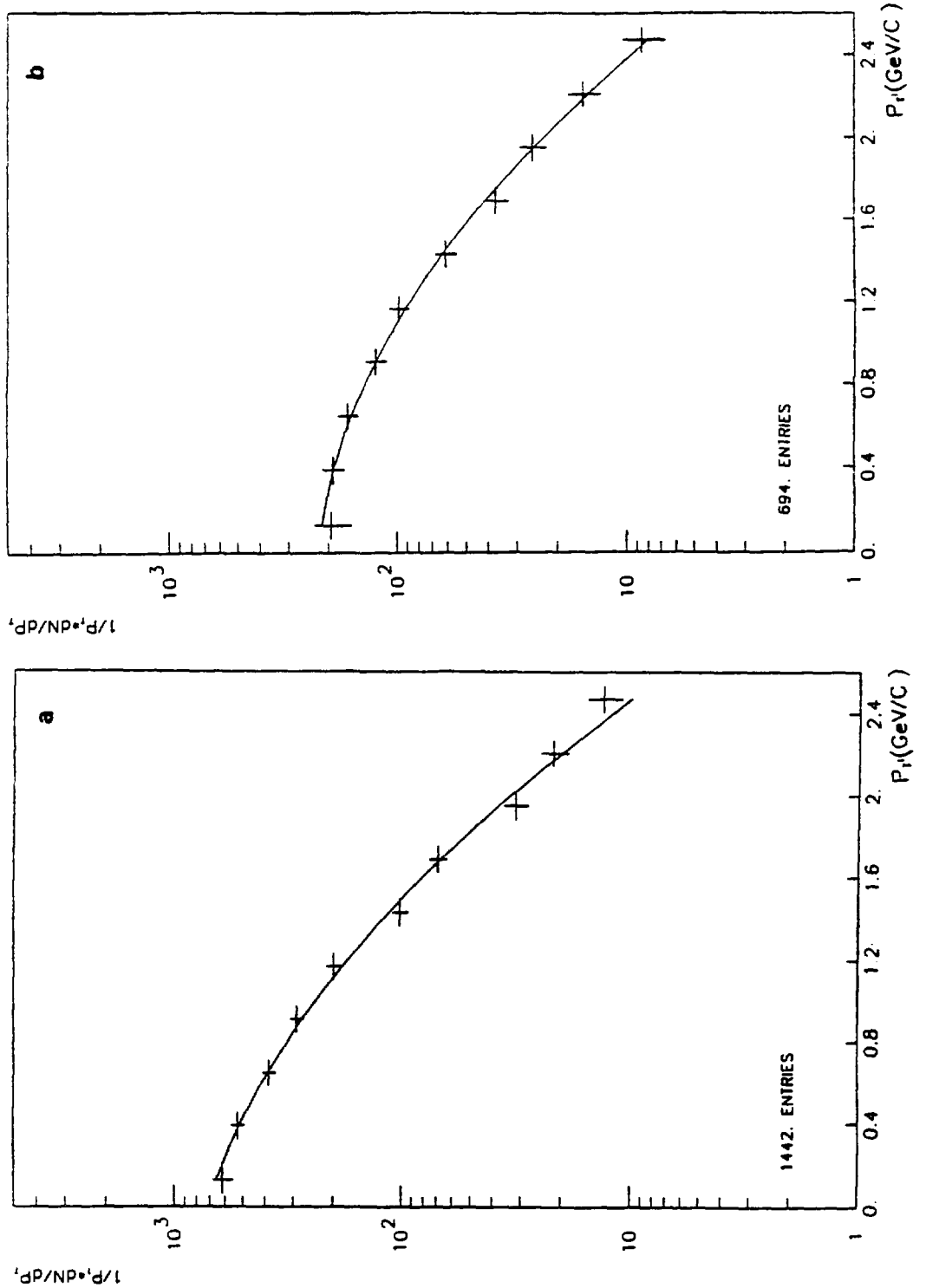

Figure 7. The p_T distributions for the a) low and b) high E_T samples of O-U events.

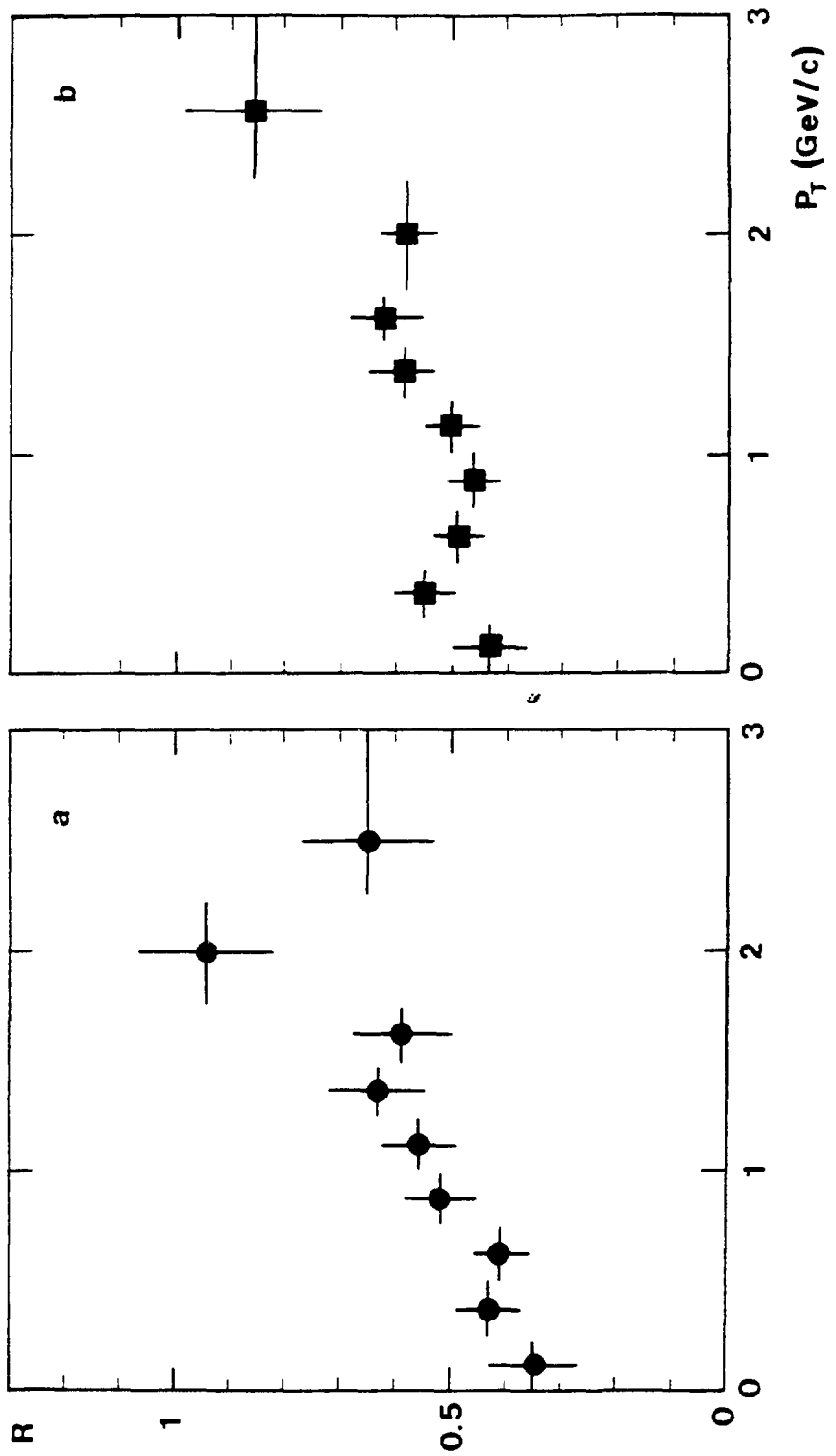

Figure 8. The J/Ψ relative suppression as a function of the J/Ψ p_T for the a) O-U and b) S-U collisions.

QCD Jets at RHIC

Frank E. Paige
Physics Department
Brookhaven National Laboratory
Upton, NY 11973
17 January 1989

QCD jets are produced at short distances and so might be a useful probe of the interior state produced in nucleon-nucleon collisions.[1] Such collisions will produce a very large amount of transverse energy, so it will not be easy to observe jets using just the calorimetric energy flow.[2] But jets contain a core of hard particles which should be observable.

A sample of QCD jets with $p_T > 20\,\text{GeV}$ in pp collisions at $\sqrt{s} = 200\,\text{GeV}$ was generated with ISAJET 6.10. The cross section from the primary partons, corresponding to the lowest order QCD process, is shown in Fig. 1. The cross section for jets defined by the UA1 cluster algorithm with $\Delta R = .5, .7$, and 1. is shown in Fig. 2. The cross section increases with ΔR but is still is significant for the smallest cluster radius. All of these cross sections should be multiplied by A^2 for A–A collisions.

The hard component of the jets was found by summing all particles with $p_T > 1$, 2, 5, and 10 GeV. The charged particle component is shown in Fig. 3 and the photon component (primarily from π^0's) is shown in Fig. 4. The sum of the two is shown in Fig. 5.

The background from soft nuclear collisions has not been evaluated, but it seems plausible that jets with $p_{T,\,\text{jet}} > 20\,\text{GeV}$ in particles with $p_T > 2\,\text{GeV}$ would be observable. The rapidity distribution for such jets is shown in Fig. 6, and the multiplicity and transverse energy flows for particles with $p_T > 2\,\text{GeV}$ are shown in Fig. 7 and Fig. 8.

References

1. J.D. Bjorken, Fermilab 82/59/59-THY (1982);
   J. Appel, Phys. Rev. D33, 717 (1986).
2. T. Ludlam, L. Madansky, and F.E. Paige, *Proceedings of the 1984 LBL Workshop on Detectors for Relatavistic Nuclear Collisions*, (L. Schroeder, ed.), LBL-18225, p. 115 (1984).

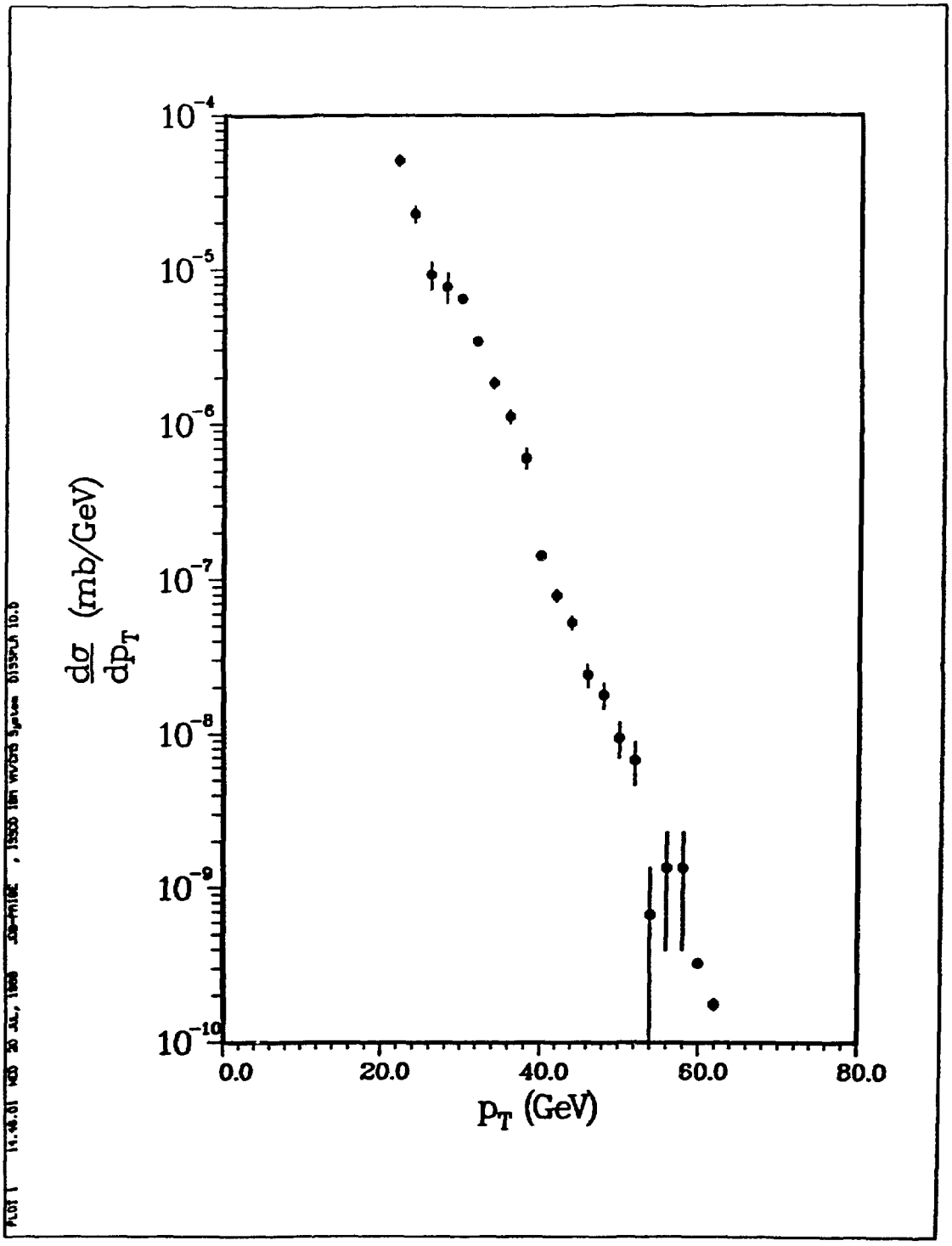

Fig. 1: Parton cross section for jets in pp collisions at $\sqrt{s} = 200\,\text{GeV}$.

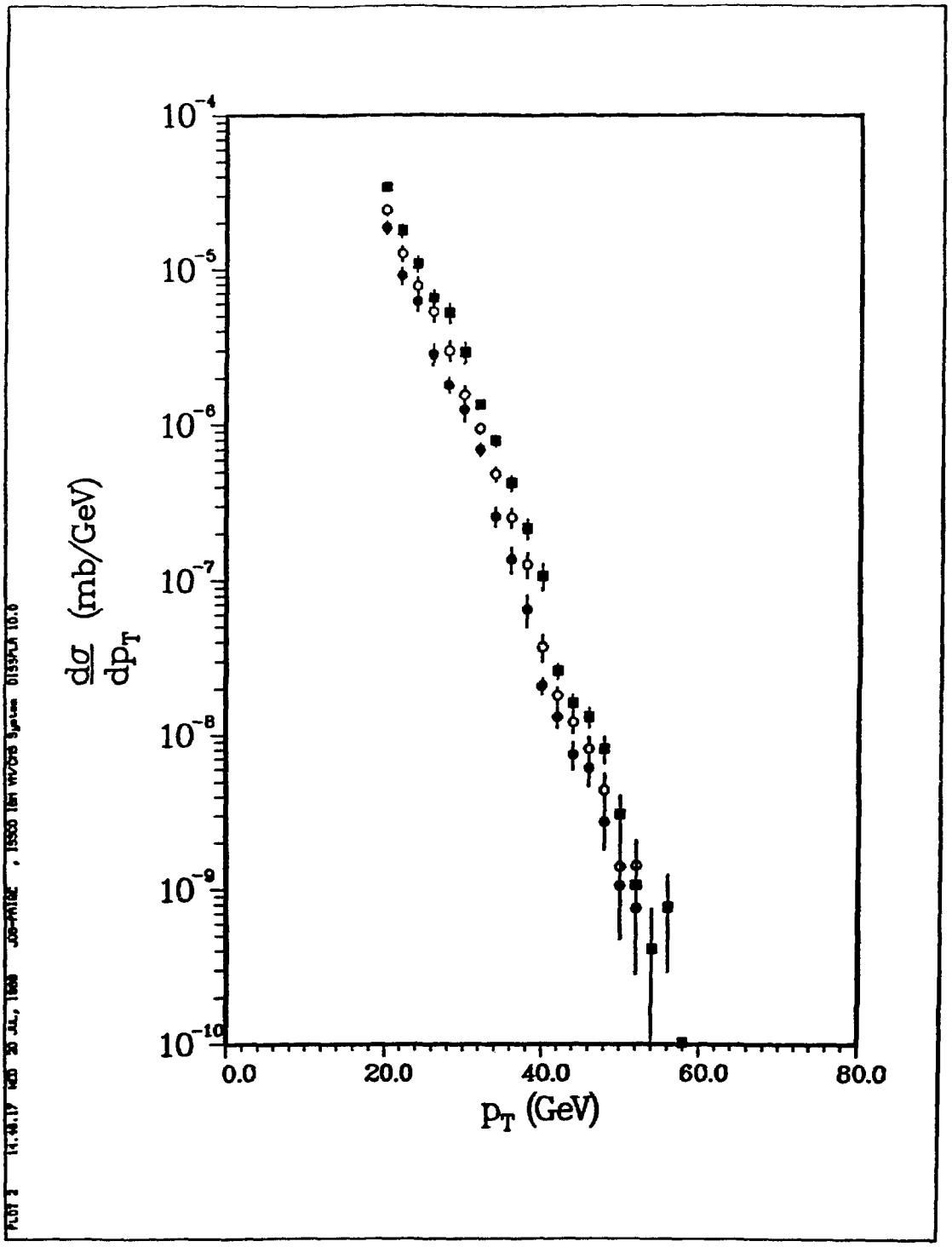

Fig. 2: *Cross sections for jets defined by the UA1 cluster algorithm with* $\Delta R = .5, .7,$ *and* 1. *in* pp *collisions at* $\sqrt{s} = 200\,\text{GeV}$.

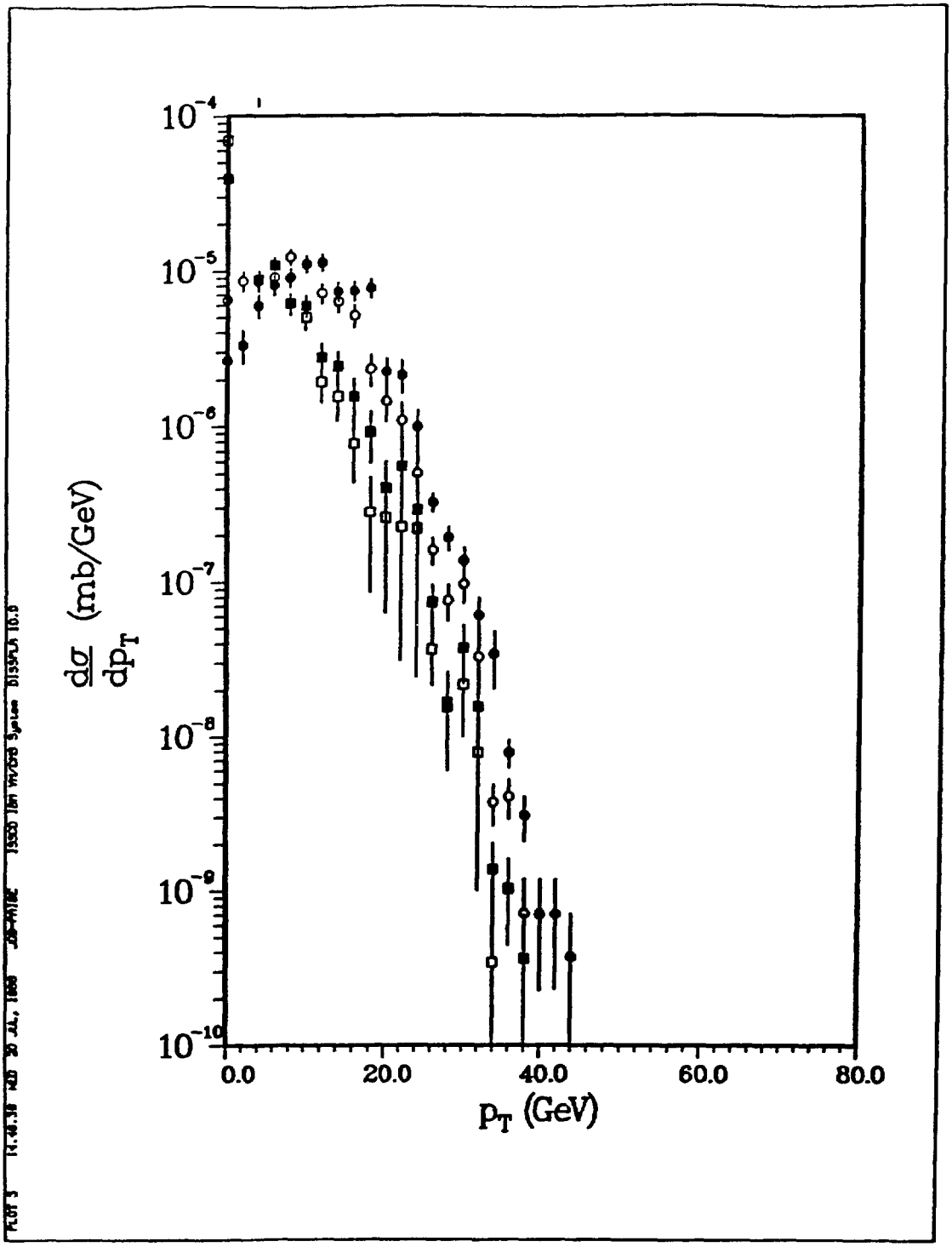

Fig. 3: Cross sections for jets defined by the UA1 cluster algorithm with $\Delta R = 1.$ for charged particles with $p_T > 1.$, 2., 5., and 10. GeV in pp collisions at $\sqrt{s} = 200$ GeV.

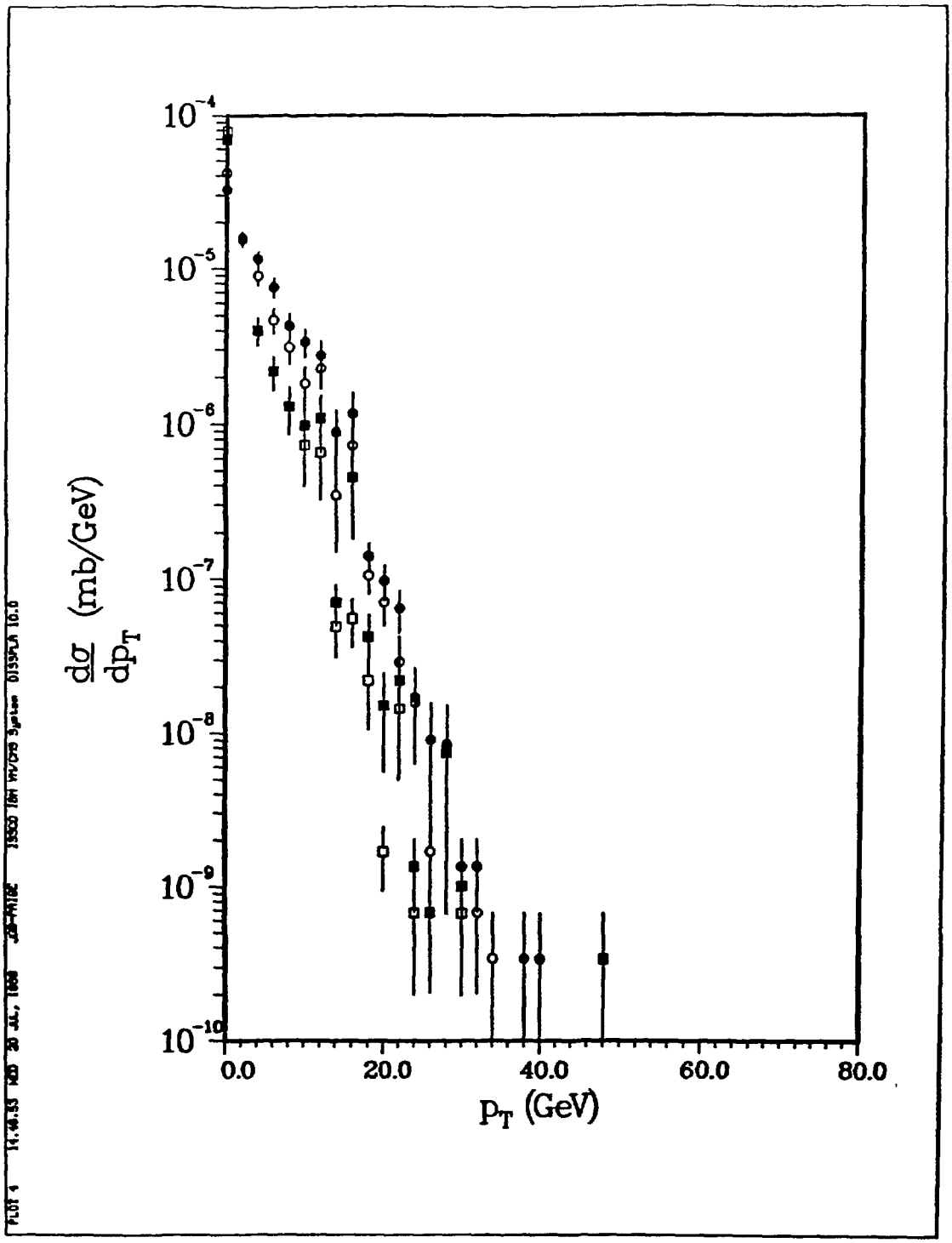

Fig. 4: Cross sections for jets defined by the UA1 cluster algorithm with $\Delta R = 1.$ for photons with $p_T > 1.$, 2., 5., and 10. GeV in pp collisions at $\sqrt{s} = 200$ GeV.

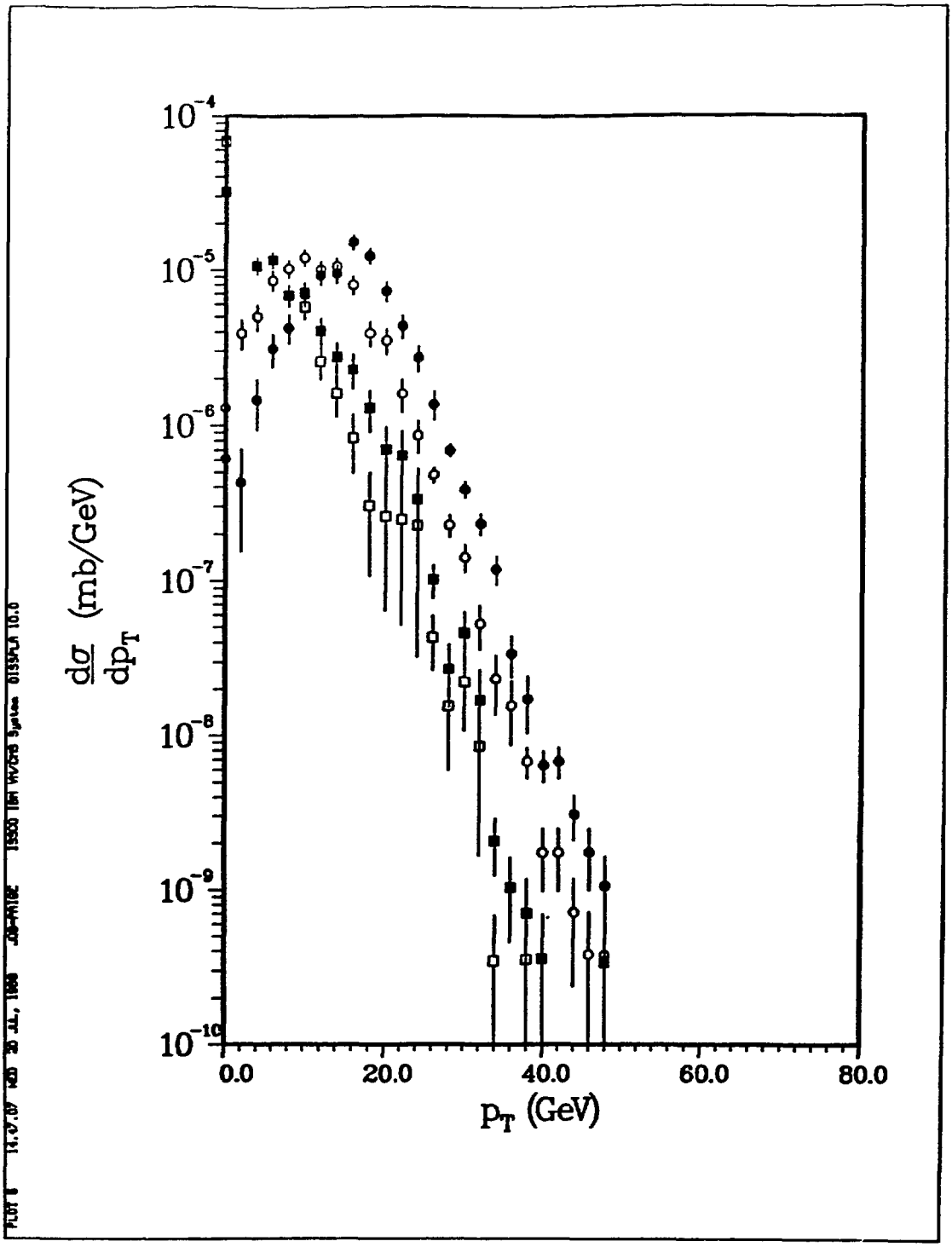

Fig. 5 Cross sections for jets defined by the UA1 cluster algorithm with $\Delta R = 1.$ for charged particles and photons with $p_T > 1., 2., 5.,$ and 10. GeV in pp collisions at $\sqrt{s} = 200$ GeV.

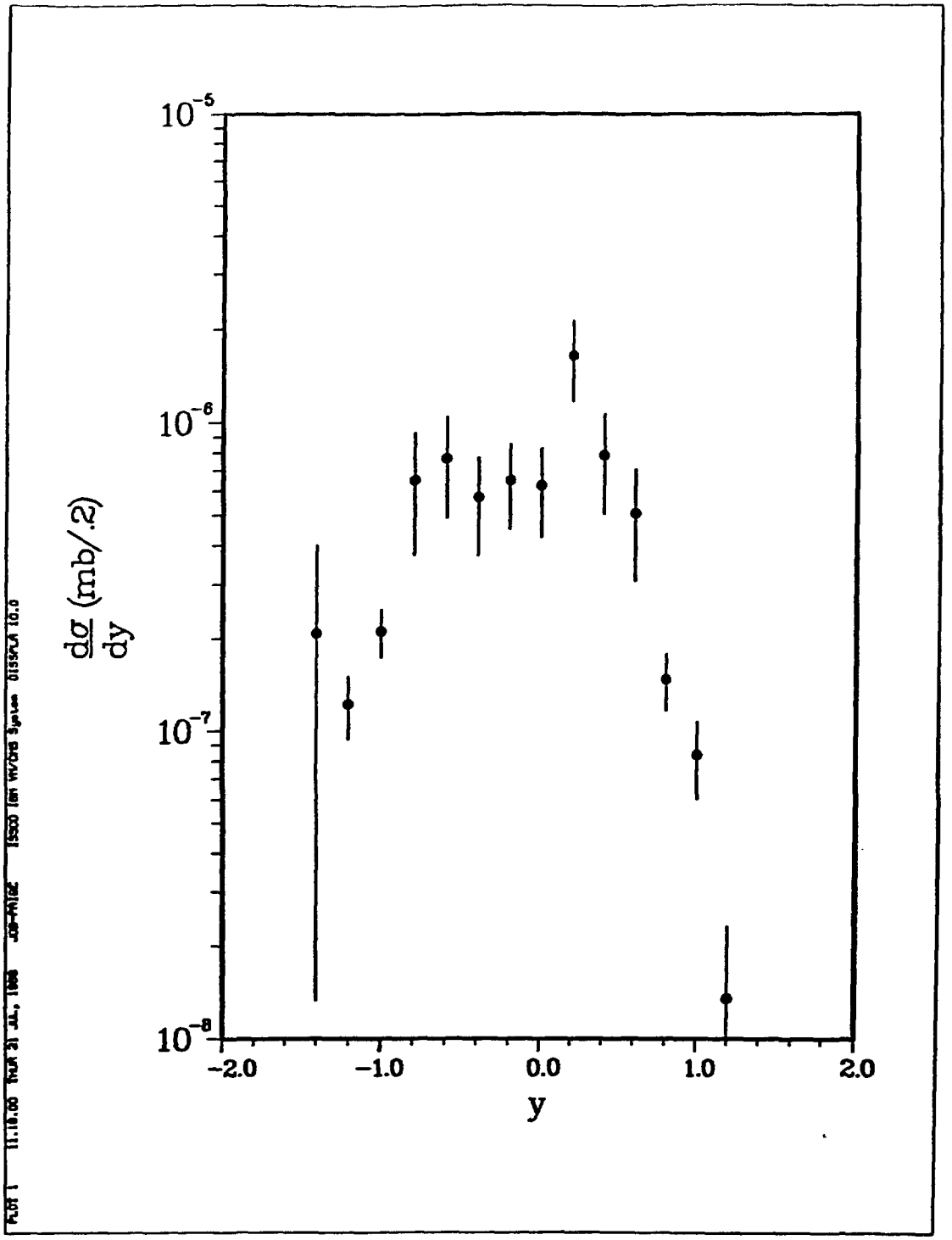

Fig. 6: Rapidity distribution for jets with $p_{T,\,\mathrm{jet}} > 20\,\mathrm{GeV}$ in particles with $p_T > 2\,\mathrm{GeV}$.

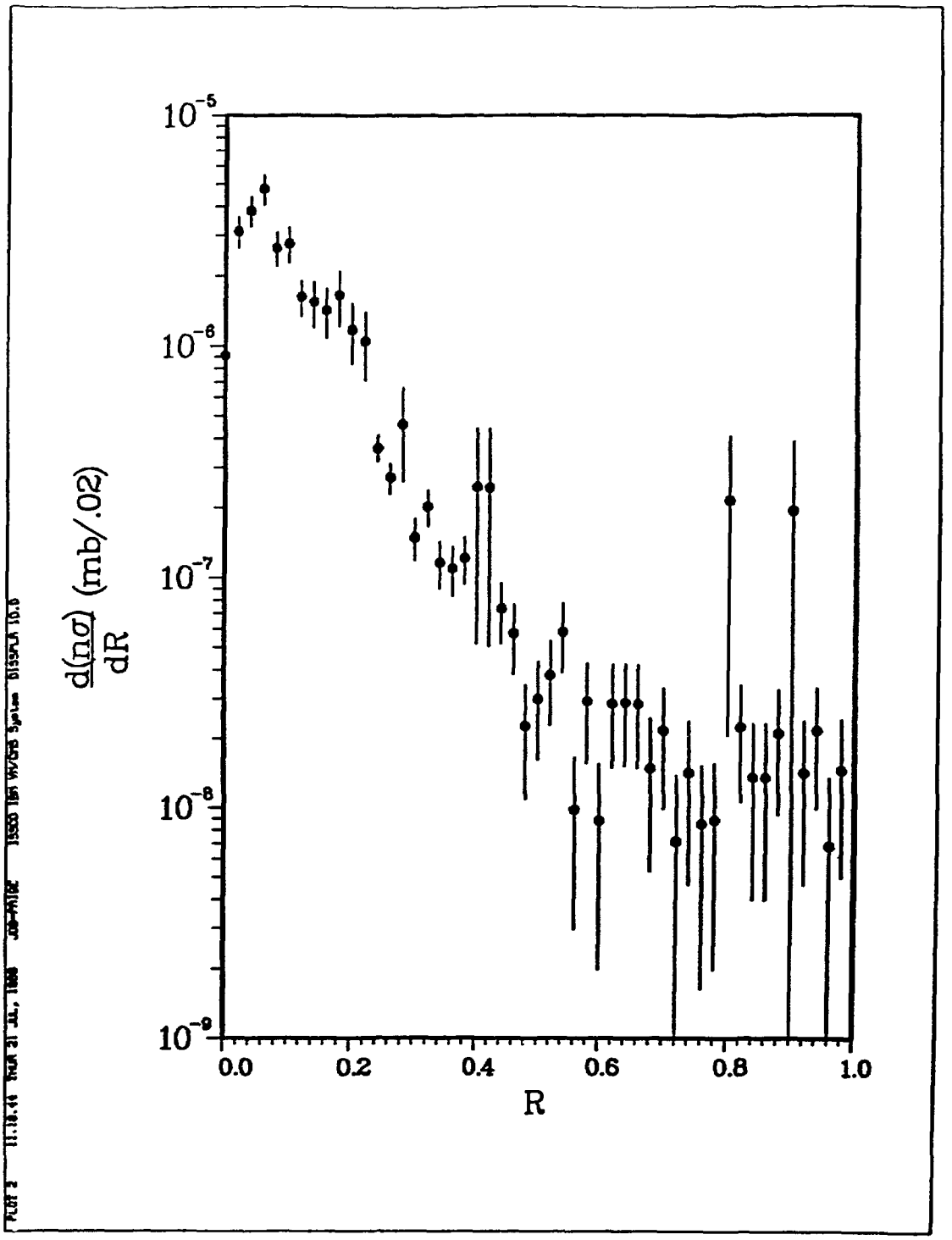

Fig. 7: Multiplicity flow for jets with $p_{T,\,\mathrm{jet}} > 20\,\mathrm{GeV}$ in particles with $p_T > 2\,\mathrm{GeV}$.

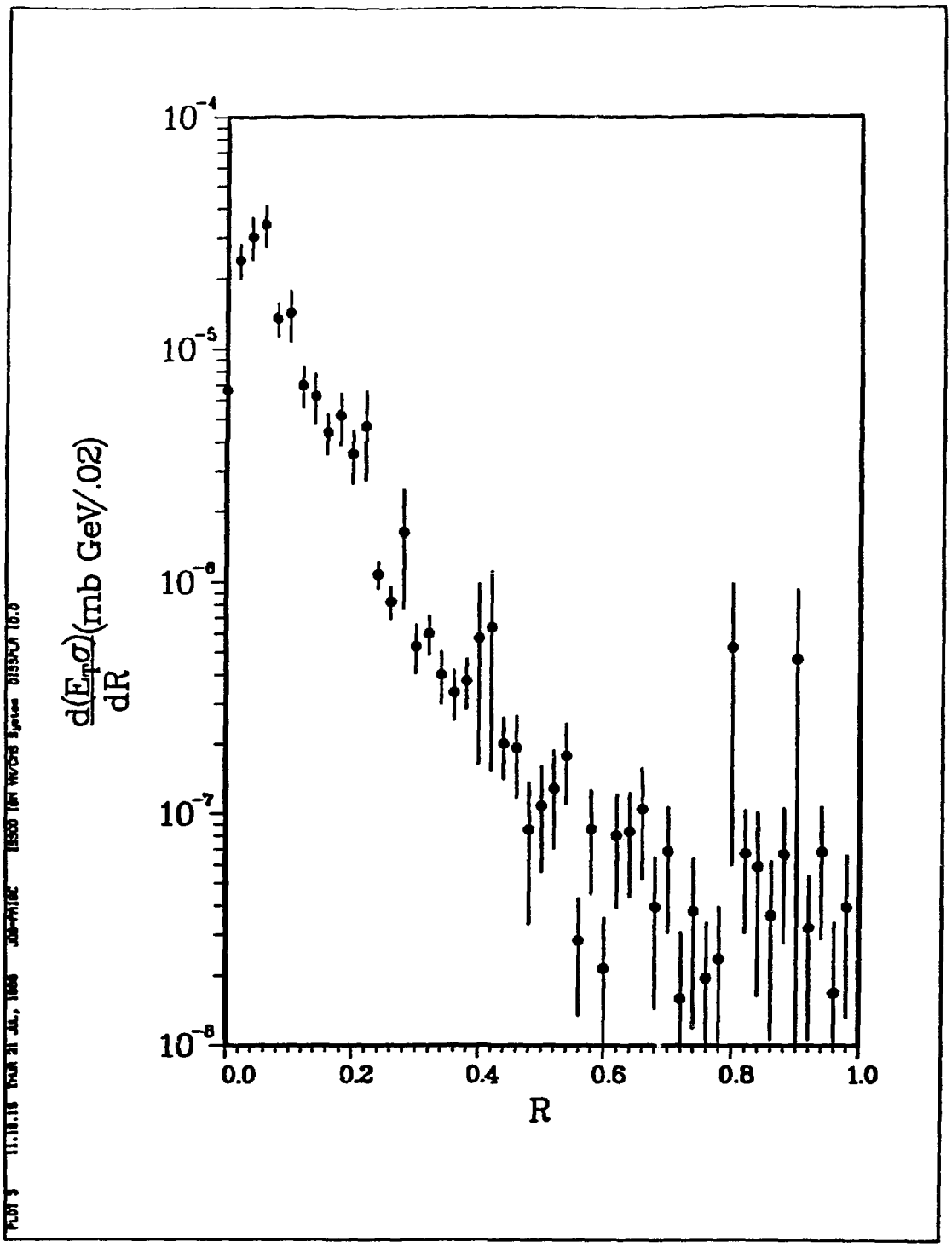

Fig. 8 Transverse energy flow for jets with $p_{T,jet} > 20$ GeV in particles with $p_T > 2$ GeV.

Tracking and Particle Identification Related Contributions

Tracking and Particle Identification

P. Braun-Munzinger, E. O'Brian, J. Carroll, C. Chasman, J. Engelage, A. Etkin, C. Findeisen, K. Foley, S. Y. Fung, S. V. Greene, H. Gutbrod, T. J. Hallman, H. Hamagaki, T. Humanic, P. Jacobs, R. Johnson, B. Kohlmeyer, M. Kramer, S. Lindenbaum, R. S. Longacre, B. Love, L. Madansky, Y. Miake, T. W. Morris, S. Nagamiya, T. Nagae, H. G. Ritter, A. Saulys, V. Steiner, T. Sugitate, J. W. Sunier, J. Thomas, K. van Dijk

Starting from the results of the last RHIC Workshop, details on detector design, in particular, the R&D issues of tracking and particle identification, were discussed in this group. The group was split into five sub-groups; two for tracking and three for particle identification. Subjects and physicists in charge of these sub-groups were as follows:

1. TPC-based 4π tracking ---- K. Foley
2. Alternatives of TPC for limited solid angles ---- T. Humanic
3. Ring-image Cerenkov counter ---- J. Carroll
4. Transition radiation detector ---- K. van Dijk
5. Time-of-flight array ---- Y. Miake

The Workshop started with several talks on the related subjects on Tuesday.

Si Vertex Counter	R. Rehak
Straw Chamber	R. Sidwell
Pad Chamber	R. Debbe
Projective Chamber	B. Knapp
TPC	K. Foley
Drift Chamber Readout	R. Vanberg
TOF	Y. Miake
CRID	R. Johnson
RICH	S. Dhawan
TRD	K. van Dijk

The individual sub-groups then met for discussion on Wednesday and Thursday. The reports from five sub-groups, which form the heart of this report, are attached on subsequent pages.

We focused on the physics in the mid-rapidity region. Constraints for the detector design are summarized here:

1. Multiplicity: In the mid-rapidity region we start with the well-known multiplicity density of $dM_{ch}/dy = 2000$ and $dM_{ch}/d\Omega = 300$. This means that at 1 meter from the interaction point we expect to have one particle per 6 cm x 6 cm pixel. For the tracking purpose we set a criterion that the ratio of double-hit to single-hit probability per pixel should be less than 1 %. That

is, the size of one pixel should be less than 6 mm x 6 mm, corresponding to 30K pixels for a 1-sr detector. On the other hand, for the particle-identification purpose we set a criterion that this ratio should be less than 10 %, corresponding to 3K pixels for a 1-sr detector. Note, however, that in this case the double-hit probability itself is still kept to be less than 1 %.

2. Luminosity & Counting Rate: At RHIC we expect $L = 5 \times 10^{26}$ for ^{197}Au beams. This implies a counting rate of 5×10^3/s. For lighter ions the counting rate will go up to 10^5/s. The design criterion for the counting rate was set to 10^5/s.

3. Momentum Region and Particle Identification: A majority of the particles are emitted in the momentum region $p < 1.5$ GeV/c. In the region of $p > 1.5$ GeV/c the particle density, $dN_{ch}/d\Omega$, is much smaller than 1. Multi-particle identification is therefore especially important in the region below 1.5 GeV/c. In this region the TOF method would be ideal, although multi-sampling measurements of dE/dx can complement it up to 0.8 GeV/c. For the low-multiplicity region both RICH and TRD were considered.

4. Momentum Resolution: The momentum resolution must be on the order of (or less than) 1 % for inclusive particle detection. For correlation work such as Hanbury-Brown/Twiss (HBT) correlations a pair resolution of (5 MeV/c)/(1000 MeV/c) = 0.5 % is required. Angular resolutions of $\Delta\theta/\theta = \Delta\phi/\phi =$ 0.5 % are also required for HBT correlation studies.

5. Other Constraints: For example: the lifetime of the detector is one concern; the stability of detectors is another concern. Magnet design is an important issue. Rescatterings of particles by the surrounding materials, such as by the calorimeter, have to be considered carefully. Tracking algorithms, in particular a V-particle trigger, have to be considered as well. Radiation length of the entire system is another item to worry about. Most of these have not been discussed during the present Workshop, but will have to be considered in the future.

TPC Based 4π Tracking

K. Foley, A. Etkin, S. Fung, M. Gutbrod, M. Kramer,
S. Lindenbaum, R. Longacre, W. Love, T. Morris, A. Saulys

Because of its 3D point readout, the Time Projection Chamber (TPC) is an ideal detector for the high multiplicity events produced in heavy ion collisions. The basic principle is as follows: Electrons from ionization produced by charged particles in the gas volume are drifted along a uniform electric field to an endcap where the (x,z) position is measured. The y is determined by measuring the time delay between the trigger and the arrival of the electrons at the endcap. Usually a magnetic field is applied parallel to the electric field in order to measure momentum, but TPC's can be designed to work in a field-free region, and designs have been considered where the magnetic field is perpendicular to the electric field. One should note that readouts on a plane give information throughout the volume, leading to a low cost per pixel. The choice of detector at the endcap is determined by the Physics goals, such as the need for particle identification via dE/dx. This greatly influences the cost and complexity of the device, so careful optimization is in order; for example, in the TPC for E-810 no attempt is made to measure dE/dx, and a high gain, low diffusion, gas is used; this gives good two-track resolution while minimizing the cost of the readout electronics.

One possible drawback in the use of TPC's at RHIC is the relatively long drift time, maybe 20 μsec for a 1m drift. However, for the reaction of most interest, Au/Au scattering, the design luminosity is $5 \cdot 10^{26}$. Assuming a total cross section of 10barns, the interaction rate is $5 \cdot 10^{3}$/second or 0.1 per 20 μsec. Since very simple trigger logic can be used to detect and so reject overlapping events the only effect is a 10% loss of data rate. Another possible difficulty is track distortion due to positive ion buildup in the drift region. The major effect is due to feedback of positive ions from the amplification region at the endcap. In a typical

case a gain of $>10^4$ is required. This potential problem can be solved by well designed gating. This could work as follows: a gating grid is normally set to collect all electrons before they reach the endcap. When a trigger is received indicating an interesting event the gate is opened to allow the electrons to enter the amplification region. After a time corresponding to the maximum electron drift the gate is closed. Since the positive ions drift much more slowly than the electrons (typically 10^{-3} times the speed) the gating grid can easily be positioned to capture the positive ions formed in the amplification region before they reach the active volume. With good gating the primary ionization then limits the interaction rate that can be tolerated. Study of this process is under way, with first results indicating that the standard RHIC luminosity can be handled. Detailed estimates of charge buildup will tell us the maximum luminosity "upgrade" that makes sense for a TPC.

Some R+D needs

1. GAS PROPERTIES

The physics should determine the chamber characteristics, which then suggest desireable properties for the TPC gas. For example, most TPC's being designed and built for e^+e^- colliders need good dE/dx and good spatial resolution in the bend plane. The choice of gas is usually Argon with ~10% methane. This gas has a very long attenuation length for drifting electrons and has a high drift velocity at low fields indicating a relatively long time between collisions. This leads to large diffusion constants, but also permits large values of ωt in a magnetic field. Since tranverse diffusion is suppressed by a factor $1/(1+(\omega t)^2)$ good precision is still possible in the bend plane. Unfortunately, the longitudinal diffusion is not suppressed, so the two-track resolution is typically ~ 2 cm for a 1 meter drift, several times that achievable with a low diffusion gas; clearly that

is not a good compromise for RHIC events. We note that the original TPC, PEP4, had lower diffusion with this gas since it was operated at high pressure. Clearly, it would be very desireable to find a gas with long attenuation length that has lower longitudinal diffusion. There are other relevent parameters to be considered including drift speed, linearity, and chamber lifetime.

A typical "toolkit" would include:

Pulsed UV lasers

Alpha, beta, x-ray sources

e, π, K, P, + nuclear beams

Pulsed ionization sources

Good gas mixing, measuring, purifying

etc

The startup cost is approximately $100K

2. READOUT ELECTRONICS

A large TPC for RHIC will need about $5 \cdot 10^5$ readout channels, most of them equipped for analog readout. This is to be compared to the 50,000 readout channels in one of today's large TPC's, ALEPH. When taking such a large step one cannot just copy the electronics, both from the point of cost and "space". For example the cost of the ALEPH TPC readout electronics was listed in the proposal as 9.2MSwFr.; 10 times that would be prohibitive. Clearly the solution is in the direction of custom monolithic IC's. At the 1987 RHIC workshop the basic design of a readout chip set was achieved.[1] It was based on an analog memory cell developed at LBL. Subsequently a segmented system was laid out to confirm the capability of such system.

The circuit was based on a low noise, low power amplifier-shaper chip and a segmented analog memory chip, each having 8 channels per IC. The amplifier design

is straight forward and should not require high priority for prototyping. Design changes to the LBL analog memory were made to implement the segmented memory function. This is important to the desparsification or compaction of the data on the fly consideration that is clearly necessary in a system of $5 \cdot 10^5$ channels. It is also important to reduction of memory size to minimize power and silicon cost. This design reached the point that prototype chips could have been produced. Subsequently the process used in this design has been replaced by a more advanced process so a redesign is required. In order to verify the efficacy of this concept it is important to proceed with prototype production test and evaluation. Most likely several iterations of the chip will be required for debugging and optimization.

Costing

A prototype chip run through MOSIS costs about $10,000. This however, is the tip of the iceberg for a major ASIC development such as this. A conservative estimate of the manpower and equipment needed to successfully develop such a chip is 5-10 man-years and several hundred thousand dollars for computer hardware and software systems, test facilities, interfaces, etc. At the end of the tunnel, however, is the prospect of very low production costs, estimated at less than $2.00 per channel for the chip component of the readout electronics.

3. RADIATION BACKGROUNDS

For Au/Au collisions the low luminosity suggests that radiation levels will not be excessive--for example, relative to the SSC, the luminosity is lower by a factor of about $5 \cdot 10^{-6}$ while the higher cross section and multiplicity lead to an increase in particle flux of about 10^4 per unit of luminosity. However, a better

estimate should be made to determine allowed locations for radiation "soft" materials like plastic scintillators, lead glass etc.

4. SOFTWARE

Many projects fall into this category. The most immediate need is for good simulation packages for the design of apparatus. Some work has already begun with the HIJET event generating program and the GEANT simulation package, but many features of both "physics" and apparatus still need to be incorporated.
A good, user friendly, package for wire chamber design would be a very useful tool; this should include a 3D electrostatics package that can easily be configured to simulate typical wire chambers.

5. CALIBRATION AND MONITORING

Extensive work is needed in this area. Much useful information is available from the efforts at the major detectors at the various high energy colliders. Most of the questions here will be quite detector-specific.

6. MECHANICAL DESIGN

As usual, we often demand infinitely strong support structures of zero thickness! Good design packages must be made available from the beginning. This includes modern workstations with good software.

REFERENCES

1. Lindenbaum, S.J. An Approximately 4π Tracking Magnetic Spectrometer for RHIC. Proc. of the Second Workshop on Experiments and Detectors for a Relativistic Heavy Ion Collider (RHIC), Lawrence Berkeley Laboratory, Berkeley, California, May 25-29, 1987, Editors, Hans Georg Ritter and Asher Shor, pp. 146-165 (Lawrence Berkeley Laboratory, 1988).

Alternatives to TPC: Small Acceptance Spectrometer

Participants: T. Humanic(spokesman), P. Braun-Munzinger, E. O'Brien
C. Findeisen, S. Greene, T. Nagae, S. Nagamiya, and J. Thomas

3-1 Introduction

Following up ideas from previous RHIC workshops, we propose an updated concept for a small acceptance hadron spectrometer which can be employed, for example, in conjunction with the 4-pi Calorimeter system. Such a device has the advantages of being relatively inexpensive to build and able to tolerate high event rates while still providing particle identification and the ability to make high precision particle correlation and pt-distribution measurements.

We consider a design in which the spectrometer is located at Ycm=0 in the 4-pi Calorimeter system and subtends an angle in theta and phi of 25 degrees for both, giving a solid angle of about 200 msr, and a rapidity bite of 0.44 units. The charged particle multiplicity in this solid angle for central collisions is about 60. Figure 3-1 shows a schematic diagram of this concept. The philosophy is taken that each tracking plane is non-projective (unique x-y position information) and has sufficient position accuracy so that track reconstruction can be carried out in this relatively high particle density environment without ambiguities and sufficient momentum resolution is obtained. Close to the intersection region (10-20 cm) there are two x-y planes of Si drift-chambers (position accuracy 5-10 microns, 2-track resolution 200 microns, 500 readout channels each) and farther away (1-2 m) pad chambers (position accuracy 1-2 mm, 2-track resolution 2-3 mm, 6000 pads each) are used, backed up by a high-granularity (6000 channels) TOF wall. This gives a modest 19,000 readout channels. It is anticipated that a momentum resolution of 1%, high event rate capabilities, and particle identification based on TOF and dE/dx (in the Si drift-chambers) can be obtained with this kind of configuration.

3-2 Description of R&D required

In order to achieve these performance goals, some R&D effort will be necessary for the Si drift and pad chambers and the TOF wall. Since the TOF wall has been studied by another sub-group, only the R&D required for the Si drift and pad chambers will be described below.

- Si drift-chambers---These devices have existed for several years at the development stage and are only now being considered for use in actual experiments such as UA6 at CERN. Thus, it is necessary to obtain some of these chambers (either from BNL where they were invented or from the MBB company in Germany who are manufacturing them for UA6) and study their characteristics, eventually under the high multiplicity conditions that will be found in the RHIC environment. Some areas of study will be 1) 2-track resolution, 2) optimal readout electronics to use, 3) position information uniformity over the chamber area, and 4) dE/dx capabilities for particle identification. These tests would be carried out using sources and test beams

from the AGS. The cost of this test program would probably be under $50K + manpower. Besides the RHIC application, these detectors would be useful for E814 at BNL and NA34 at CERN.

- Pad chambers---R&D efforts are already underway to study pad chambers for use in existing experiments at BNL (E814) and CERN (NA35). The problems that must be addressed in the present application are 1) to optimize pad geometry (e.g. chevron or rectangular shape) and pad layout to satisfy 2-track resolution requirements for particle correlations and to get sufficient momentum resolution, and 2) to deal with the resulting high readout density of the electronics. Test beam studies at the AGS with high particle multiplicity conditions will also be necessary for this development effort.

3-3 Vertex detector for Muon Spectrometer

In addition to their use in the small acceptance hadron spectrometer described above, Si drift-chambers could be employed in a vertex detector for the Muon Spectrometer. Using mosaics of Si drift-chambers to construct two concentric barrels about the beam with 5 cm and 10 cm radii, respectively, and barrel length 60 cm one could uniquely reconstruct interaction vertices along the length of the interaction region (sigma=25 cm). This would require about 150 chambers at 250 readouts per chamber, giving 40,000 readout channels in total. The radiation dosage for the inner barrel is calculated to be 10**4 Rad/year, which is considered to be acceptable for Si-detectors.

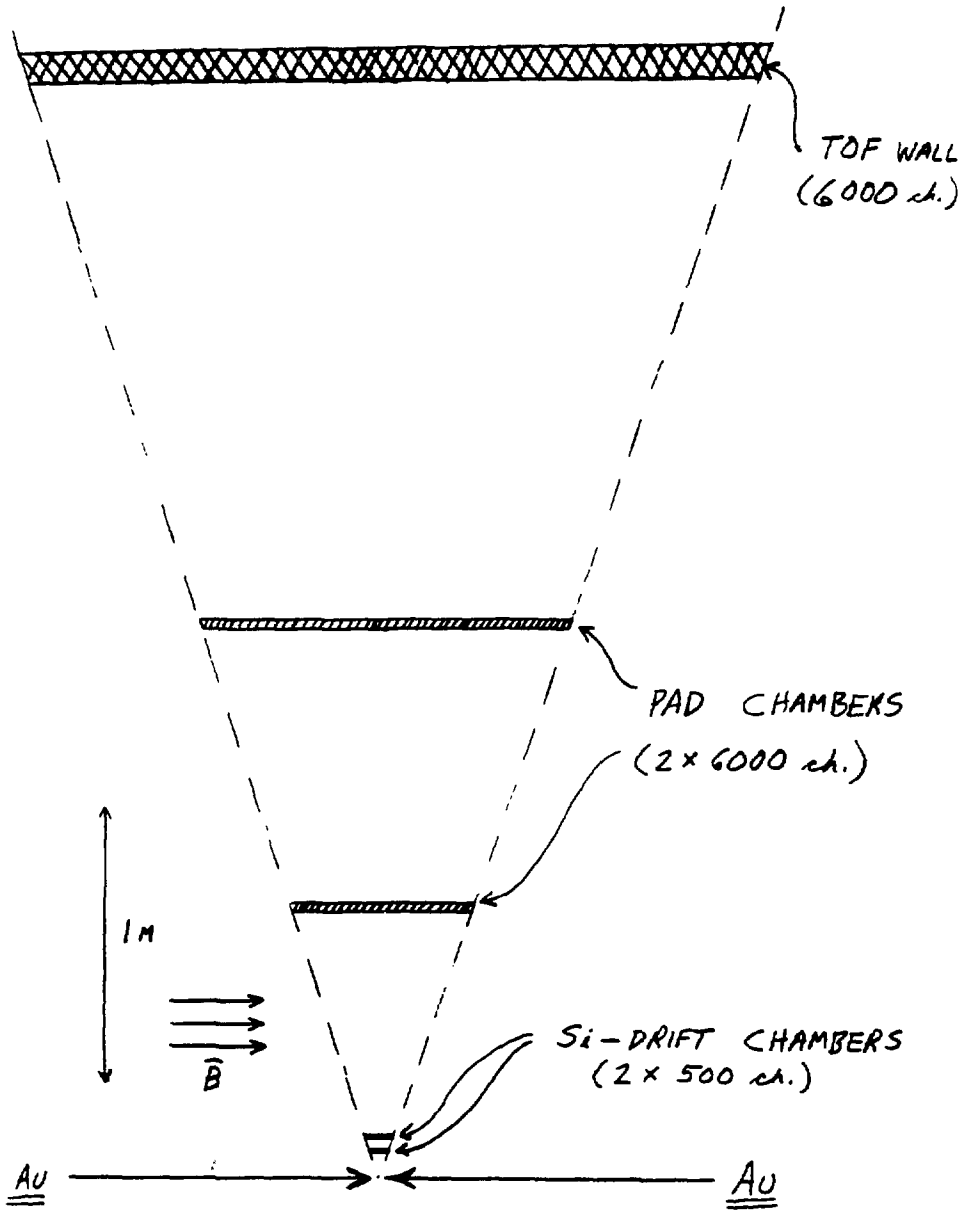

Figure 3-1 Conceptual design of small acceptance spectrometer

PARTICLE IDENTIFICATION WITH RING-IMAGING CHERENKOV (RICH) DETECTORS

J. Carroll, T. Hallman, H. Hamagaki, R. Johnson, L. Madansky, H.G. Ritter, V. Steiner, T. Sugitate; participants (H. Gutbrod, S. Nagamiya; consumers)

The working group considered the use of RICH detectors at RHIC both as general particle ID devices and as specific detectors for electrons. The present state of the art was reviewed with particular emphasis on areas where further development is needed.

In a RICH, Cherenkov light emitted in the characteristic cone by a charged particle traversing an appropriate medium is transformed by a focussing device (eg - a mirror) into a ring-image. See Fig 1. A suitable detector then gives the spatial location of the photons. From the ring diameter one can obtain the magnitude of the particle velocity, and the location of the ring center gives the direction cosines of the velocity vector. Since the device does not require a specially prepared, parallel beam in order to give good resolution, it finds a natural home in detector systems covering large solid angles.

Table 1 shows a comparison of some of the types of RICH detectors presently in use, or in construction.

TABLE 1

PROPERTY	E665 RICH	SLD CRID	BRESKIN RICH
Photocathode	TEA	TMAE	TMAE
Detector pressure	?	1 ATM	20-100 TORR
Drift length	SHORT	LONG	SHORT
Amplification	SINGLE STEP (low noise electronics)	SINGLE STEP (shadow shields)	MULTI-STEP (with gate)
Detector 'in beam'	NO	YES	NO
Cherenkov radiator	1 ATM. GAS	1 ATM. GAS FC-75	1 ATM. GAS
Focussing	SEG. MIRROR	SEG. MIRROR	SEG. MIRROR
Digitization	2-D (parallel process. of pad array)	3-D (multiplex- drift time, wire #, charge div.)	2-D (para. proc. pads or CCD camera)
Pattern recognition	---STARTS FROM TRACKING---		STAND ALONE

As a specific example, a RICH of the CRID type was considered as a possible particle identifier for a 2-pi detector at RHIC. We arrived at the following conclusions-

1. The particle density at central rapidity is roughly the same as is expected in a detected jet at SLC, therefore the pattern recognition techniques from the SLD CRID should work at RHIC.

2 .To get the same spatial resolution (and thus the same velocity resolution, and particle separation) as the CRID would require about 2 x

10^6 pixels for a detector at 3 meters from the beam. 2000 tracks with 20 detected hits per ring would then give 4 $\times 10^4$ hits per event, or about 2% occupancy of the pixels, which should be OK. (All pions are above threshold for FC-75 radiator.)

3. To cover the required area would mean either a drift time of about 50 microseconds or 2 $\times 10^6$ pads.

The above concept uses only a liquid radiator (FC-75, $n \sim 1.27$) and proximity focussing, and is therefore radially thin. It would be possible to reduce the number of detected rings, and therefore the effort in pattern-recognition if there were an appropriate radiator with $n \sim 1.02$ and the RICH were to be used to complement a time-of-flight system - but one would still need 2 $\times 10^6$ pixels to obtain the desired resolution.

There are a large number of both practical and fundamental areas in which advances in RICH detector technology would significantly improve the usefulness of this kind of detector; we list some of these in Table 2. From among these, we identify two that are of large importance for RHIC.

• In the area of general particle identification, we point to the 'index gap' between the liquid radiators ($n \sim 1.27$) and the gases (C5F12 $n \sim 1.0017$). The aerogels that have been developed to partially fill this gap are not suitable for RICH's because they both absorb and scatter the UV light. What is required is a 'super aerogel', $n \sim 1.02$, that is transparent for wavelengths down to 160 nm.

• For RICH's that would be used to identify only electrons, in

experiments measuring electron pairs, the most pressing requirement is the development of a fast electron trigger from the Cherenkov signal. Since the existing RICH's use only the far UV photons, the visible component of the Cherenkov radiation remains for use as a prompt trigger if an appropriate means can be found to direct it to an appropriate detector.

Table 2

Research and Development Areas for RICH Detectors

- Direct detection of ring image with image intensifier (eliminate gas detector). Needs larger, cheaper image intensifiers; improved CCD's for readout; some way of obtaining a trigger signal.
- Reduced avalanche size to improve pattern recognition.
- Reduce photon conversion length - to give higher precision and reduce detector dead-time. Can be achieved by higher operating temperatures (construction techniques/materials), or by developing new photocathode gases with higher vapor pressures.
- Reduce mirror thickness to reduce multiple scattering and photon conversion; while retaining good optical quality and high UV reflectivity.
- Extend lifetime (tolerable radiation dose) of TMAE-containing detector. (Gating final amplifier helps.)
- Understand and control avalanches not associated with rings.
- Make a 'smart' mirror that will separate visible and UV photons.
- Develop a fast, pattern recognition trigger from RICH.
- Improve pattern recognition aglorithms (with and without tracking information to start from.)
- Develop low-noise, multiplexed electronics for pad readout.
- Develop thin, UV-transparent, 0_2 impermeable windows.
- Improve CCD readout speed.

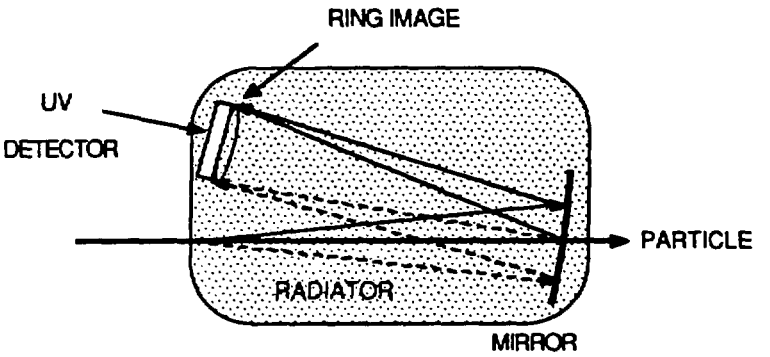

Fig 1. Schematic picture of a RICH.

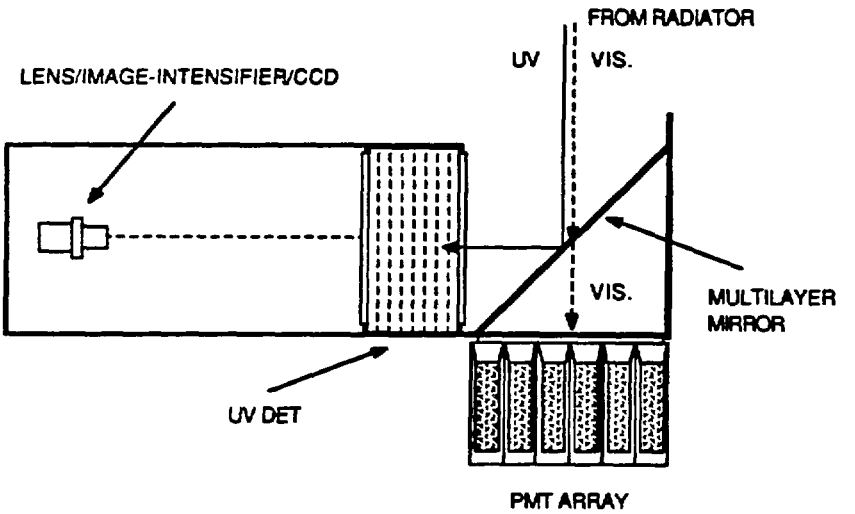

Fig 2. Spectrum splitting mirror used for fast trigger.

Transition Radiation Detectors

J.H. van Dijk, C. Chasman, H. Hamagaki, P. Jacobs

A detector is needed in electron and di-electron experiments (one of the measurements that may be important in determining the properties of the quark-gluon plasma) that can provide tracking information for the electrons in an environment in which the hadron/electron ratio is ~10**4. One device which has the potential for large pion suppression and good electron efficiency is a transition radiation detector(TRD)(1). Another device which has been proposed for this purpose is the Ring Imaging Cerenkov Detector(RICH).
Difficulties yet to be completely resolved with the RICH's include:
1)
the threshold gamma for convenient pressures is about 30 which means that 4 GeV pions will be mis-identified and that 15 MeV electrons will be counted(one would rather have a somewhat higher electron threshold)
2)
the photo-detecting counter may be placed in a large pion flux (as in the design proposed at the 1987 RHIC workshop) and register false events;
3)
The device does not provide space points but rather vectors making tracking difficult;
4)
the device tends to be long because of the small amount of Cerenkov radiation emitted per centimeter of radiator.

We propose that some effort be made to design TRD detectors specifically for the needs of the Relativistic Heavy Ion program. We believe these detectors have the advantages of being effective at large gamma, can be built to be substantially hadron blind, and can provide space points.
However, some research and development is needed to make these assertions convincing. At present TRD's are designed to work at gamma values of several thousand which is much greater than the gamma of about 500 needed for RHIC. In addition the fact that the detectors will have to be part of the trigger will have an important impact on both detector design and read_out.
The main parts of the development effort are directed then to these objectives by designing a counter with a gamma threshold

of roughly 500 an overall pion rejection factor of 10**(-4), (10**(-2) at the trigger level), and space point tracking. The pion rejection factor is defined as R = e(pion)/e(electron), at e(electron) = 90% , e(pion,electron) being the detection efficiencies for pions and electrons respectively.
As a first step we expect to set up the computer programs to simulate radiators and detectors. To this end, one of us (JHvD), visited members of four different experiments that are using or are in the process of constructing TRDs: NA34 at CERN which has a TRD working in a fixed target experiment, as well as UA2 at the collider at CERN, and H1 and ZEUS who are constructing detectors for the collider at HERA. The software obtained will facilitate the job of setting up our own simulation programs.
Next we plan to build one or more radiators, which will consist of a stack of foils. The specific material, thickness, spacing and number of foils in a stack will be determined on the basis of computer-simulation results.
We will further design and build a drift-chamber which will serve as the photon-detector. The read_out of this detector needs special attention with emphasis on a fast current sensitive low noise preamplifier that should preserve the shape of localized ionization clusters given by photon absorption.
The design of the trigger logic might be seen as a separate effort from the building of the detector itself.
Although it is hard to specify precise what the cost of the R & D effort will be, we estimate that about $50,000 will be required.
The device will need both electron and pion beams for testing. The pion beams are available at the AGS and electron beams of the higher energies can be gotten at the AGS with the lower energies available from Bates where it is also easier to do a threshold scan with electrons in the energy range from 200 to 500 MeV.

(1) For review of transition radiation detectors see:
Practical theory of the multilayered transition radiaton detector.
X. Artru, G. B. Yodh and G. Mennessier
Phys. Rev. D Vol 12,no 9(1975) p 1289-1306
and
Transition Radiation Detectors and Particle Identification
Boris Dolgoshein
Nucl. Instr. and Meth. A252 (1986) 137-144
or references given there.

Subgroup #5: Time of Flight (TOF)

Participants: Y. Miake, J. Engelage, B. Kohlmeyer, J.W. Sunier

The design goals for a RHIC TOF system were established at the 2nd RHIC Workshop[1]. An upper limit on the TOF resolution of $\sigma_{TOF} = 100\ ps$ was set, sufficient to allow $\pi - K$ separation up to 1.6 GeV/c, $K - p$ separation up to 2.8 GeV/c, and $p - d$ up to 5.7 GeV/c. The segmentation and angular resolution requirements for RHIC TOF systems are dictated by a combination of the expected charged particle multiplicities and projected HBT correlations. Incorporating a desired confusion probability of 0.5% or less, leads to a detector segmentation in the neighborhood of 6000 and an angular resolution on the order of $\Delta\theta \approx \Delta\phi \approx 1\%$.

The current working group identified two detector geometries capable of meeting the above design goals, a multifaceted or mosaic system and a bar-like configuration. For the spectrometer systems currently under consideration (radii on the order of 3m and covering a rapidity region $|\ y\ | < 1$) this translates into either a $4cm \times 4cm$ facet or a $0.5mm$ diameter bar over 3m long. Beyond resolving suitable detector geometries, the working group was charged with

1) identifying known technologies through which the desired design goals could be achieved
2) indicating problems that might exist with those technologies
3) proposing possible solutions to those problems

[1] LBL Report #24604 (1987) 129.

4) and determining those areas requiring further research or engineering.

all the while remaining mindful of probable costs. Further, great interest was expressed in developing a TOF system which either incorporated, or was compatible with, some kind of electron calorimetry.

Several possibilities were considered for the mosaic configuration, including a flashlight-like scintillator/photomultiplier tube (PMT) setup, Si(Li) wafers, and Pestov chambers. The PMT signal from the flashlight construction has the advantage/disadvantage of being a superposition of the scintillation light emitted from the scintillation material and the Cerenkov light produced in the glass window of the PMT. It is possible that the Cerenkov component can be effectively eliminated by employing thinner windowed PMTs or faster scintillation materials. Conversely, by incorporating some form of multiple sampling or multiple threshold, multi-hit TDC electronics, the Cerenkov component may be used for electron calorimetry. Clearly, this construction is too massive to allow electron calorimetry in a subsequent detector system. Research into this type of detector system is currently in progress by the BNL E802 collaboration. Silicon based TOF systems have produced subnanosecond timing resolutions and may prove to be the most cost effective solution. A UCSSL/LLNL collaboration has begun to conduct feasibility tests of a Si(Li) based TOF system at the LBL Bevalac. The disposition of a TOF system involving Pestov chambers remains in question because they only operate in a pressure containment vessel.

Scintillating fibers or ribbon connected to multi-anode PMTs are the obvious solution for a bar-like TOF system. Several experimenters are presently using scintillating fibers; however, no one has been able to achieve a timing

resolution of $100ps$. If this level can be attained, this system would be the most compatible with a subsequent electron calorimeter or RICH system.

Much work remains before any of the above systems can be recognized. Common to all systems is a complicated TOF versus detector position which needs to be thoroughly investigated. The problem of integrating some form of electron calorimetry with the TOF system is also not quite a reality and demands further consideration. All systems as now envisioned rely on the timing difference between counters since no "central" TOF start counter is planned in any of the proposed spectrometers. The answers to these problems are not considered unattainable, nor are these studies expected to be expensive. Indeed investigations of the above questions are expected to cost in the between \$25K and \$100K. Further, these studies should be completely achievable by small physics teams of five or less persons with access to a few shifts of parasitic beam time.

A 4π Tracking Magnetic Spectrometer for RHIC *

S.J. Lindenbaum
(Convenor Report on Working Group)
Brookhaven National Laboratory and City College of New York

Membership of the Group

G.T. Danby, K.J. Foley, S.E. Eiseman, A. Etkin, R.W. Hackenburg, R.S.Longacre, W.A. Love, T.W. Morris, E.D. Platner, A.C. Saulys (BNL); C. Chan, M.A. Kramer (City College of New York); B.E. Bonner, J.A. Buchanan, J.M. Clement, M.D. Corcoran, J.W. Kruk, H.E. Miettinen, G.S. Mutchler, F. Nessi-Tedaldi, M. Nessi, G.C. Phillips, J.B. Roberts (Rice University).

Abstract

A tracking magnetic spectrometer based on large Time Projection Chambers (TPC) was previously proposed[1-2] to measure the momentum of charged particles emerging from the RHIC beam pipe at angles larger than four degrees and to identify the particle type for those beyond fifteen degrees with momenta up to 700 Mev/c, which is a large fraction of the final charged particles emitted by a low c.m. rapidity quark-gluon plasma. Experimental progress in the successful performance of a TPC developed for AGS E-810 is reported. We have also included typical results of our event generator which contains an interface of an improved HIJET and a plasma bubble model. Typical plasma signals one can expect from this model are presented.

---

* This research was supported by the U.S. Department of Energy under Contract Nos. DE-AS05-81ER40032, DE-AC02-76ER03274, DE-AC02-76CH00016, DE-AC02-83ER 40107 and the City University of New York PSC-BHE Research Award Program.

Introduction

We had previously proposed a large ($\approx 4\pi$) magnetic spectrometer to track and momentum analyze a very large fraction of the charged particles emitted in a heavy ion collision.[1-2] The TPC system proposed was described in Ref. 2 and is illustrated in Figs. 1 and 2. A diagram of the TPC readout electronics[2] not previously published is shown in Fig. 3.

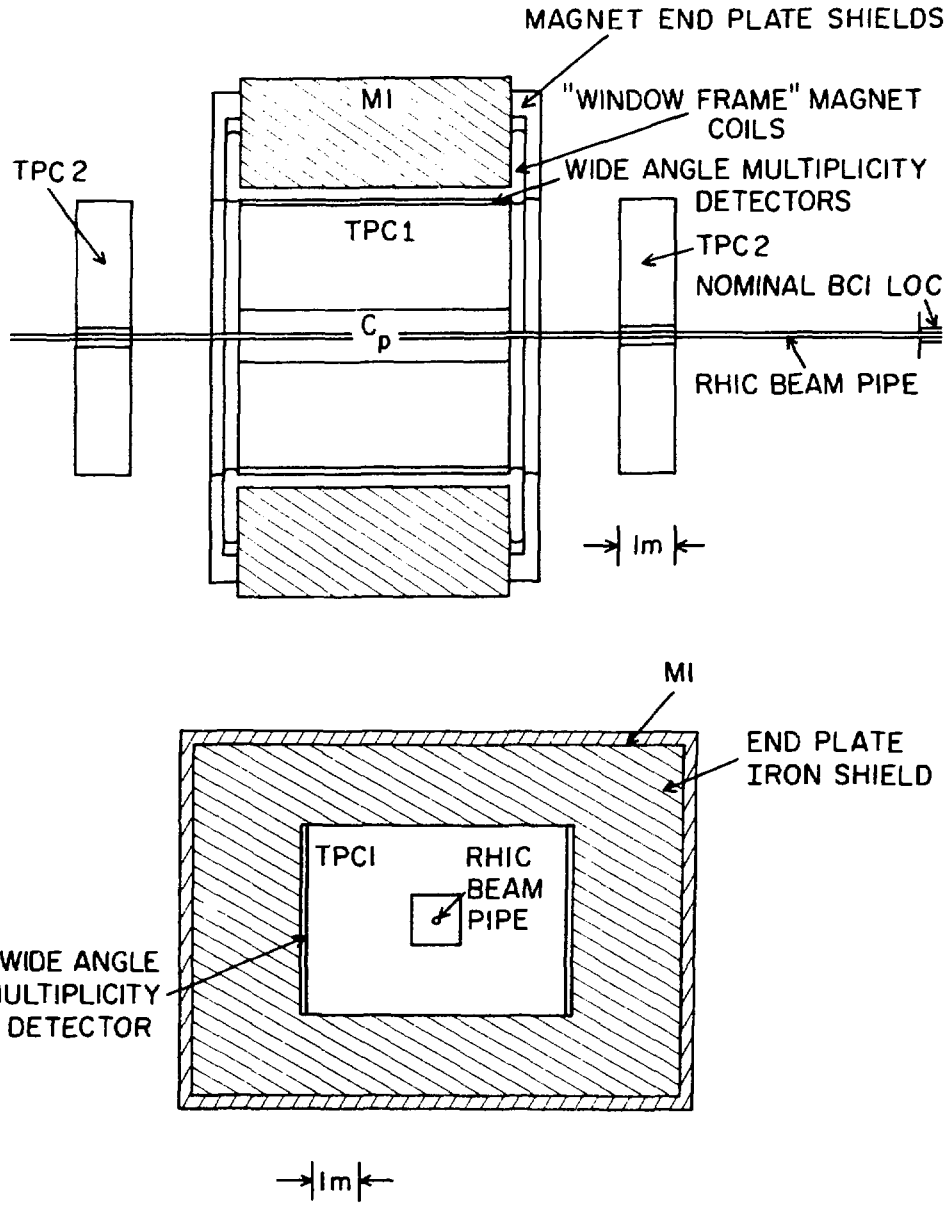

Fig. 1. Plan (above) and elevation (below) views of the proposed device.

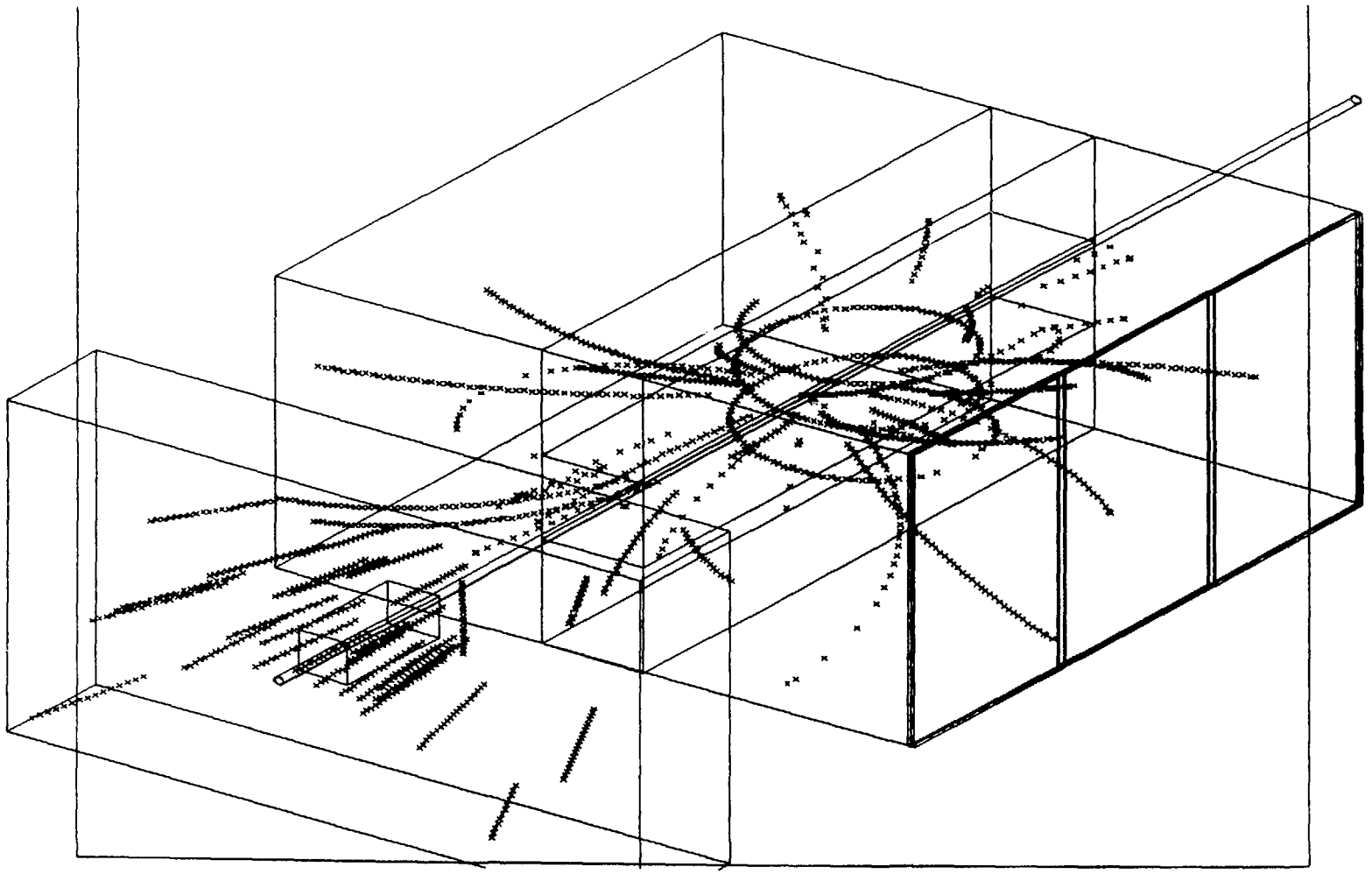

Fig. 2. **Plot of the detector with hits from about 2% of the charged tracks of one central event. Only one of the TPC2 modules is shown.**

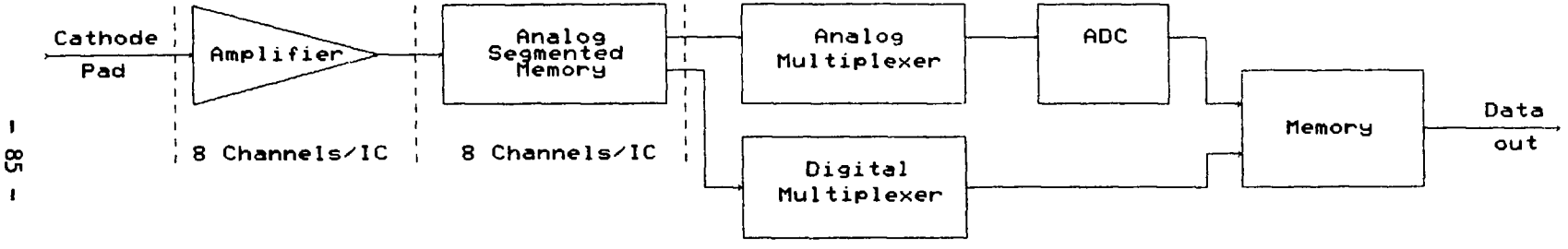

RHIC TPC on Chamber Electronics
256 Channels/Hybrid

Figure 3

The most important part of this update paper is the results on the successful performance of the AGS E-810 TPC since this is a clear indication that the project is technically viable and that we have the appropriate expertise for this project.

AGS 810 Progress on TPC System

Four modules* comprise the AGS 810 TPC system. They are placed along the beam in the MPS 5KG magnet (Fig. 5) with the S (or Si) and O ion beams passing through the TPC to provide large solid angle coverage. From ion beam tests we conclude that this will be satisfactory for these runs. However it should be noted that one can deaden the beam area if necessary. When the booster becomes available at AGS to accelerate Au ions; this will likely become necessary. The anode readout wires are 20 μ gold-plated tungsten 1 cm long rows parallel to the beam direction. There are 10 wires to the inch between cathode structures. A gate which opens only when events of interest occur is included for operation at high ion beam rates (~ 1/2 10^4/pulse). See Figs. 4a and 4b for details.

A TPC module was tested in > 25K Si ions per pulse beam without magnetic field. The hits can clearly be associated with several tracks consistent with beam particles dispersed in y because of late arrival. When we reduced the anode structure gain to correspond to detecting minimum ionizing particles the silicon ions were detected with high efficiency > 90%. The next tests were in an 18 GeV/c proton beam. Figure 6a shows accidental tracks from several million per pulse incident 18 GeV/c protons. Figure 6b shows detected events from a target. Our pattern recognition program led to fits with efficiencies of > 90%. Figure 6c shows the TPC module inside the MPS magnet with a 5 KG field. A 3 GeV π^- beam is incident and low momentum tracks from a target are clearly reconstructed with high efficiency (> 90%). The resolutions in x (transverse to the beam and magnetic field) and y (along the drift and magnetic field direction but perpendicular to the beam) were both measured to be < 1 mm. The two track separability was measured to be ≈ 1-5 mm. The gas is a stable high gain, low diffusion mixture of Argon, Isobutane and Methylal which is a slightly modified mixture of the standard MPS II drift chamber

---

* For technical reasons three modules of twelve anode rows each will be used in the fall 88 runs.

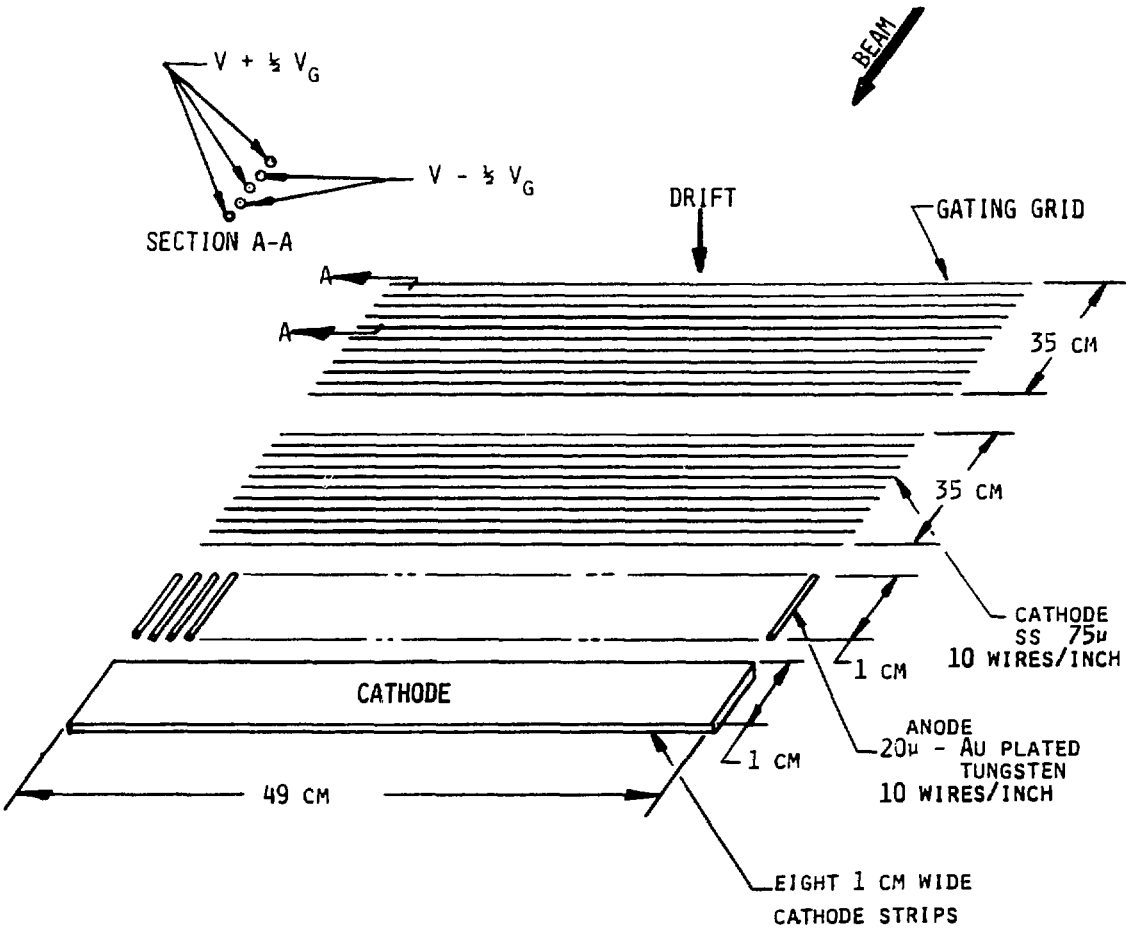

Fig. 4a: Anode Readout Structure. Each section lies above the other physically with gating grid at top.

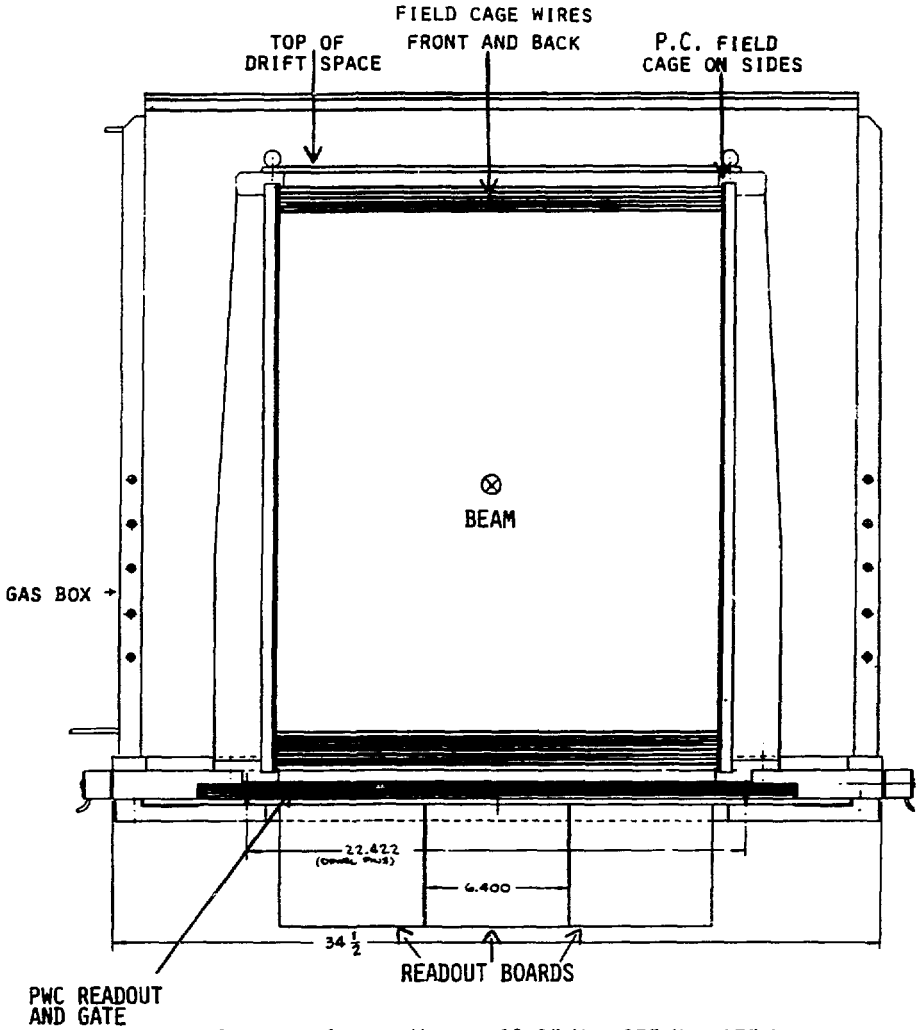

Fig. 4b: Construction details of TPC Module

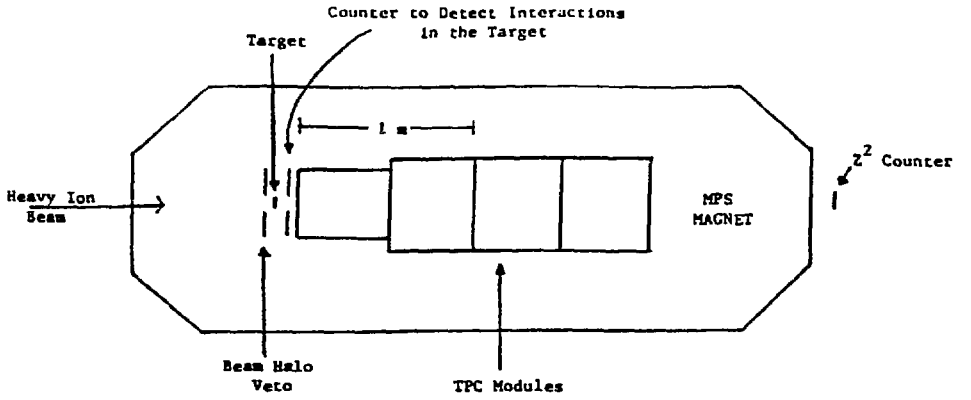

NOTE: Counters and target are not to scale

Figure 5: AGS E-810 Setup

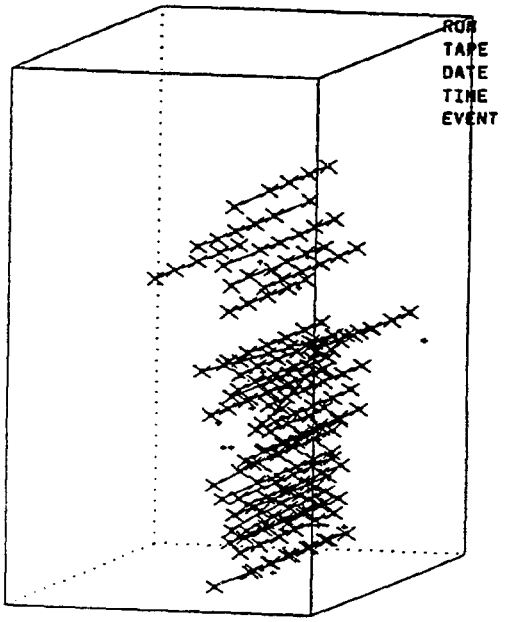

Fig. 6 a: High Rate 18 GeV/c Protons

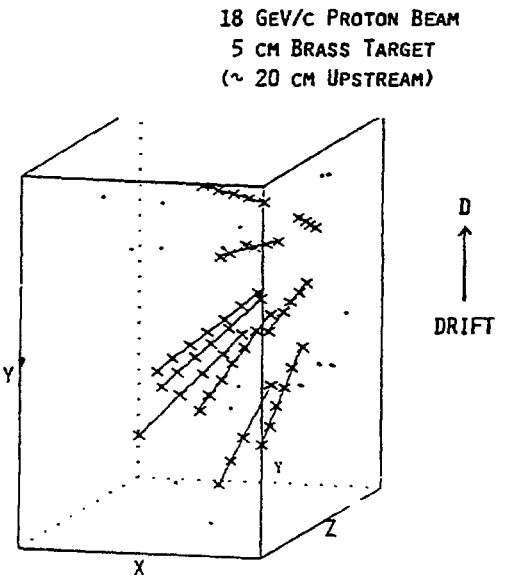

Fig. 6 b: Interaction Detected

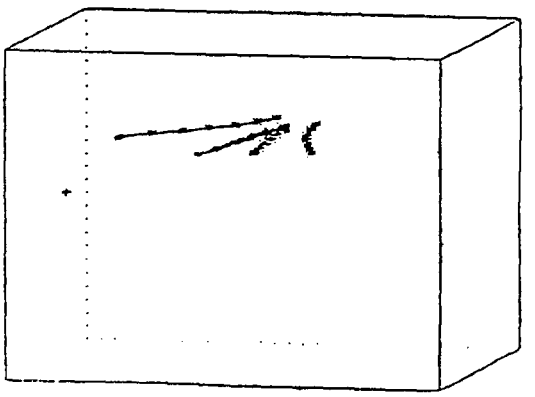

Fig. 6 c: TPC in MPS Magnet

gas. Minimum ionizing particles gave clear well-shaped pulses averaging 8 μamps with peaks of > 20 μamps. Setting a threshold of 2-3 μamps ensured clean pulse operation with very high efficiency. The readout electronics was vintage 86 LeCroy hybrids we designed for TPC readout. An improved version has in recent tests in AGS Oxygen ion runs shown that even lower thresholds (i.e. < 1/2 microamp) are useable with the new readout system.

Thin targets will be used to minimize secondary interactions. The triggering system includes beam halo counters in veto, counters to detect interactions in the target and a $\sum Z^2$ counter to select candidates for events varying from central to peripheral depending on the setting (see Fig. 5). We prefer minimal triggering in the early stages since according to our Monte Carlo's and plasma model one can get surprises if one triggers tightly. For example our plasma model calculations predict that plasma events have a smaller multiplicity distribution than cascade events at AGS energies. The pattern recognition program previously developed by BNL/CCNY was described in Ref. 3. It has been modified somewhat. A local pattern recognition forms a single hit from adjacent and nearby readout wires. A subroutine corrects $\vec{E} \times \vec{B}$ effects which varies from less than 2 mm to a fraction of a mm. Track recognition and reconstruction starts downstream. The PR forms and fits > 3 consecutive hit chains. Finally the chains are joined to form tracks. The existing MPS vertex finding and fitting program has been adapted to the TPC analysis. High efficiency track reconstruction > 95% has been attained in Monte Carlo's and actual MPS and beam tests which were monitored on-line.

We have just obtained preliminary results on an Oxygen ion beam incident on a thin Pb target. Figures 7 and 8 show the preliminary reconstruction of these events via our pattern recognition. The pattern recognition efficiency is nominally estimated to be 75%. The TPC obviously can stand high track density events caused by the several thousand Oxygen ions per second which course through the chamber and still yield very clean chamber operation for the triggered events. The target is just upstream of the chamber.

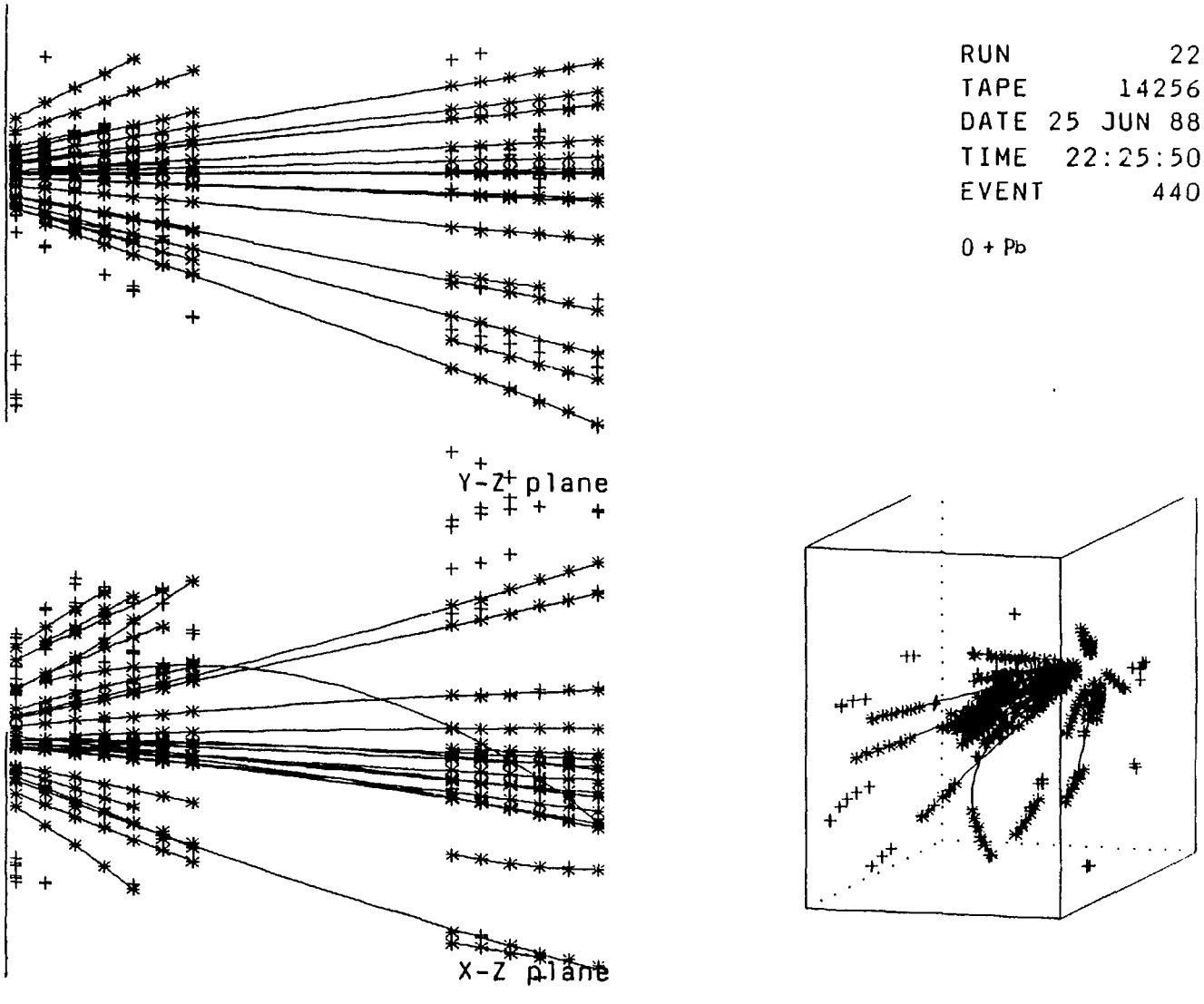

Figure 7: 28-prong event produced by 14.5 GeV/c Oxygen Ions incident on a Pb target

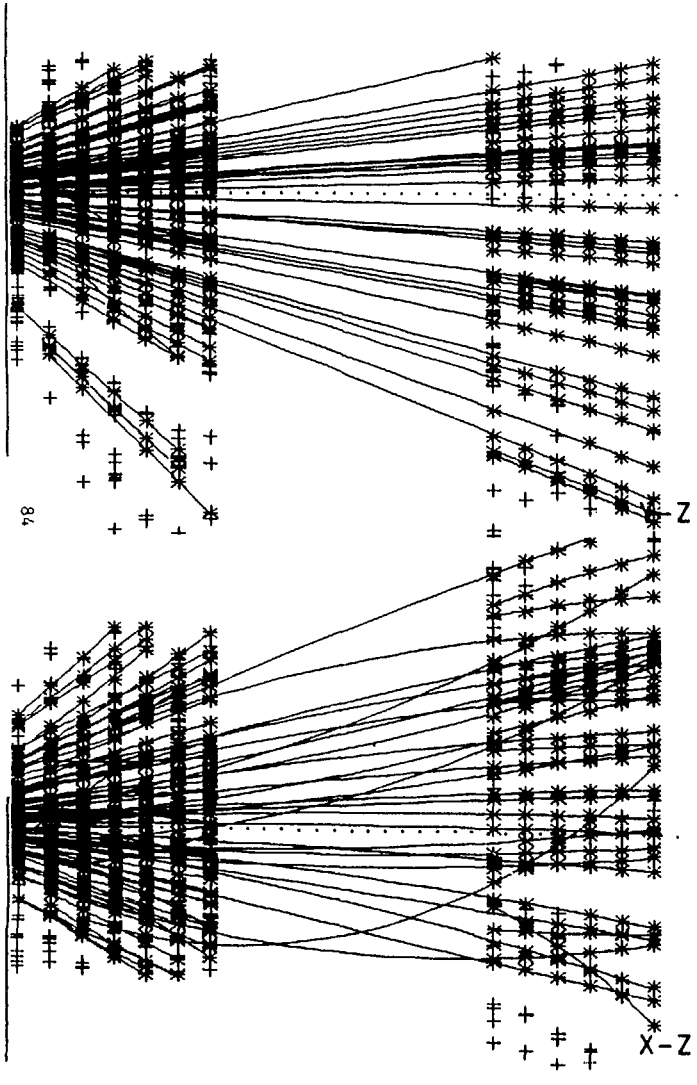

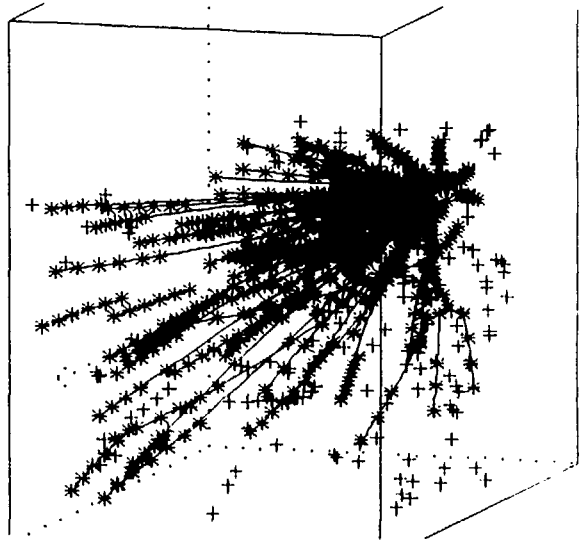

RUN 22
TAPE 14256
DATE 25 JUN 88
TIME 22:42:00
EVENT 2037

O + Pb

Figure 8: 78-prong event produced by 14.5 GeV/c Oxygen ions incident on a Pb target

Figure 8: 78-prong event produced by 14.5 GeV/c Oxygen ions incident on a Pb target

Monte Carlo Event Simulation

Events have been generated by a variant of the HIJET code which allows for simulation of Quark-Gluon Plasma formation. The plasma then hadronized according to Ref. 4. The CERN GEANT program was used to investigate the detector response to these events. This was described previously.[2] However an important point to note is that each particle exhibits a rapidity peak with a different enhancement over background and thus their correlations make an excellent Quark-Gluon Plasma signal. Typical examples are shown in Figs. 9a-b. The rapidity bump signals in plasma events are striking.

Magnet and Estimated Detector System Costs

The magnet design, estimated detector costs etc. remain about the same as described in Ref. 2.

Conclusion

The successful tests of a TPC system in AGS E-810 have clearly indicated the technical feasibility of a 4π tracking magnetic spectrometer for RHIC. The track densities reconstructed in AGS E-810 are adequate to show the technical feasibility of the RHIC system. Future work on AGS E-810 and future R&D on dE/dx should clarify the situation even further.

Plasma bubble Monte Carlo studies indicate that this proposed technique has a good chance of convincingly detecting a QGP at RHIC.

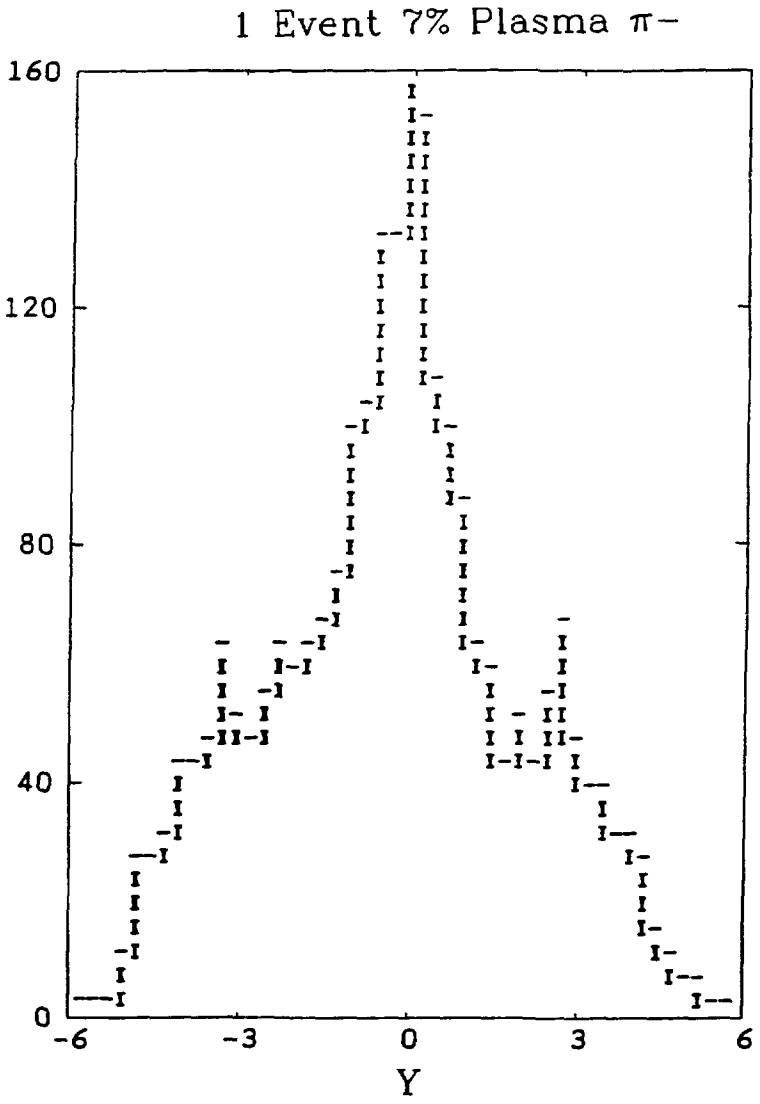

Fig. 9a. **Rapidity distribution from one plasma event for π^-. The plasma energy is approximately 7% of the total available collision energy.**

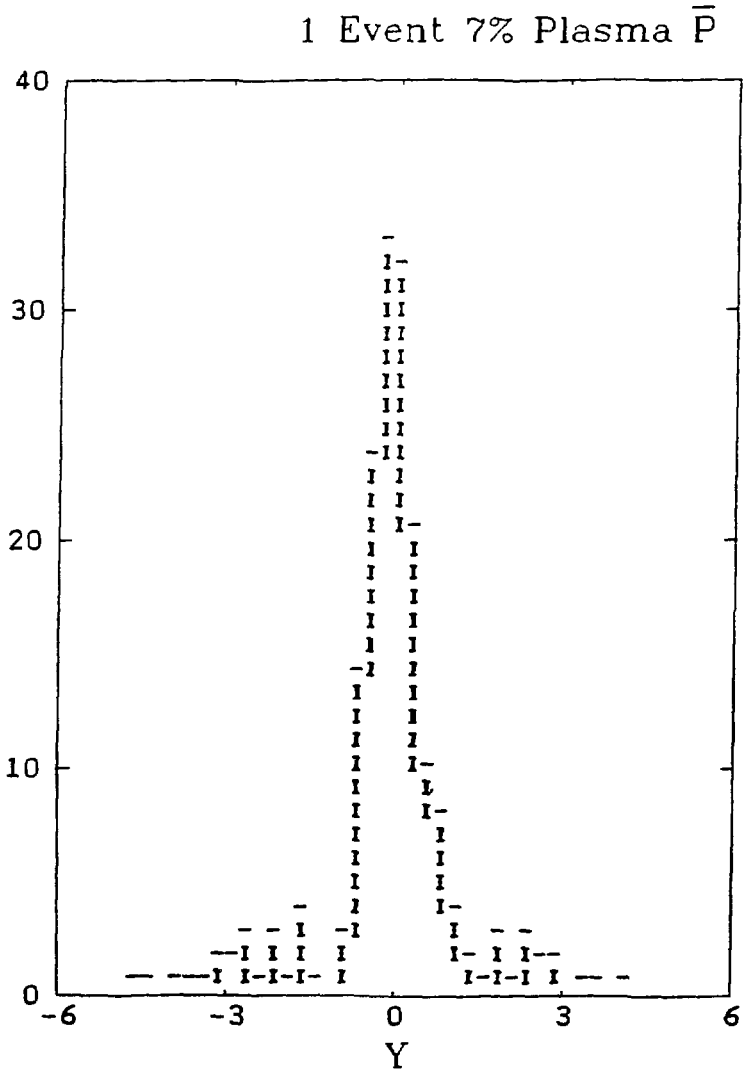

Fig. 9b. **Rapidity distribution from one plasma event for $\bar{p}$. The plasma energy is approxiately 7% of the total available collision energy.**

References

1. Lindenbaum, S.J. and Schroeder, L. Large Magnetic Spectrometer. RHIC Workshop: Experiments for a Relativistic Heavy Ion Collider, April 15-19, 1985, P.E. Haustein and C.L. Woody, Editors, pp. 211-252 (Brookhaven National Laboratory, Upton, New York, 1985).

2. Lindenbaum, S.J. An Approximately 4π Tracking Magnetic Spectrometer for RHIC. Proc. of the Second Workshop on Experiments and Detectors for a Relativistic Heavy Ion Collider (RHIC), Lawrence Berkeley Laboratory, Berkeley, California, May 25-29, 1987, Editors, Hans Georg Ritter and Asher Shor, pp. 146-165 (Lawrence Berkeley Laboratory, 1988).

3. Lindenbaum, S.J., Etkin, A., Foley, K.J., Hackenburg, R.W., Longacre, R.S., Love, W.A., Morris, T.W., Platner, E.D., Saulys, A.C., Asoka-Kumar, P.P.V., Chan, C.S., Kramer, M.A. Large Solid Angle Tracking of Monte Carlo Events of Heavy Ion Collisions in TPC Magnetic Spectrometers. Proc. of the 5th Intern. Conf. on Ultra-Relativistic Nucleus-Nucleus Collisions (Quark Matter '86), Asilomar, California, April 13-17, 1986, L.S. Schroeder and M. Gyulassy, Editors. Nucl. Phys. A461, pp. 431c-442c (1987).

4. Koch, Müller and Rafaelski, Physics Reports, February 1986.

BOSE-EINSTEIN MEASUREMENTS AT RHIC IN LIGHT OF NEW DATA

William A. Zajc
Physics Department
Columbia University
New York, NY 10027

Abstract

The implications of the NA35 Bose-Einstein data for two-pion interferometry in the central region at RHIC are discussed. It is shown that naive rate estimates may greatly over-estimate the effective rates for such measurements.

1 Introduction

Bose-Einstein measurements are generally advertised as providing a direct measurement of the spatial extent and lifetime of pionic sources. Recent work has extended this formalism to include the case of expanding hadronic matter[1]-[4], particularly in the context of collisions at RHIC. Typically, these analyses predict differences in the behavior of the correlation function with respect to the direction of relative momentum. Only a modest improvement of conventional spectrometer resolutions is required for experiments employing these techniques, since most of the impact lies in the methods by which the data is analyzed. (Here, of course, one must insure that the experiment can obtain sufficient data to support the projection of the correlation function into more complicated phase space bins.)

Recent experimental data, on the other hand, have dramatic implications for the feasibility of Bose-Einstein measurements at RHIC. In this note, I would like to examine the requirements imposed on tracking detectors by these new data.

2 Recent Heavy Ion Data

The NA35 collaboration has performed the first Bose-Einstein analysis for $^{16}O + {}^{197}Au$ Collisions at 200 $A \cdot GeV$ [5]. Their result for the average radius, uncut on rapidity interval, is of the order of 4 fm, and is therefore consistent with a simple $A_p^{1/3}$ scaling observed at lower energies[6]. What is provocative is the value for the radius obtained in the central region ($2 < y < 4$), where the transverse radius is found to be 8.1 ± 1.6 fm. This is much larger than the geometric size of

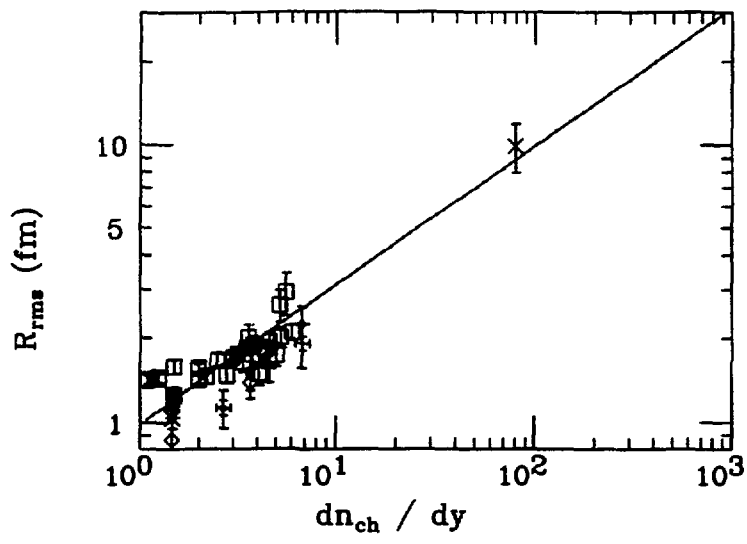

Figure 1: The root-mean-square radius measured via two-pion interferometry at ISR and CERN energies as a function of charged rapidity density.

the assumed collision region. This discrepancy motivated the authors of Ref. [5] to interpret their result in terms of a freeze-out radius, R_{FO}. They obtain, for N_π pions interacting in a spherical (expanding) volume, a freeze-out radius given by $R_{FO} \approx 1.2\sqrt{N_\pi}$ fm, which provides an estimate of order 8 fm for their data, in good agreement with the measured value.

Taken by itself, the result of NA35 of a multiplicity-dependent radius is intriguing but not quite compelling, based as it is on only one data point (although in principle NA35 could study this effect as a function of N_π). However, such a dependence has already been observed at the ISR, both by the AFS collaboration[7] and by the SFM group[10]. Futhermore, these results extrapolate smoothly to the NA35 point, as shown in Fig. 1. (The various radii have been scaled, as suggested by Bartke and Kowalski[6], so that rms values are always compared, using the various scaling factors found in[11]. In addition, the AFS and NA35 multiplicities have been converted from charged multiplicity to charged particle rapidity density.) Having done this, we see that all three data sets are consistent with a dependence $R_{BE} \cong \sqrt{dn_{ch}/dy}$ fm. This result, if valid, has significant consequences for HBT analyses at RHIC, which we explore in the next section.

3 Experimental Implications

For convenience, I have concentrated on a "limited aperture" central tracking detector at RHIC, covering ~ 1 sr of solid angle. For example, requiring an aperture roughly symmetric in $p_{||}$ and p_T gives $|y| < 1$, $\Delta\Phi = 60°$. A conceptual design for such a device may be found in the proceedings of the previous workshop[12]. It is straightforward to extend these results to other regions of phase space, paying due

attention to the opposite momentum dependences of multiple scattering and spatial resolution.

3.1 Required Momentum Resolution

The Bose-Einstein enhancement is expected for pairs with relative momentum of order $\delta p \sim 1/R$, where R is the characteristic dimension of the source in the direction of $\vec{q}$. (In what follows, I will use $\vec{q}$ to denote $\vec{p}_1 - \vec{p}_2$, $\delta p \sim 1/R$ to indicate the range of $\vec{q}$ exhibiting a Bose-Einstein enhancement, and Δp for the single-particle momentum resolution.)

3.1.1 Single Particle Spatial Resolution

Clearly, a single-particle momentum resolution Δp significantly smaller than δp is required in order to resolve the peak. If we assume standard four-point tracking with a lever arm L then

$$\frac{\Delta p}{p} = \frac{p}{p_K} \cdot \frac{2\sigma}{L} \quad , \tag{1}$$

where σ is the spatial resolution for each measured point and $p_K = \frac{e}{c} \int B\, dl$, i.e., the p_T kick of the magnetic field. (Somewhat different numerical factors apply for tracking in a uniform field volume. A complete discussion has been given by Gluckstern[13]. For equally-spaced points, approximately 36 measurements are required for this configuration to give the same results as an equivalent length lever-arm spectrometer. Nonetheless, this does not affect the basic conclusions of this section.) Suppose we require, as a minimum, that $\Delta|p_1 - p_2| \sim \delta p/R$, or that $\Delta p \approx \delta p/6$. This leads to an expression for the maximum radius that can be measured:

$$R < \frac{1}{6} \frac{p_K}{p^2} \cdot \frac{L}{2\sigma} \quad . \tag{2}$$

Making quite modest assumptions for p_K (0.5 T-m = 0.15 GeV/c), σ (500 μm) and L (1 m) leads to a maximum measurable radius of 200 fm (using $\langle p \rangle$ = 0.5 GeV/c). Presumably, the barrier to such measurements must (and does) lie elsewhere.

3.1.2 Multiple Scattering

Multiple scattering will lead to a single-particle momentum resolution of

$$\frac{\Delta p}{p} = \frac{0.021\,\mathrm{GeV/c}}{p_K} \sqrt{\frac{L}{L_0}} \quad , \tag{3}$$

where L_0 is the radiation length(s) of the spectrometer material(s). Applying the same criteria as before, and for the same spectrometer parameters, one obtains the condition that

$$R < 0.4 \sqrt{\frac{L_0}{L}} \quad , \tag{4}$$

for R measured in fermis. For large values of R, this represents a stringent condition. For example, R = 10 fm then requires that the total spectrometer material be less

that 0.2% of a radiation length (!). Note also that one loses as the square of the radius to be measured.

3.1.3 Two-track resolution

All of the single-particle momentum resolution in the world will prove useless unless one can in fact measure each track of a closely correlated pair. Here I will provide only the crudest of considerations, since it is somewhat meaningless to quote a required two-track resolution in the absence of definite details of the detector geometry and reconstruction algorithms. Simply requiring that the spatial separation everywhere between two tracks of momenta p be adequate to resolve a source of radius R leads to the condition (assuming tracking starts at a radial distance of 10 cm.)

$$\Delta s_2 < \frac{7\,\mathrm{mm}}{R} \quad , \tag{5}$$

where again R is in fermis and a mean momentum of 0.5 GeV/c has been assumed. This is undoubtedly an optimistic estimate, but as noted above, more realistic values require a much more sophisticated approach. Note that such an effect could in principle be studied in existing Monte Carlo simulations[14].

3.2 Rates

The remark is often made that Bose-Einstein rates improve as the square of the mean multiplicity. This is of course true if the source radius does not depend on multiplicity. If, however, there is such a dependence, then this no longer true. The number of pion pairs in an event will of course still be given by $\langle N_\pi(N_\pi - 1)\rangle$, but the number of *useful* pairs in an HBT analysis will depend on the explicit form of the $R(N_\pi)$ dependence. This is illustrated below.

Consider a measurement of the transverse dimensions of the source. For convenience, we will restrict our attention to equal-energy pairs of momenta $\langle p_T\rangle$. For a pair to be "useful" in determining the correlation function, the relative momentum q must be in or near the enhancement region. For definiteness, I will define the effective region to be for those relative momenta satisfying $q < 6/R$. (All that pairs outside this region do is increase our knowledge of the baseline, which is useful for studies of systematics but contributes nothing to the measurement of source dimensions.) The solid angle in which such pairs will exhibit an enhancement is thus[15]

$$\Delta\Omega \sim \left(\frac{6}{\langle p_T\rangle R}\right)^2 \quad . \tag{6}$$

The mean multiplicity in $\Delta\Omega$ will be (for the central region of rapidity)

$$\langle n_-\rangle = \frac{dn}{d\Omega}\Delta\Omega = \frac{1}{2\pi}\frac{dn_-}{dy}\frac{36}{\langle p_T\rangle^2 R^2} \quad . \tag{7}$$

Assuming a rapidity density variation of R as given in Fig. 1, this gives a mean multiplicity in each sub-region of

$$\langle n_-\rangle \approx 1 \quad . \tag{8}$$

Thus, any large-aperture spectrometer of solid-angle Ω_S breaks up into small "patches" of size $\sim \Delta\Omega$. The number of such patches, and hence the Bose-Einstein rate, is only *linearly* dependent on the aperture. In fact, the result that the mean multiplicity in such a patch is of order unity tells us directly that the number of such patches is on the order of the number of (like) pions in the overall region (here the central region) under consideration. In other words, an event with ~ 1000 like-sign pions in the central region produces about ~ 1000 "useful" pairs in a correlation function, not $\frac{1}{2}1000 \cdot 1000$. While still sufficient to provide a rough estimate of the radius on an event-by-event basis (assuming we can measure all 1000 pions!), this is much worse than one might hope for 500K pairs.

4 Speculation

It is striking that the number of pions per patch is of order unity. Our "patches", after all, are closely related to the number of (transverse) phase space cells. Again, assuming the validity of $(dn/dy)^{1/2}$ scaling of R_{BE}, we are faced with a system where the multiplicity, rather than the phase space volume, determines the effective number of cells. Regardless of the origin of this behavior, the end result (roughly one pion per phase space cell) is reminiscent of the condition for Bose-Einstein condensation. For a source at temperature T and of volume V, Bose condensation occurs at a spatial density of

$$\frac{N}{V} = f\frac{2.61}{\Lambda^3} \quad , \quad \Lambda \equiv \sqrt{\frac{2\pi}{mT}} \quad . \tag{9}$$

(Λ is known as the thermal de Broglie wavelength. The factor f is unity in the non-relativistic limit; it is approximately 2 for $m = T$.) Applied to the NA35 data, Eq. 9 requires a (like) pion density of about 0.18 fm^{-3}, which is substantially lower than the freeze-out density of 0.02 fm^{-3} these authors infer from their data. However, assuming the validity of their interpretation of a spherically expanding source, and calculating the like-pion density at the time the source has the radius of the incoming projectile (i.e., at production time), one finds that *initially* the pion source density is $\sim$0.35 fm^{-3}, well above the threshold for Bose condensation. Even if one allows $\sim$1 fm of proper time for the production of these pions, the conclusion remains that the source is at or near the critical density.

An experimental consequence of Bose-Einstein condensation would be an enhanced population of particles in the lowest momentum state. Such an effect is in fact seen by NA35[16] in this same data set: In the central region, the negative pion transverse momentum spectrum has a significant enhancement (relative to pp collisions) for $p_t <\sim T$. It is important that this phenomena be understood and pursued via further measurements. For example, the enhancement could be studied as a function of the negative pion multiplicity n_- in $2 < y < 3$ (for central events). An interpretation based on flow of the surrounding matter[16]-[17] would presumably show little dependence on n_-, while Bose condensation would depend directly upon it.

5 Conclusions

Nearly all the arguments in this note revolve around the conclusion, derived on the basis of Fig. 1, that $R_{BE} \cong \sqrt{dn_{ch}/dy}$ fm. Clearly, the lever arm is dominated by the NA35 point, with a large desert of data in the region of intermediate rapidity density. As I have tried to make apparent, it is essential for the design of Bose-Einstein experiments at RHIC that measurements in this region are made with existing experiments to confirm or disprove the dependence of R_{BE} on dn/dy hypothesized here. Among the present heavy-ion experiments, NA35 at CERN and E802 at BNL (and perhaps NA34 and E810 as well) should be able to determine radii via Bose-Einstein measurements in the region $10 < dn_{ch}/dy < 200$. These same experiments could explore the connection, if any, to the low p_T enhancement, as noted in the previous section.

If in fact nature requires that we must measure radii of order 30 fm at RHIC, traditional interferometry methods may prove totally impracticable. In that case, the appropriate technique, as noted by Chasman and Willis[18], becomes speckle interferometry, which may be thought of as the study of global fluctuations in phase space density. Thus, we are presented with the attractive possibility of simply measuring multiplicities of like-sign particles in our small patches of $\Delta\Omega$, rather than doing a detailed relative momentum analysis. It can be shown that, per pair, this carries the same information content as traditional two-particle interferometry studies[19]. However, note that we are still faced with the task of PID for all such patches we wish to use, so that some crude momentum and timing analysis will still be required. Regardless of the method used, it is safe to say that interferometry should play an important role in the design considerations for any spectrometer at RHIC.

6 Acknowledgments

Remarks by H. Gutbrod were instrumental in directing my thoughts to these matters.

References

[1] S. Pratt, Phys. Rev. Lett. **53**, 1219 (1984).

[2] K. Kolehmainen and M. Gyulassy, Phys. Lett. **180B**, 203 (1986).

[3] A.N. Makhlin and Yu.M. Sinyukov, Z. Phys. **C39**, 69 (1988).

[4] G. Bertsch, M. Gong and M. Tohyama, Phys. Rev. C37, 1896 (1988).

[5] A. Bamberger *et al.*, Phys. Lett. **203B**, 320 (1988).

[6] J. Bartke and M. Kowalski, Phys. Rev. **C30**, 1341, (1984).

[7] T. Akesson *et al.*, Phys. Lett. **129B**, 269 (1983).

[8] A. Breakstone *et al.*, Phys. Lett. **162B**, 400 (1985).

[9] T. Akesson *et al.*, Phys. Lett. **187B**, 420 (1987).

[10] A. Breakstone *et al.*, Z. Phys. **C33**, 333 (1987).

[11] Bose-Einstein Correlations: From Statistics to Dynamics, W.A. Zajc, to appear in *Hadronic Multiparticle Production*, World Scientific Press, P. Carruthers, ed.

[12] S. Nagamiya in Proceedings of the Second Workshop on Experiments for a Relativistic Heavy Ion Collider (RHIC), H.G. Ritter and A. Shor, ed., LBL-24604 (1988).

[13] R.L. Gluckstern, Nucl. Instr. and Meth. **24**, 381 (1963).

[14] S.J. Lindenbaum in Proceedings of the Second Workshop on Experiments for a Relativistic Heavy Ion Collider (RHIC), H.G. Ritter and A. Shor, ed., LBL-24604 (1988).

[15] This argument is not quite valid for hadron-hadron reactions, where the size of $\Delta\Omega$ is of the order of the entire central region, but it should apply for $R \geq\sim 2$ fm.

[16] H. Ströbele *et al.*, Z. Phys. **C38**, 89 (1988).

[17] T. Atwater, P.S. Freier, and J.I. Kapusta, Phys. Lett. **199B**, 30 (1987).

[18] W. Willis and C. Chasman, Nucl. Phys. **A418**, 413 (1984).

[19] Monte Carlo Methods for the Generation of Events with Bose-Einstein Correlations, W.A. Zajc, Phys. Rev. **D35**, 3396 (1987).

Summary of Working Group On Readout Electronics

Summary of the Working Group on Readout Electronics

W. E. Cleland (convener), J. Hall, R. Ledoux, E. Platner,
S. Rescia, J. Stachel, H. Takai, B. Wadsworth, and G. Young

Other working group participants:
S. Dhawan, O. Dietzsch, S. Eiseman, M. Newcomer, I. Pless, M.Purschke,
V. Radeka, R. Scharenberg, S. Steadman, R. Van Berg, and Bo Yu

1. Introduction

RHIC poses two principal challenges for readout electronics. The first is the short time between bunch crossings, which will be of the order of 100 ns, compared to the several microseconds enjoyed by the $S\bar{p}pS$ and Tevatron. This necessitates speed in making trigger decisions and ingenuity in providing analog delay. The second is the very large number of channels to be read out. This could lead to problems with power consumption, cabling cost and data rate restrictions. A new means of dealing with the problems in a coherent way and the needed R&D work to realize this goal are described in the following.

The working group concentrated primarily on the part of the electronics chain which will be common to all detectors which deliver "prompt" signals, i.e. those detectors with no inherent delay. The principal problem concerning the readout of such detectors is that the spacing between crossings is too short to permit even a very low level trigger decision to be made. Although the different types of detectors require preamplifier–shaping amplifier chains which are matched to their characteristics, the problem of storage of amplitude or timing information is quite common.

Typical RHIC events will be characterized by a large multiplicity of produced particles. In contrast to fixed target experiments, these will be fully distributed over 4π, with a moderate decrease in density in the central region. Requiring good granularity in a detector over 4π leads to large numbers of readout channels, easily several times 10^4 per detector, and of the order of several times 10^5 in a single experimental apparatus. This large number of detector channels would require a similarly large number of cables for readout if conventional techniques were used. Multiple detector layers will have to be read out, requiring that cables for the readout introduce unwanted inactive material causing undetected energy loss as well as multiple scattering. The readout of tens of thousands of detector channels using coaxial cable or even multiple–twisted–pair cables would require allocating considerable space just for cables. The sheer size of the needed cable bundle will impose severe constraints on the location and hermeticity of the detectors and magnets. Therefore, also from the viewpoint of detector performance, it is highly desirable to reduce the number of readout cables and connectors to the minimum possible.

We therefore explore, as has been done for the SSC [1] and HERA [2], the concept of an

analog pipeline. Since granularities are usually designed to give double hit probabilities of less than 5%, most of the channels are empty for a single event. In addition, there is on the average less than a 10% chance per bunch crossing of having an interaction. These coupled features suggest a way to economize on the storage requirements for the analog signals. A pipeline would need only to provide enough storage to accommodate the hits expected in a single detector element during the entire (first and second level) trigger decision time, not the much larger storage needed to allocate a bucket for each of the bunch crossings occurring during this period.

Because of the large quantity of detector channels, it is also important to incorporate elements that have little need for adjustment, calibration and correction to the data. For example, if power, size and cost considerations permit, time can be digitized directly (i.e. with counters, shift registers, etc.) where no adjustments, calibrations or corrections are required. This kind of circuit behavior is extremely valuable in detectors with 10^5 or more channel elements. In analog to digital conversion applications, direct conversion (i.e. flash ADC) may be prohibitive in cost, size and power. Thus major effort must be given to minimize the magnitude of offset and conversion gain variance. Where possible, self-correction and adjustment should be applied at the subsystem level.

2. Analog Pipeline Storage at RHIC

Beam bunches will intersect every 114 ns at RHIC, implying that there will not be enough time to make even a first level trigger decision before the next bunch crossing occurs. Thus, all analog information from detectors will need to be stored in some manner while awaiting a trigger decision to be made. A circuit to provide active delay and storage of data while trigger decisions are being made would be a welcome solution to the problem. An intelligent circuit could store data for a given detector element together with a label indicating from which beam crossing it came. The circuit would pass on the data if and only if a positive trigger resulted for the particular beam crossing. Such a concept is being exploited for a time-to-digital chip (TVC) being developed by the Penn group [1, 3].

Because of the low probability that a given detector element is 'hit' in a given event, and the additional low probability that a given beam crossing will result in an event, a circuit of rather modest storage capability could store analog information long enough for rather sophisticated

trigger decisions to be made, i.e. for times of the order of several tens of microseconds. The circuit could be made even more useful if it passed on only digitized data after the receipt of a valid trigger. Then a single cable would transfer data from a large number (perhaps 100) detector elements, thus reducing the number of cables required in the experiment and consequently the power required to drive them.

From the viewpoint of data acquisition the amount of data has to be reduced about 3 orders of magnitude between the detector output and storage medium [4]. This reduction has to come from selective triggers and suppression of empty channels. Since this step has to be taken in any case, we feel that the only cost- and time-efficient strategy is to keep data on the chip until needed and the appropriate decisions can be made. This will also lead to considerable reduction in cost for event buffer memory, which typically increases as the square of the data. It is also envisioned that the use of monolithic technology for amplification, shaping and data storage will lead to considerably lower power consumption.

A desirable goal is therefore to have detector-mounted (a) amplification (preamplifier and shaping), (b) signal storage in an Analog Memory Unit (AMU) until the second level trigger decision is made, (c) digitisation of the analog information on the chip in response to a valid second level trigger, and (d) compaction followed by serial transfer to memory buffers in preparation for a third level trigger. The number of "interesting interactions" in a given experiment will usually be very small after a higher level trigger. Therefore, after de-sparsification, one would usually have a fairly large amount of time (milliseconds) for the transfer of the data.

The principal element needing development work on such a chip would be the analog memory unit (AMU). The most promising technology today for such a memory unit involves the use of switched capacitors. Much of the readout and control logic could use standard digital cells available from chip manufacturers, although a dedicated design of the entire chip would have to be performed eventually. Estimates of the needed precision and dynamic range for the AMU's are given in Table 2-1 for various detector types.

Presently, capacitors on monolithic circuits can be constructed with varying degrees of accuracy (see Table 3-1). A development effort to meet the requirements given in Table 2-1

Table 2-1: Approximate requirements for an analog memory storage element for RHIC detectors.

Charge Measurement Devices:

Detector type	Precision	Dynamic range
Calorimeters	0.1 %	15 bits
Scintillation counters	1 %	9 bits
Silicon diodes	1 %	9 bits
Pad chambers	0.1 %	12 bits
TPC (dE/dX data)	1 %	12 bits

Time Measurement Devices:

Detector type	Precision	Dynamic range
Drift chambers	1 nsec	1 μsec
Time of flight	25 psec	25 nsec
TPC (time slices)	10 nsec	20 μsec

is clearly needed and seems eminently feasible. Given that much of the information at RHIC will come from devices producing analog data, an effort dedicated to developing monolithic low noise preamplifiers and shaping amplifiers is also required. The effort should concentrate first on developing standard cells (e.g., for preamplifiers, shaping amplifiers and analog memory units) which would then be available for further use in developing application-specific circuits.

The potential benefits of this development are large. At costs of $10/chip and a power consumption of 5 mW/chip, it would be possible to instrument 2×10^5 channels at a cost of only $2M for the basic readout and 1 kilowatt of power, vastly better than present-day figures.

3. Current Status of Switched Capacitor Technology

In order to obtain a perspective on the usage of switched capacitor analog storage devices in high energy physics, we present here a brief survey of the devices which have been designed and/or constructed, of which we are aware. The technical data on these devices are summarized in Table 3-1.

Table 3-1: Survey of switched capacitor technology used in high energy physics

Name	Size (ch x depth)	Process	Sampling Rate (MHz)	Readout Rate (MHz)	Mplx	Dynamic Range	Precision	Power Consumption (mW/ch)	References
MPX2,MPX3	128x2	5μNMOS	2.5	4	128:1	15:1	3%	20	[5, 6, 7, 8]
Microplex	128x2	5μP-well CMOS	1	3	128:1	10:1	5%	0.5	[9]
Microstore	1x256	3μNMOS (HMOS-1)	200		none	2000:1	5%	200	[10]
CDU	32x4	3μNMOS (HMOS-1)	7	~1	32:1	4000:1	2%	3	[11, 12]
TWR	16x128	3μCMOS	50		none				[13]
SVX	128x1	3μCMOS	2	20		14:1		1.3	[14]
ZEUS	4x58	2.5μCMOS	10	0.8	none	8000:1	0.25%	25	[2]

3.1. The Microplex Chips MX2 and MX3

A 128 channel VLSI chip has been developed for readout of silicon strip detectors [5, 7, 8]. Each channel is provided with a calibration line and overvoltage protection. An amplifier integrates the signal and also charges a storage capacitor which is connected to the gate of a transistor. This transistor modulates an output current which is directed to each channel in turn by a shift register. A duplicate output channel with a storage capacitor which is isolated just before the signal comes in, permits the subtraction of noise and switching transients. As many as 10 chips have been successfully multiplexed onto a single output channel. Tests have been performed in minimum ionizing beams. The most probable signal height from minimum ionizing tracks was 15 times the rms noise in any single channel. The average gains of two readout chips were equal to within 3%. MX2 and MX3 designs have been irradiated with a ^{60}Co source up to doses of 100 Krad. Large differences in their behavior after irradiation have been seen which are thought to be due to the different fabrication processes between MX2 and MX3 (they are structually very similar). The MX2 and MX3 are usable if irradiated unpowered up to 100 and 20 Krad, respectively. If powered, both fail after approximately 15 Krad exposure.

3.2. The Rutherford Microplex Circuit

A Microplex system has been developed by Rutherford Appelton Lab [9] as a readout for silicon strip detectors. It consists of an array of 128 amplifiers with a single multiplexed output. This VLSI circuit can be bonded directly to silicon strips. Analog storage is accomplished by charge storage on two capacitors. The use of two capacitors, one charged at the beginning and one at the end of the sampling period (correlated double sampling), provides some noise filtering. The amplifiers give a linear response up to 5 x 10^6 electrons with 3% gain spread over a single chip and 10% variation between chips. The uniformity of the analog storage capacitor was better than 5% across any chip. The circuit showed no change in operation for ^{60}Co gamma dosages of less than 3 Krad. By 10 Krad the device was unusable. A new device is being developed using 3 micron technology.

3.3. The Stanford Microstore Chip

A switched capacitor Analog Memory Unit IC has been developed by SLAC and the Stanford Center for Integrated Systems [10]. The IC contains 256 analog storage cells consisting of pass transistors, a storage capacitor and a differential read out buffer. Fast response and good amplitude resolution were the design goals. Variations in cell response at the level of 5% and non-uniformities in gain of 1.5% were measured. The RMS error for repeated samples at the same input level was 1/1000 of full scale. It is expected that cell by cell corrections could achieve significantly better accuracy.

3.4. The SLAC Calorimeter Data Unit

A multi-channel sample-and-hold Calorimeter Data Unit (CDU) has been developed at SLAC and the Stanford Center for Integrated Systems [11, 12]. The IC consists of 32 input channels, each with 4 storage cells which allows samples to be taken at 4 time intervals. The design goals for the development were wide dynamic range and long hold times. Therefore, each storage cell is laid out in a fully differential way and consists of a sampling stage for the signal and another identical stage for a reference voltage. The chip can be read out in a voltage or current mode. The current mode gives a faster transient response and better transfer curve linearity. RMS noise levels of 1 part in 4096 (12 bit resolution) have been obtained on single shot measurements. Approximately 2% non-uniformities in the gain among the cells are observed. However, a 2 parameter fit (pedestal and gain) of the output response yields a 0.4% accuracy. A curvature correction with 8 sets of values for the 128 channels improves the accuracy to 0.07%.

3.5. The LBL Transient Waveform Recorder

S. Kleinfelder [13] at LBL has developed a 16 channel transient waveform recorder on a 6.8 by 6.8 mm chip. Each channel has an individual analog input, a linear array of 128 sample and hold elements, clock drivers, a few steering switches, a read amplifier and an individual output. Each sample and hold storage element consists of a 1pf capacitor an n-channel sample gate, and a master-slave shift register bit. In this scheme, the voltage stored on the capacitor is important, not the charge, so small variations in the capacitor values do not affect accuracy. The 128 bit shift register is implemented as 2 interleaved 64 bit registers so as to relax internal and external timing requirements and to reduce power consumption. A prototype which has run at 50 MHz has already been produced and is in the process of being thoroughly tested.

3.6. The LBL SVX Chip

The SVX IC has been developed at LBL [14] for the Silicon Vertex Detector system for CDF. The IC contains 128 parallel data acquisition channels and considerable peripheral circuitry. Each channel consists of a low noise, low power charge sensitive amplifier, a multi-stage auto-balanced comparator, an analog multiplexer, nearest neighbor logic, priority search logic and a share of a position encoding read-only memory. The analog system can subtract both detector pedestal and leakage current on a channel by channel basis. On-chip sparse readout circuitry allows for efficient management of low occupancy events. A dedicated test chip has been designed for clean evaluation of the input amplifier. A signal-to-noise ratio of 14 has been obtained for a 10 pf silicon detector for minimum ionizing particles. Early tests of new versions of the SVX show improved signal to noise ratios.

3.7. The ZEUS Analog Pipeline

The ZEUS analog pipeline has been developed at Fraunhofer Institut fuer Mikroelectronische Schaltungen und Systeme at Duisburg for the ZEUS calorimeter at DESY [2]. It will be used in both the uranium-scintillator calorimeter and in the silicon planes within the calorimeter to store the analog data until the first level trigger signal has come, namely for 5 μs.

The most important features are summarized in Table 3-1. To achieve the very large dynamic range which is needed, the charge injection which causes the pedestal has been minimized and kept constant by putting the storage switch on the ground plate of the storage capacitor. The pedestal is only 20 mV with 2.5 mV rms variation from channel to channel,

which guarantees a dynamic range of 8000:1 after pedestal correction. By a careful layout, the capacitors are matched to 0.25% within a pipeline. The pipeline shows no degradation up to 5 Krad of γ-rays from a ^{60}Co source. This pipeline is to be followed by a second IC which performs the function of buffer-multiplexer. This second IC is still being designed.

In summary, it is clear that a number of successful attempts to develop AMUs of the type needed at RHIC have been made. A comparison of the device requirements (Table 2-1) with the achieved characteristics (Table 3-1) indicates that the technology to carry out this project is available, although none of the devices built to date have precisely the required characteristics.

4. Radiation Effects

In designing electronic components for RHIC detectors the effects of radiation damage must be considered. The requirements of a high degree of integration, speed, and a low level of electronic noise will indicate the type of technology to be used, but radiation hardness may be an overriding factor. The damage induced in the electronic devices can be caused by slow neutrons (from albedo), in which case displacement damage are produced, or by ionizing particles such as electrons, hadrons or photons. At this point no accurate estimates for radiation levels exist for the RHIC environment, but reasonably good estimates can be obtained from previous SSC studies [15, 16]. In making this estimates, one should keep in mind that although RHIC is a low luminosity machine for heavy ion beams, a typical event is expected to produce a multiplicity of final products of the order of 3000.

First, we focus our attention to damage produced by neutrons. Neutrons produce mostly dislocation damage, which is somehow recovered by thermal agitation (even at room temperature). At SSC luminosities, $10^{33}/cm^2s$, it is estimated that a integral flux of $2.4x10^{12}$ cm^{-2}/yr should be produced inside a cavity 2 m in diameter. Based on this estimate, we could expect a flux of the order of 10^{11}-10^{10} cm^{-2}/yr for the RHIC environment. According to the study by Raymond and Peterson [17], such a flux of neutrons should not produce any harm to the circuitry, whichever technology is chosen. However, one should have in mind that these numbers can be off by at least a factor two. As pointed out by Raymond and Peterson, the most susceptible technology to neutron damage is bipolar, which comes from degradation in the transistor gain. If the damage were all due to neutrons the best technology to be employed would be the CMOS.

The second type of radiation damaged suffered by the electronic circuits is due to ionizing particles. Ionizing particles are more likely to produce permanent damage in circuits, due the interaction with matter. At low energies (E<100 MeV), protons should behave as neutrons producing mostly dislocation damage. Due to the differing nature of the shower formation for hadrons and photons, hadrons are likely to produce less damage then photons for the same incident energy. In fact calculations done by Mokhol [18] show that the total integrated dose for hadrons is about a factor of 30 less than that produced by photons at the SSC. If now we take the numbers pertaining to the SSC and scale to RHIC luminosities, we find that the total dose due to photons is about 10^2 to 10^3 rad/year.

Such doses, according to the work of Raymond and Peterson [17], can start to produce some harm to circuits based on CMOS or bipolar technology as shown in Figure 2 of their paper. They also point out that there are ways of improving the radiation hardness for CMOS technology, which comes as a byproduct of circuit development for artificial satellites. However, it is not clear that such a technology would compromise the response of the devices for the purposes needed for RHIC detectors.

In summary, on the basis of previous SSC and Raymond and Peterson studies, the radiation damage produced by slow neutrons does not seem to be a problem at RHIC. On the other hand, in the case of ionizing particles, which produce more permanent damage, studies are needed for the RHIC environment in order to get more precise values for accumulated doses.

5. Practical Considerations in Carrying Out an ASIC Project

As mentioned in Section 3, it appears that the technology to carry out the development of an analog memory unit for RHIC exists, and some demonstrations of this type of circuit exist in the field of high energy physics. Nevertheless, if we are to achieve the performance which is demanded of RHIC detectors (see Table 2-1) and take into account the time structure of the accelerator, it will be necessary to carry out a development project specifically for RHIC. This is a major undertaking. In this section we outline the magnitude of the effort required and report on the experience of two past efforts of a similar nature.

Their are many levels of involvement of a laboratory or university group in the development and production of Application Specific Integrated Circuits (ASICs). The simplest level is to

specify device properties, locate vendors capable of meeting these specifications, select the vendor, usually after a bidding process, and verify that prototype and production devices meet these specifications. These minimal requirements might include logic simulation of digital devices or SPICE type simulation of analog circuits. A minimum organization to successfully carry out such an ASIC project would include a project manager, preferably with ASIC experience but at least having a broad knowledge of available technologies. The organization should include one or more persons with logic or analog design simulation experience. It should include people capable of developing test facilities. Testing of ASICs is a major effort. For example, gate array ASICs are generally tested by the manufacturer for logic functions but usually require the user to perform his own detailed testing because of the unique speed or function demands of ASICs in this field. Substantial efforts in both hardware and software will be required. Ordinary gate arrays can often be tested with commercial pattern generators and logic analyzers but invariably interfaces must be constructed, control devices designed and constructed to do parameter or margin tests. Even a simple gate array or memory device will require large combinational test sequences that can only reasonably be practical under software control and analysis.

In this simple example of ASIC development for which detailed silicon or gallium arsenide design is left to an outside vendor, a short list of personnel and equipment might read as follows:

Personnel:
- Project Leader (experienced)
- Logic design and simulator (digital)
- Analog design and simulator (analog)
- Test system designer for hardware implementation
- Test system designer for software implementation

Equipment:
- Computer and software for simulations & test management
- Pattern Generator
- Logic Analyzers -- Digital and Analog
- Application Specific Interface and Controller
- Ordinary lab equipment (i.e. scope, meters, power supplies, etc.)

This list is suitable for the simplest of ASIC development and would only apply where the

appropriate Cell libraries are available to the vendor. If circuit elements not available from Cell libraries are required a new level of complexity is encountered. This may involve in house chip layout and SPICE type simulations even for digital circuits. In this case the above list quickly expands to include silicon level design and layout capability with a perhaps extended learning curve plus chip level probe and test facilities probably including a clean room.

The MPS II drift chambers shift register project at BNL is illustrative of the process of ASIC development. This device is a 1024 bit 4 channel shift register capable of running at greater than 330 MHz while dissipating 200 mW. The project was funded in 1978. The first step was to canvas the industry. Some 30 companies were visited and in most cases high level technical discussions were held. Only three of these vendors were convincing as to their capabilities to meet the requirements. Two of them responded to the RFQ. The contract was awarded to RCA. Their design was an advanced CMOS-SOS process in which all logic Cells had to be designed and simulated since no circuits in their Cell libraries could approach the speed requirement. The output circuit led to a patent. Many months of design reviews were held before a prototype run was attempted. In fact, the first three prototypes runs failed for a variety of reasons.

Early on in the project (before the contract was awarded) it was clear BNL had to take responsibility for all testing, even at the wafer level since the speed of this ASIC was more that an order of magnitude beyond RCA's in house test capability. This effort alone accounted for more that a man year of engineering and development. The tester had to measure time to 100 ps, operate the chip from DC to 330 MHz and exercise parameters for margin tests. All of this under software control and in a fraction of a second. The instrument was designed to test chips at the wafer level or as packaged parts.

After prototype runs yielded successful parts on the pilot line, the processing was moved into production facilities. Wafers were produced and returned to the pilot line for testing. At one point 60 wafers were damaged beyond repair because of misaligned fingers on the probe card. The vendor should have found this problem before destroying $10,000 worth of wafers; they didn't until the BNL group convinced them of their faulty probe card. This is an example of how closely an ASIC development group must follow the manufacturing process to maintain

cost control. Device yields varied greatly, in part because this ASIC was an advanced state-of-the-art technology and the vendor had a poor understanding of the effect of production parameter variations on device performance. This is a situation that is likely to prevail whenever ASIC properties deviate from those of normal production devices. Chip development this far from the mainstream of production chips can only elicit cost plus fixed fee agreements or foundry only vendor responsibility. For the shift register, the final cost was three times the "budgetary" figures initially given. The time from contract signing to delivery of 20,000 working channels was about 36 months.

An ASIC project to develop analog memories has some features similar to the shift register ASIC. Some elements of the design such as amplifiers, memory Cells and switches are not available from Cell libraries. Thus design and simulation of these elements are required either within the project group or as part of a vendor contract. The accuracy, stability and reproducibility characteristics of this ASIC will require clever ideas in circuit design and extensive test and evaluation capability first at the prototype level where design changes are still possible and later during production where less flexibility is required but speed and efficiency become important. Since the Analog memory specification has not yet been set it is possible only to create a typical set of test requirements of things to be measured:

1. Transfer gain and linearity
2. Offset and stability
3. Rise and fall response times
4. Memory decay time
5. Noise
6. Dynamic range
7. Cross talk
8. Clock to data acquisition timing
9. Sensitivity to supply voltages
10. Sensitivity to temperature

This review of problems encountered in ASIC design and production may seem somewhat daunting but suggests such projects require careful personnel and equipment planning. In particular some of the design tools may require extensive training and practice along the learning curve.

Another experience in the design of an ASIC was presented by Larson at a recent IEEE meeting [19]. Larsen also describes many of the pitfalls which may be encountered in

carrying out such a project. He emphasizes that it is important to realize that there is a threshold level of manpower and support, below which it makes no sense to begin an ASIC project. He emphasizes that a team of specialists with the right mix of skills must be assembled and retained, and they must have proper mechanical and electronic engineering and technical support. The team members will become proficient in the use of CAD/CAE tools, and one risks losing them to industry. Testing of complex ASICs require at least as much engineering effort as the design itself. This problem becomes more severe as the complexity of the system increases. Testing needs to be done at several levels (Larsen suggests six), from tests at the production line all the way through tests of the full system, each requiring a separate hardware and software effort. Finally the problem of dealing with vendors is addressed, which is complicated by the fact that different vendors use different design rules for their ASICs. Care must be taken to create a "portable" design, if one is to take advantage of competitive bidding.

The conclusion the working group drew from discussions of these problems is that a serious effort to produce ASICs for readout electronics must be well supported and properly managed. It is possible that this work can be done through the combined efforts of several (4-5) groups at universities and/or national labs, if their efforts can be well coordinated. The total manpower level required is 15-20 people, among which must be several people with specialized training. The effort will probably require 5-6 years.

6. Conclusions and Recommendations

The working group concluded that a major problem will exist at RHIC which will affect nearly every detector. We will be unable to store the vast amount of electronic data in the usual way of using delay cables. An attractive alternative exists, namely the use of an analog pipeline, but although the technology to construct an IC to do the job is at hand, it will be necessary to mount a sizable effort to take advantage of it.

If such a device is to be developed for the first round of experiments at RHIC, the effort must be started immediately. The working group developed the following schedule, which illustrates the urgency of the situation:

1989	Design start, group assembled
1990	First chip element prototypes
	System design started
1991	Complete protyping and testing of chip elements
	System design completed
1992	Prototypes of system produced
	Full bench tests of system units
1993	Early production modules available for test beam trials
	Design refinements
	Arrangements for full scale production
1994	Full production
	Installation into completed detector elements
	Calibration of detector elements in test beams
1995	Assembly of full detector
	Detector systems tests
	First operation with collider beams

We recommend that high priority be given to the development an AMU for RHIC experiments, as we see no viable alternative to this device. The group concluded that the effort would be best carried out through the combined efforts of several groups which are centrally coordinated.

REFERENCES

1. H. H. Williams, "Detectors for the SSC: Summary Report," in Physics of the Superconducting Supercollider, Snowmass 86, p. 327.
2. W. Buttler, et al., "Design and Performance of a 10 MHz CMOS Analog Pipeline," Contribution to the San Miniato 1988 Topical Seminar, 7-11 March, 1988.
3. R. Van Berg, "The TVC Project," talk presented at this workshop.
4. M. Levine, "Report of the Data Acquisition Working Group," these proceedings.
5. J. T. Walker, et al., Nuclear Instruments and Methods 226, 200 (1984).
6. G. Anzivino, et al., Nucl. Instr. and Methods A243, 153 (1986).
7. C. Aldolphsen, et al., IEEE Trans. in Nucl. Science NS33, 57 (1986).
8. P. Dauncey, et al., IEEE Trans. in Nuclear Science NS35, 166 (1988).
9. P. Seller, et al., IEEE Trans. in Nuclear Science NS35, 176 (1988).
10. D. R. Freytag, et al., IEEE Trans. in Nuclear Science NS32, 622 (1985).
11. G. M. Haller, et. al., IEEE Trans. in Nuclear Science NS33, 221 (1986).
12. G. M. Haller, et. al., IEEE Trans. in Nuclear Science NS34, 170 (1987).
13. S. A. Kleinfelder, IEEE Trans. in Nuclear Science NS35, 151 (1988).
14. S. A. Kleinfelder, et al., IEEE Trans. in Nuclear Science NS35, 171 (1988).
15. D.E. Groom, ed., "Radiation Levels in the SSC Interactions Regions," SSC-SR-1033.
16. M.G.D. Gilchriese, ed., "Radiation Effects at the SSC," SSC-SR-1035.
17. J. P. Raymond and E. L Peterson, IEEE Trans. on Nuclear Science NS34, 1822 (1987).
18. N. V. Mokhol, tt, edited by D. E. Groom, SSC-SR-1033, uu, aa, 1988.
19. R. S. Larsen, IEEE Trans. on Nuclear Science NS35, 138 (1988).

Data Acquisition for RHIC: Report of the Working Group

Data Acquisition for RHIC
Report of the Working Group

M. Atiya, B. Gibbard, R. Hackenburg, M. LeVine*, T. Throwe, W. Watson
Brookhaven National Laboratory, Upton, NY 11973

J. D. Cole, M. Drigert
Idaho National Engineering Laboratory, Idaho Falls, ID 83415

H. Huang
Massachusetts Institute of Technology, Cambridge, MA 02139

I. Juricic
Columbia University, New York, NY 10027

C. Lourenco
CERN, CH-1211 Geneva 23, Switzerland

* Convenor

1. INTRODUCTION

As experimental configurations for RHIC become better defined [1], the requirements for data acquisition for each of the evolving experiments becomes susceptible to detailed analysis. An earlier contribution [2] made it clear that the scale of these experiments makes demands on data acquisition that are at least as severe as some of the large–scale collider experiments being mounted at Fermilab and LEP. In this report, we attempt to answer the following questions:

- What sort of performance is required by each of the experiments?
- Is there a single architecture flexible enough to accommodate all of the proposed experiments?
- What are the costs associated with such an implementation?
- How far in advance of beam does a data acquisition implementation need to be started?

The RHIC accelerator design, with 114 bunches in each ring, allows approximately 100 nsec between crossings. Depending on the physical scale of an experiment, this may not be enough time to distribute a first–level trigger decision to all components of the detectors. It certainly is not enough time to allow for a sophisticated decision. In order to avoid dead time imposed by the first–level trigger, a mechanism must be provided to store [for eventual digitization] the pulses arising from each detector element, for several crossings.

In carrying out this analysis, we were forced to anticipate the outcome of the development efforts for the readout electronics for RHIC (see [3]). The impact of the readout electronics on the data acquisition system architecture and costs cannot be underestimated. In the following discussion, it is assumed that the digitization of all signals takes place in chips mounted on the detectors and that the resulting digital signals are highly multiplexed before being shipped to the data acquisition crates. We also assume that sparse data scan [suppression of zero descriptors] takes place in the readout crates. This latter assumption has as a consequence that the limiting factor in number of channels per crate is no longer the number which can be physically accommodated [e.g., 96 channels/slot for a Fastbus crate], but, rather, the bandwidth limitation of the crate backplane.

The following discussion is carried out in terms of an architecture based on Fastbus crate segments. Computers manufactured by Digital Equipment Corporation are also mentioned. Focusing on specific implementations was necessary to calculate costs and performances; they are not to be construed as recommendations.

2. ARCHITECTURAL REQUIREMENTS

Data acquisition, in this report, is taken to begin at the point where level 2 trigger decisions have allowed the digitizers to run to completion. Event rates, therefore, refer to events which have survived a level 2 trigger decision.

Event rates of 5-50 kHz are possible from the point of view of digitizing hardware. A 50 kHz event rate for a tiny event size [10 kByte] corresponds to 0.5 Gbyte/sec data rate. Most of the experiments being discussed will have event sizes ranging from 100 kByte to a few Mbyte. We see immediately that the event rate quickly becomes irrelevant; it is the input data rate [event rate×event size] which is the limiting factor.

The output of a data acquisition system's front end is the event stream sent to the host for logging. This output stream is limited in data rate by available logging media to approximately 1 Mbyte/sec. Thus another important property of the data acquisition system is its ability to reduce the input data rate to the acceptable output rate via software [level 3] trigger decisions.

3. A COMMON ARCHITECTURE

We present an architecture for discussion in terms of the requirements outlined above.

3.1. The Readout Crates

The readout crates (Fig. 1) contain slaves which are likely to be receivers for the digital data streams, highly multiplexed on to optical fibers, from the detector-mounted digitizers. These modules will have pedestal memories and will suppress channels that are zero after pedestal subtraction. We estimate that the level of multiplexing at each fiber will be 100 and that as many as 24 fibers could be accommodated by a single Fastbus module. Thus a single Fastbus crate full of such slaves might represent as many as 48000 detector elements. The analysis presented assumes the bandwidth of the Fastbus backplane to be 40 Mbytes/sec. Even if only 10% of the detector elements fire in a typical event, a single such crate would produce 20 kByte/event, limiting the system to 2000 level 2 triggers/sec. If a higher rate is desired, fewer receiver modules can be accommodated in a single crate.

3.2. The Readout Controller

Mounted in each receiver crate is a readout controller which is responsible for reading the slaves in that crate and passing the resulting data on to a Fastbus cable segment. Each readout controller proceeds in parallel with the others, limited only by bandwidth in its crate.

It can be seen from the preceding discussion that it is essential to be able to read the contents of the slaves at the maximum possible rate. Thus the readout controller must be a bit–slice engine. [Several Fastbus masters based on bit–slice engines already exist.] The data stream from the crate segment is output directly on a cable segment. Thus each event fragment corresponding to the contents of a single readout crate is present on a distinct cable segment.

The bit–slice engine is controlled by a general-purpose microprocessor which is accessible via an Ethernet port (not shown in Fig. 1). Thus bit–slice instructions may be down–loaded from the host via this Ethernet port. Multiple Ethernet segments connected by bridges may be used here, as well as the 100 Mbit/sec systems which should be readily available in 3 years.

To facilitate subsequent processing, the readout controller will embed word counts for logical detector subdivisions in the data stream. This allows for rapid and efficient construction of pointers so that downstream processing is not required to search for descriptors.

Hardware would be provided to generate cyclical redundancy check words as the data is transmitted; corresponding hardware at the receiving end will check the integrity of the data on the cable segment.

3.3. The Spy

A spy on the cable segment functions as a frame grabber: it stores in its memory the contents of an entire event fragment. Analysis programs running on the host or on workstations can access these fragments via the spy's Ethernet port. Providing these spies at the readout crate level allows for monitoring of detector performance without wasting the Ethernet bandwidth by needlessly transmitting an entire event when only a small part of it is necessary. Spies at the next level provide access to the complete, assembled, event. While the spy is shown as functionally distinct from the readout controller, it might be implemented as part of the readout controller.

3.4. The Event Buffer Memories

Each cable segment is connected to a series of memories in event buffer crates. Each buffer crate has a separate memory, connected by a cable segment, corresponding to each readout crate. If the experiment is input–data–rate limited, then, to preserve total bandwidth up to the microprocessor farm level, there must be as many of these buffer crates as there are readout crates. In an experiment where the number of readout crates is determined by the number of detector cells to be read out, and where the data rate is not the determining factor, the number of event buffer crates may be reduced considerably, with a commensurate savings in cost. The use of multiple cable segments, with data flowing independently in each, allows the assembly of an entire event in one event buffer crate, without compromising the input bandwidth.

A synchronizing processor (not shown) selects an available event buffer crate as destination for the next transfer from the readout crates. A complete event is represented by the event fragments present in a single crate. These whole events are transferred from the buffer memories via a second cable segment to the third level trigger system. A second set of spies residing on these cable segments provides access to integral events for online monitoring.

The bandwidth limit assumed for all segments has been 40 Mbyte/sec, corresponding to a 100 nsec transfer time. This is a conservative estimate, based on some uncertainty about the reliability of the cable segment at higher speeds. Equally important are economic considerations arising from high speed memories required in the event memories; tens of Mbytes of 40 nsec memory will be costly! These are factors to be considered when operating parameters are defined.

3.5. The Third Level Trigger System

The third level trigger decisions are carried out by a farm of microprocessors arranged in banks; each bank serves a single event buffer crate. Events which survive the third level decision are collected by a dedicated microprocessor which transmits them to the host.

The microprocessors will be commercial, board–level products, based on one of several RISC chip sets appearing in the marketplace. These chip sets already have a processing power of 17 MIPS. It is conservative to estimate that 25 MIPS versions will be available in 3 years. A processor equipped with 16 MByte of memory should be available for under $10K. These processors will run code written in Fortran.

3.6. Limitations of the Architecture

Because there is an upper limit (approx. 24) to the number of event memories which fit into a single event buffer crate, and because there must be a buffer memory in each event buffer crate for each readout crate, this architecture cannot easily expand beyond 24 readout crates. This implies an input bandwidth limit of 1 Gbyte/sec.

The limited number of readout crates also implies that an experiment with a very large number of cells would have to provide multiplexing on a large scale. For example, an experiment with 10^6 detector cells, would require 40000 cells to be fed into a single readout crate.

4. ESTIMATE OF HARDWARE COSTS FOR AN EXPERIMENT

It should be apparent from the above discussion that a wide range of input bandwidth requirements, as well as a range of third level triggering demands, can be accommodated by the architecture outlined; it remains to be determined whether it is economically feasible.

Table I details a cost estimate for the case of:

1. Input bandwidth = 0.5 Gbyte/sec
2. Third level processing requirement = 1000 MIPS

The first item corresponds to readout crates equipped with readout controllers and spies, but otherwise empty. Too little is presently known about the readout electronics to be able to estimate the cost of the slaves. The number of readout crates required is dictated by the input bandwidth.

The number of event buffer crates is equal to the number of readout crates. The number of memory boards for this example is equal to the square of the number of readout crates: for input bandwidths much larger than 1 Gbyte/sec, the cost of this item quickly begins to dominate the total system cost. The cost of the event memory crates includes the necessary readout controllers and spies.

The device which synchronizes the readout controllers with available event buffer memories has not been included; its cost is expected to be small.

The microprocessor farm cost scales independently of the input bandwidth: here the number of MIPS required is given by the computing needs per event for the third level filter algorithm, together with the input event rate. For this example we use a farm with aggregate power of 1000 MIPS. With chip sets now beginning to be available, the power of 1000 VAXes can be compressed into 50 boards!

A host computer is required to control the front end, handle a reasonably large number of users, run database programs, and develop online and monitoring software. For an experiment of

the scale expected at RHIC, a machine of the class of a DEC 6240 [12 MIPS] is required, outfitted with magnetic tapes, and an array of disks.

The host computer is meant to be the nucleus of the computing resources at the experiment. Its power is inadequate to serve the needs of a large collaboration; it also lacks the essential bit-mapped graphics required to generate rapidly the experimental views we have all come to find indispensable. These gaps are filled by an array of workstations. Some of the workstations will certainly need to be equipped with color graphics, while most of them will serve adequately with monochrome displays. The costs shown in this example include the file servers necessary to avoid saturating the host with the I/O demands of multiple workstations. The 18 workstations detailed here represent an additional 30 MIPS.

Finally, some third-party software will have to be purchased, notably a distributed database.

5. DEVELOPMENT COSTS AND SCHEDULE

We have estimated the development costs assuming that a single group would develop the hardware and software for all of the experiments. These estimates are not very different, however, from the costs each experiment will have to bear if, for example, four different efforts proceed independently.

The schedule for development is based on the assumption that the system should be essentially finished 2 years before physics running [BEAM-2] is anticipated. This allows the system to be used for detector debugging and calibration, and provides adequate time for resulting problems to be corrected. With this goal in mind, the group would begin to be put in place at [BEAM-5]. Figure 2 shows the expected staffing profile, ranging from five people the first year to 23 people at BEAM-2. An average salary (including overhead) is estimated at $100K. The cumulative cost of manpower over the development cycle would be $10M. If each of four experiments proceeds independently, the total cost will be four times this amount.

An additional capital cost of $1.5M would be required to purchase tools, developmental hardware and prototypes, and a small-scale host computer system. Here again, if each experiment pursues an independent development path, the cost to purchase developmental hardware, etc., for four experiments will be $6.0M.

6. SUMMARY

We have outlined an architecture which is flexible enough to meet the needs of a wide variety of experiments. Use of a single architecture allows for consolidation of development of both hardware and software. A number of arguments can be made to proceed in this direction:

- Duplication of manpower is avoided (saves $30M !!)
- The software development task can be carried out correctly:
  - Documented software
  - Diagnostics for both hardware and software
  - A single set of RHIC standards and formats facilitate adaptation of outside [e.g., CERN] software
- Enhanced buying power, for both hardware and software
- Duplication of development hardware and tools is avoided (saves $4.5M)

REFERENCES

1. *RHIC Workshop, Experiments for a Relativistic Heavy Ion Collider*, April, 1985, P. E. Haustein and C. L. Woody, editors, BNL–51921, and *Proceedings of the Second Workshop on Experiments and Detectors for a Relativistic Heavy Ion Collider (RHIC)*, May, 1987, H.–G. Ritter and A. Shor, editors, LBL–24604.
2. J.W. Sunier, *Proceedings of the Second Workshop on Experiments and Detectors for a Relativistic Heavy Ion Collider (RHIC)*, May, 1987, H.–G. Ritter and A. Shor, editors, LBL–24604, pp. 243–250.
3. Report of Readout Electronics Working Group, contribution to this workshop.

TABLE I: Experiment Data Acquisition
Budget Example
Assumption: 0.5 Gbyte input rate

• 12 Fastbus crates (empty) including readout controller @$20K	$250K *
• Event Buffer Memories 12 Crates, 12 Memories each @$3K	$450K **
• 12 Event Buffer Crates including Readout controller @$20K	$250K *
• Microprocessor Farm overhead	$ 75K
• Microprocessor Farm 1000 MIPS	
• 50 Nodes [20 MIPS/16 Mbyte] @$10K	$500K
• Host Computer [DEC 6240]	$500K
Disk, Tapes, etc.	
• 6 High quality color work stations @$30K	$150K
includes file server overhead	
• 12 monochrome, less powerful stations @$13K	$150K
• Purchased software	$100K
Total:	$2425K

* Scales as (input bandwidth)

** Scales as (input bandwidth)^2

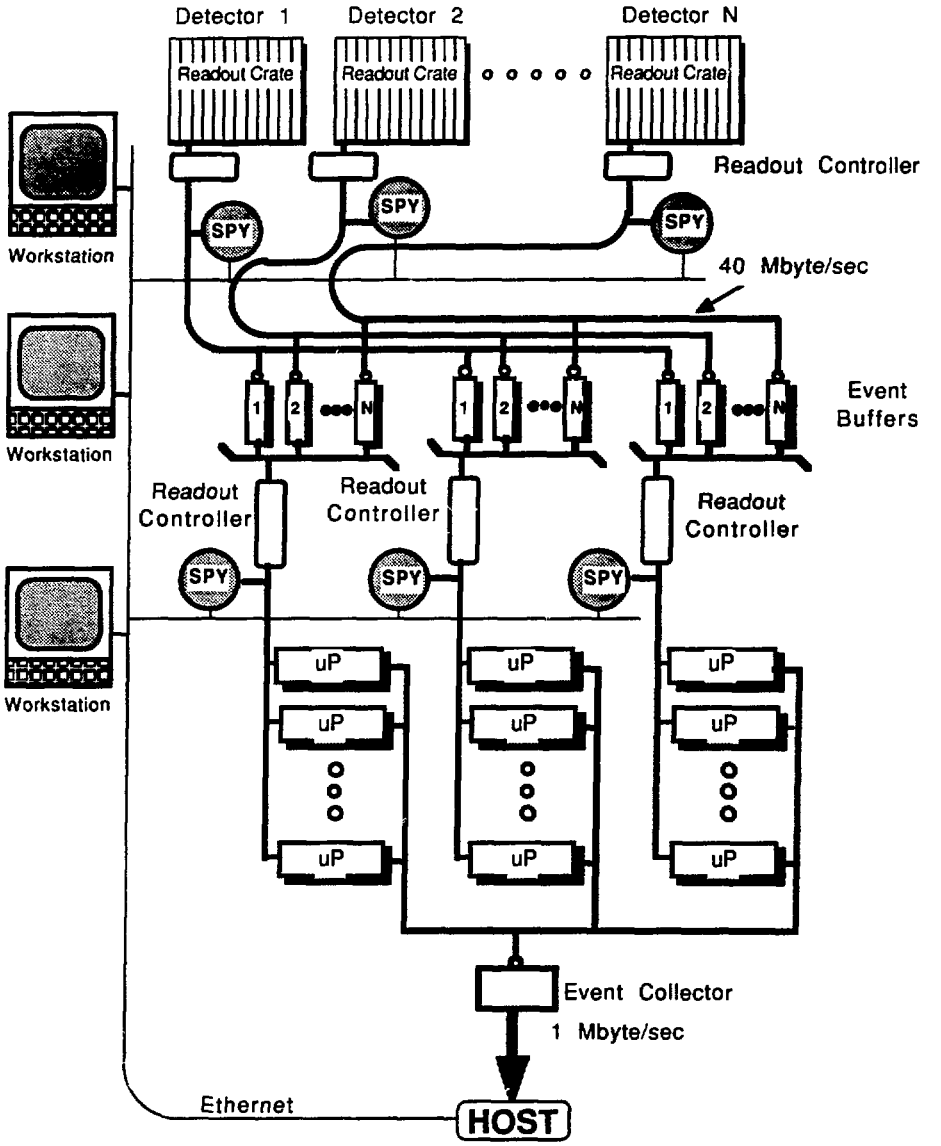

Figure 1. A data acquisition architecture for RHIC experiments

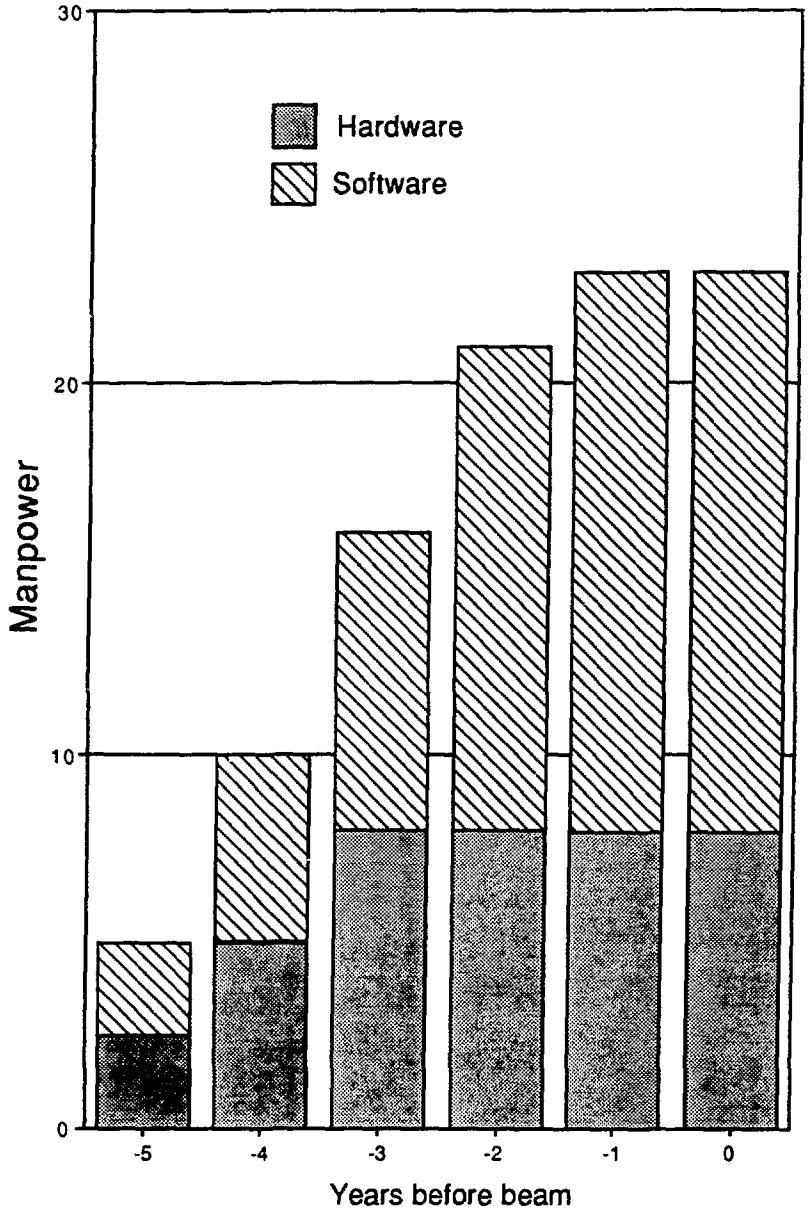

Figure 2. Required staff profile to implement data acquisition for RHIC experiments

Summary of the Working Group on Detector Simulation

SUMMARY OF THE WORKING GROUP ON DETECTOR SIMULATION

B.Shivakumar [a](Convenor)
F.Berger[b], B.Erlandsson[c], A.Gavron[d], N.Herrmann[e], K.Kadija[f], C.Lourenco[g], C.Merino[h], C.Muller[i], W.Schulz[i], S.P.Sorensen[j], J.Tran Than Van[k], and W.Zajc[l]

Other Working group participants
F.Paige[m], A.Shor[m], T.Throwe[m], P.Vincent[m], K.Werner[m]

a) Yale University, New Haven, CT, U.S.A..
b) University of Munster, Munster, West Germany.
c) University of Stockholm, Stockholm, Sweden.
d) Los Alamos National Laboratory,Los Alamos, NM, U.S.A..
e) State University of New York, Stony Brook, NY, U.S.A..
f) Max Planck Institute, Munich, West Germany.
g) C.E.R.N., Geneva, Switzerland.
h) University of Santiago, Santiago, Chile.
i) University of Marburg, Marburg, West Germany.
j) University of Tennessee, TN, U.S.A..
k) University of Paris - Sud, France.
l) Columbia University, Irvington, NY, U.S.A..
m) Brookhaven National Laboratory, Upton, NY, U.S.A..

INTRODUCTION

A major component of a successful experimental program at the proposed Relativistic Heavy Ion Collider (RHIC) is in the understanding of the detectors being used to study the physics. This involves complementary efforts in the testing of hardware, and in the use of these test results, in conjunction with predicted event characteristics, in simulations to ascertain how well the capabilities of the detectors are matched to the physics needs. The above group set forth to identify some of the requirements for carrying out a successful program to simulate RHIC detectors. The following summarizes our discussions on a set of varied topics related to detector simulation.

EVENT GENERATORS

In order to determine the multiplicity and energy distributions of the particles being produced in RHIC collisions, we compare the predictions of two event generators HIJET [1] and VENUS [2] with each other. Figures 1 and 2 plot the numbers of negative particles and baryons per unit of pseudorapidity, as functions of pseudorapidity, respectively. Each plot shows predictions of HIJET for minimum bias and central collisions.

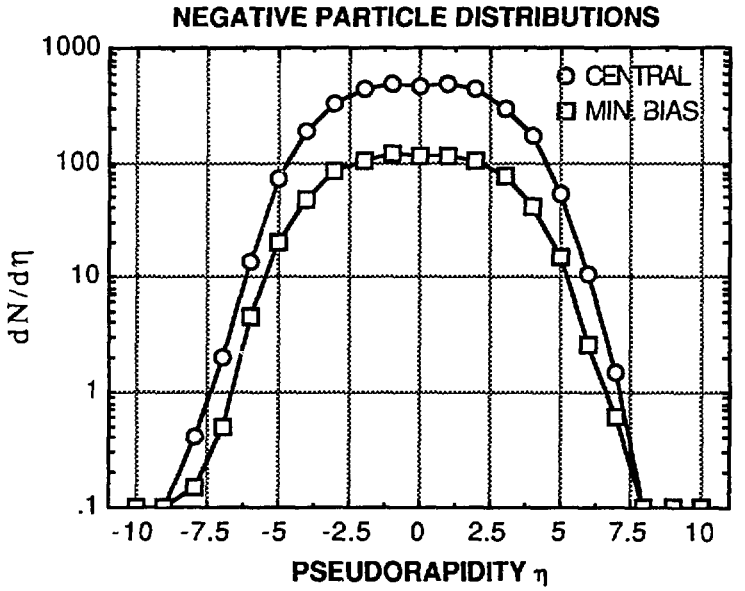

FIGURE 1:
Negative charged particle distributions predicted by HIJET for central and minimum bias Au+Au collisions at energies of 100+100 GeV/A.

[1] HIJET, T. Ludlam, A.Pfoh, A.Shor, p. 373 in RHIC workshop on experiments for a relativistic heavy ion collider, P.E.Haustein and C.L.Woody , editors, BNL 51921, 1985.
[2] VENUS, K.Werner, Z.Phys. C38, 193 (1988)

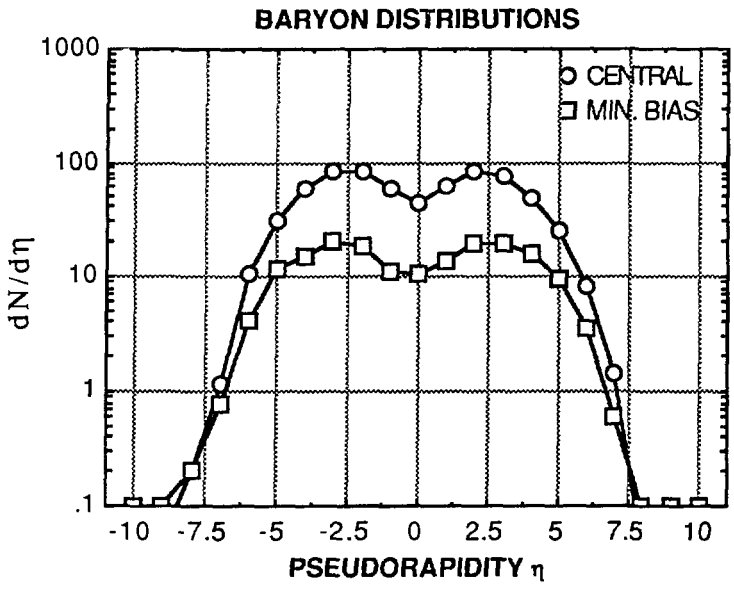

FIGURE 2:

Baryon distributions as predicted by HIJET for central and minimum bias Au+Au collisions at energies of 100 + 100 GeV/A.

Shown in figures 3 and 4 are the negative charged particle multiplicity, and the proton and antiproton multiplicity plotted as functions of rapidity for minimum bias and central collisions, as predicted by VENUS.

Two Track Separation

The density of particle tracks expected in central collsions is an important consideration in the design of tracking detectors and determines the eventual choice of detector pixel resolution. Shown in figure 5 is the numbers of charged particles per square centimeter at a distance of 1m from the target, as predicted by HIJET, plotted as functions of laboratory angles. This calculation implies that for the region of central rapidity, there are approximately 3×10^{-2} particles per square cm in a central collision. Using Poisson statistics one can determine that a 1% probability of two particles being found within a pixel translates to a pixel size of approximately 2cm x 2cm. One has to keep this in mind in determining the design considerations of a TPC or other tracking detector as have been proposed for use in RHIC experiments.[1]

---

[1]H.Gutbrot.et al., p 134 in Proceedings of the Second Workshop on Experiments and Detectors for a Relativistic Heavy Ion Collider, H.G.Ritter and A.Shor, editors, LBL 24604, Jan 1988.

Any simulation effort requires the characterization of the detector environment. What kinds of particles will the detectors see, how many of them are there of each kind, what are their energies, and how do these factors depend on angle, are some of the kinds of questions that influence the design of experiments. Such questions can be answered by computer programs which simulate the appropriate nucleus nucleus collisions, taking into account known physics processes, to predict event characteristics. Once these are determined, we can then proceed to understand how any proposed detector configuration will respond to these particles. There are two aspects that are of interest in the interaction of detectors with incident particles. The first involves the ability of the detector to study the physics. The focus here is on establishing whether the detectors have adequate position and/or energy resolution, geometric acceptance etc. The second aspect involves radiation damage. How long will detectors last when subject to the kinds of radiation doses they will experience on the experimental floor?

In the following, we begin by establishing the characteristics of events that RHIC detectors will experience. This discussion will be in the context of the various detection techniques discussed elsewhere in this volume. Folowing this we discuss standardization of event generator output. Our recommendations herein, if implemented, will greatly facilitate the simulation of detectors. The simulations themselves, when performed in detail, are rather computer intensive. There are aspects of these computations that are amenable to parametrization, and consequential reductions in computational time. We highlight some such efforts that could benefit from experimental measurements. The second aspect of detector studies, the radiation damage to detectors, can also be simulated. Herein, we only go as far as determining the levels of radiation doses that detectors will experience in RHIC experimental areas. Our discussions conclude with estimations of the computational and manpower needs of a successful RHIC detector simulation program.

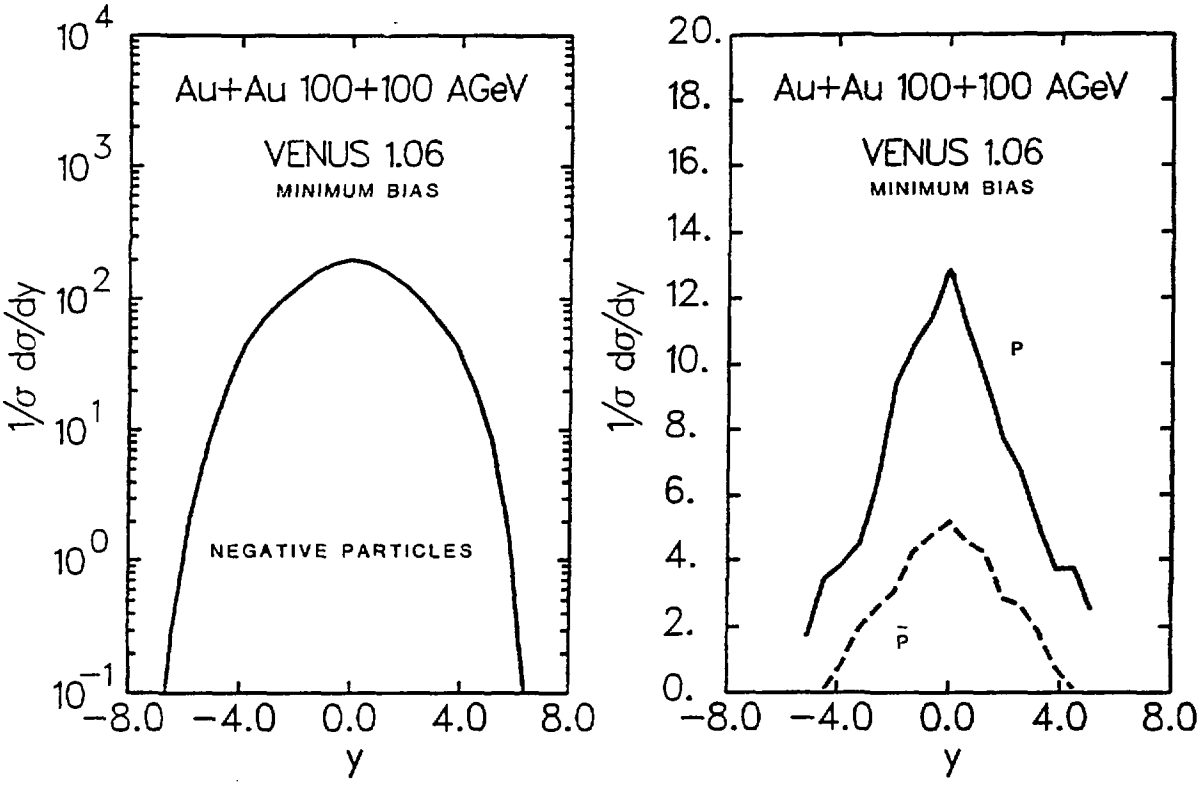

FIGURE 3:
Multiplicity of (a) charged particles and (b) protons and antiprotons predicted by VENUS for Au + Au collisions at energies of 100 + 100 GeV/A in minimum bias collisions.

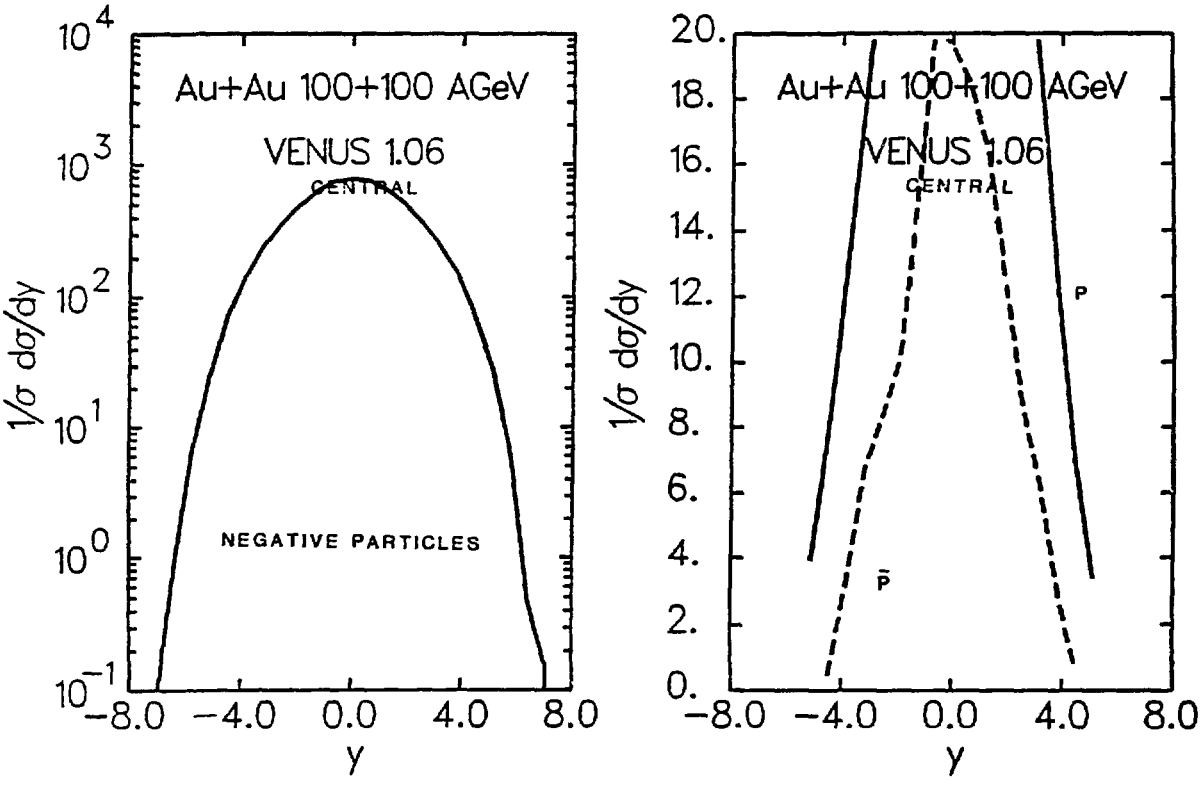

FIGURE 4:
Multiplicity of (a) charged particles and (b) protons and antiprotons predicted by VENUS for Au + Au collisions at energies of 100 + 100 GeV/A central collisions.

Particle Identification

Shown in figure 6 are the momentum distributions of pions, kaons, antiprotons, and protons for central RHIC events. It is clear that most of these particles have momenta in the range 0-2 GeV. Experiment 802 at Brookhaven has successfully demonstrated the use of time of flight techniques to achieve pion/kaon/proton separation to momenta up to 2.5 GeV[1]. One can therefore expect to achieve such separation with relatively minimal expense considering that such experimental accuracies can be achieved by todays state of the art technology. For more forward angles one has to resort to the use of techniques other than time of flight.[2]

Calorimetry

Figure 7 shows the double differential cross section $d\sigma/dEd\theta$ plotted as functions of laboratory angle θ and energy E. Evident is a steep rise in the momenta of the particles at angles forwards of 30 degrees. Projections of these figures on the energy axis are shown in figure 8 for ranges of angles in the central and forward rapidity regions. It bears emphasis that the bulk of the energy is carried by particles of low energy, and this poses a major challenge to calorimetry. The response of calorimeters to electrons and hadrons differs substantially at these energies. The relative response is also a strong function of energy. This will be an important consideration in the design of triggers based on particle blind total energy deposit.

---

[1] Y.Miake et al., E802 Collaboration, Z.Phys **C38**, 135 (1988).
[2] S.Nagamiya,, this volume.

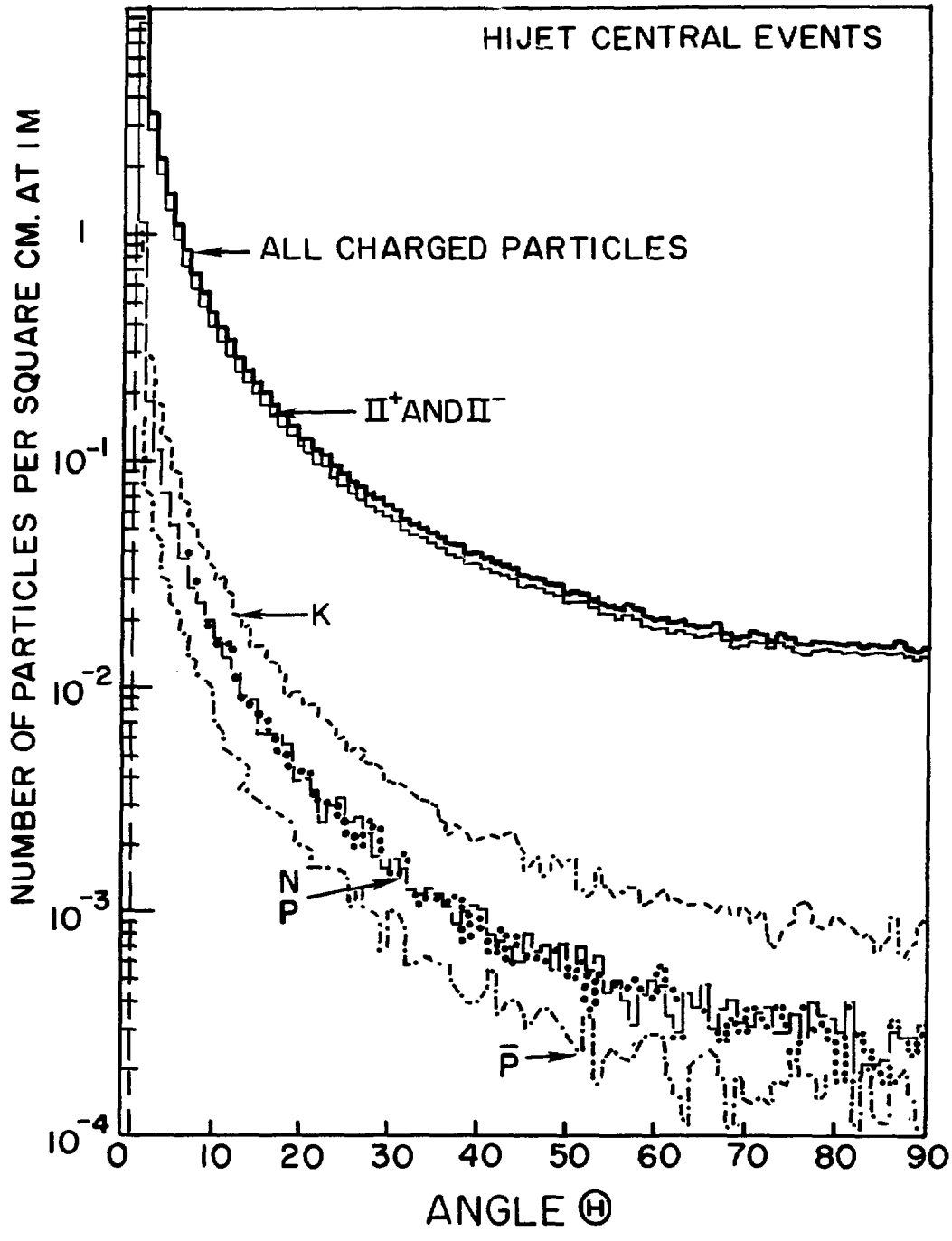

FIGURE 5:
Fluxes of charged particles per square centimeter at 1 meter from an interaction plotted as functions of angle, as predicted by HIJET for central Au + Au collisions at energies of 100 + 100 GeV/A.

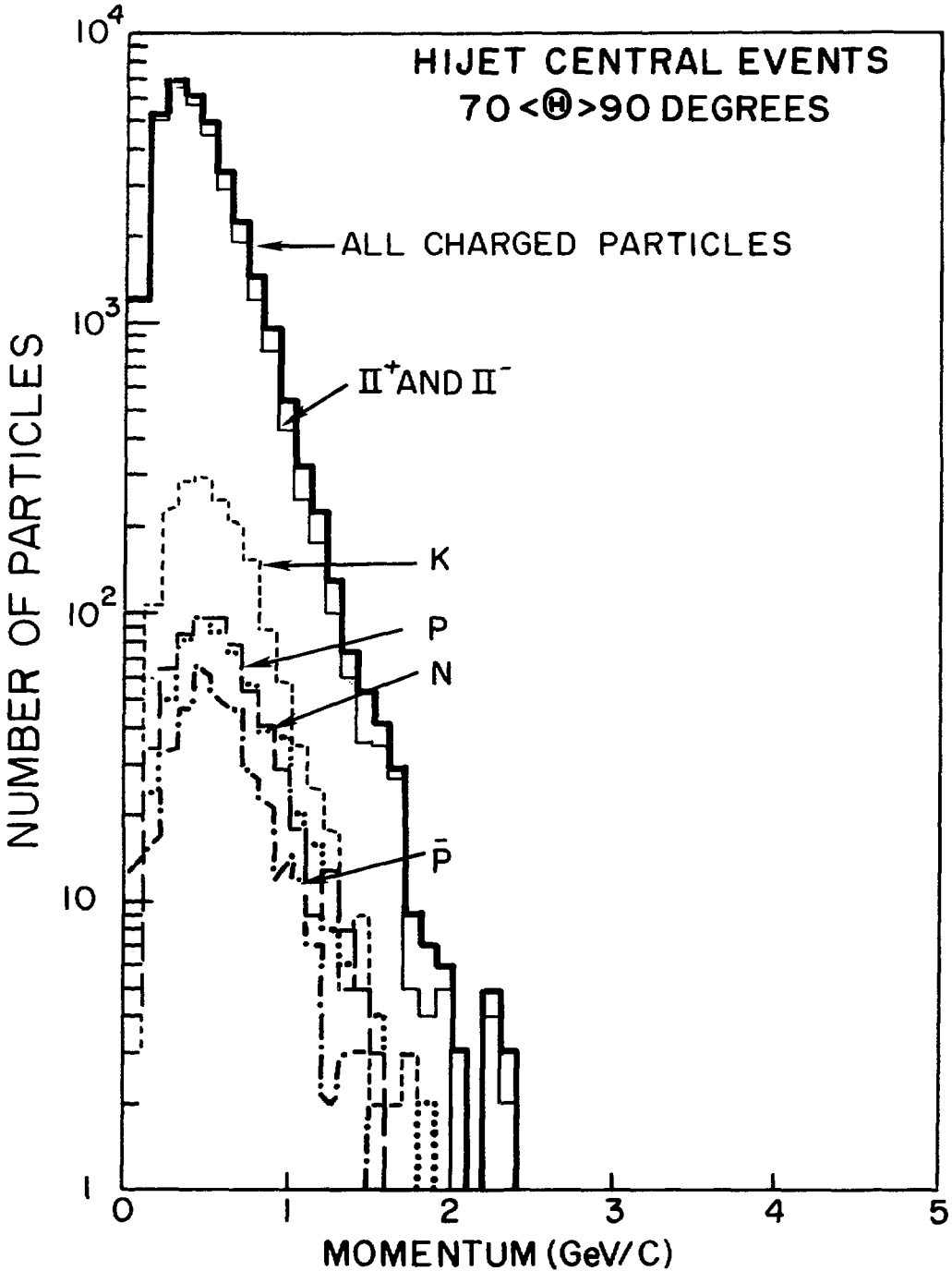

FIGURE 6:
The numbers of charged particles plotted as functions of their momenta, as predicted by HIJET in the angular range 70 to 90 degrees, for Au + Au collisions at energies of 100 + 100 GeV/A.

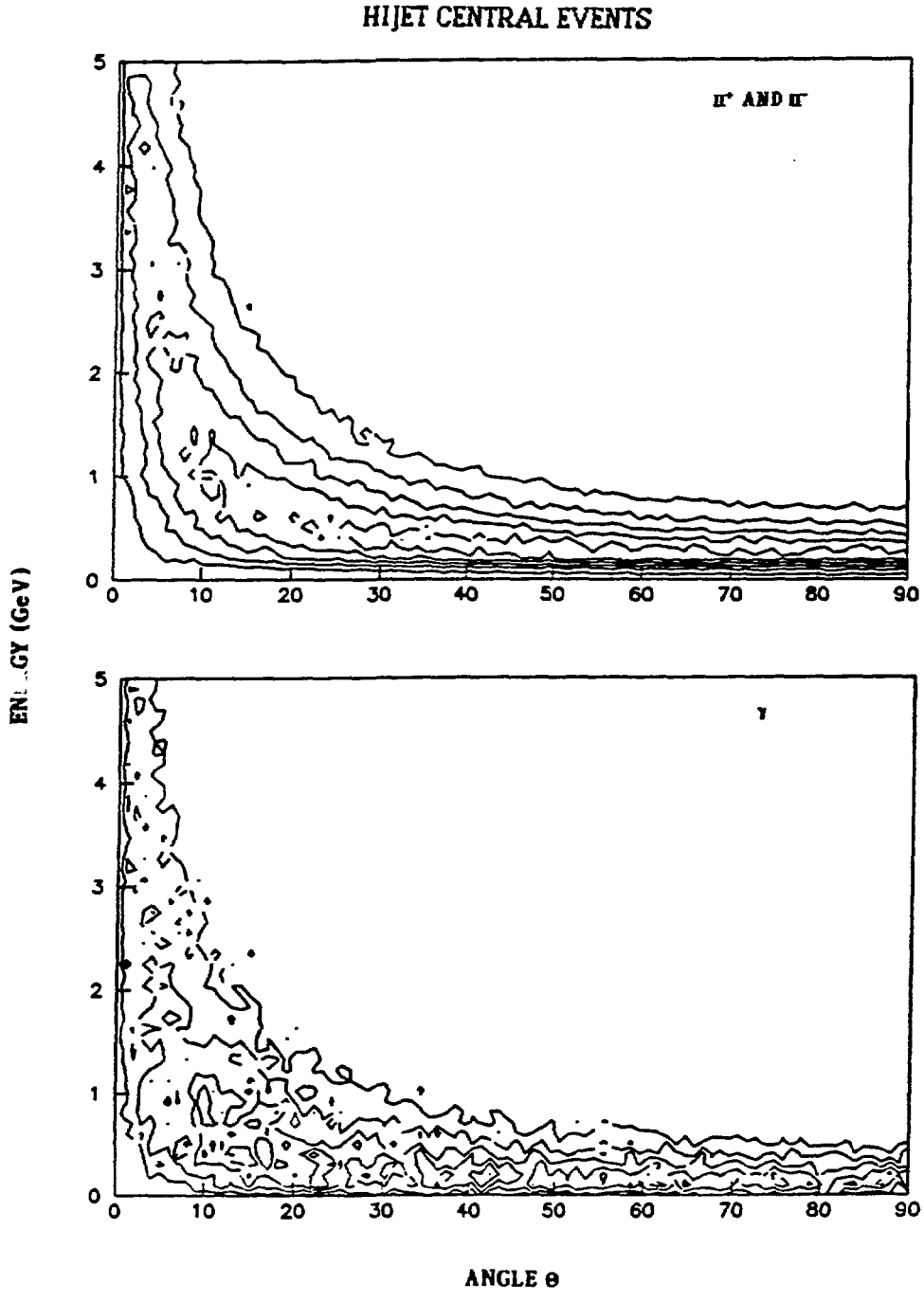

FIGURE 7:
The numbers of pions and photons plotted as functions of their energy and angle, as predicted by HIJET for central Au + Au collisions at energies of 100 + 100 GeV/A.

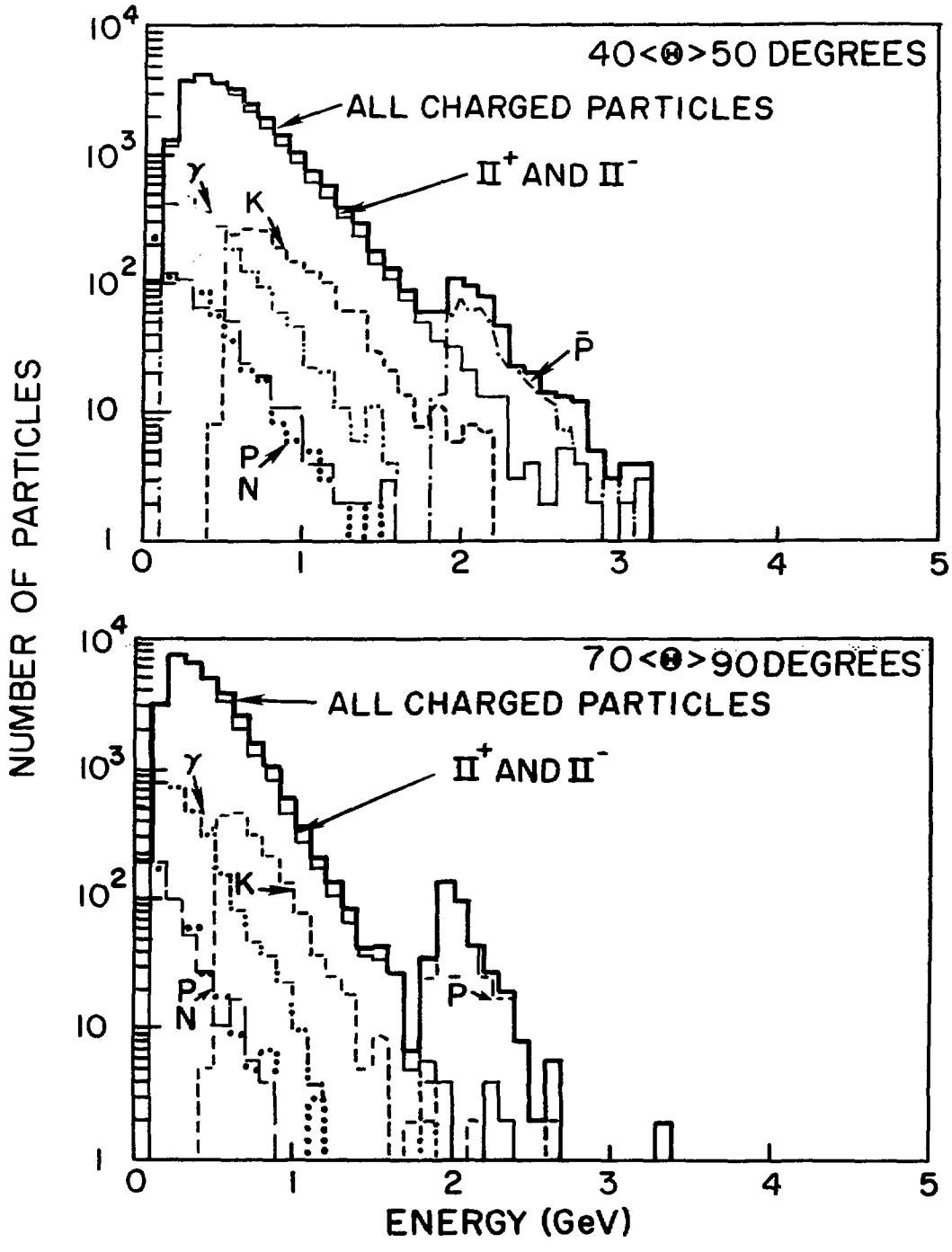

FIGURE 8:
The numbers of charged particles plotted as functions of their energies as predicted by HIJET in the angular ranges 40 to 50, and 70 to 90 degrees respectively for Au + Au central collisions at energies of 100 + 100 GeV/A.

STANDARDIZATION OF EVENT GENERATOR OUTPUT

There are several event generator computer codes that attempt to reproduce the physics of relativistic heavy ion collisions at RHIC energies. The information generated by these codes typically includes information on the four momenta of the particles produced on an event by event baisis. There is an acute need for uniformity in the way this information is presented, in the numbering conventions of particles, and in the manner in which events are stored. Standardization can be achieved by either direct changes in the source code, or through the provision of interface routines which convert the existing format into a standard format. A convention that seems to be both attractive and popular is that used by the program ISAJET[1]. Further, we felt it desirable to store this information in a format compatible with the ZEBRA[2] program of the CERN library.

[1]F.E.Paige and S.D.Protopopescu, ISAJET, Proc. 1982 Summer Study on Elementary Particle Physics and Future Facilities.
[2]R.Brun and J.Zoll, CERN program library.

It was decided by consensus that the kind of information we would like to get from an event generator should consist of the following.

1. Header	
Z_p	Projectile Charge
A_p	Projectile Mass
Z_t	Target Charge
A_t	Target Mass
E_p	Projectile Energy
E_t	Target Energy
MC ID	Identifier for Monte Carlo Code
b_{min}	Minimum Impact Parameter
b_{max}	Maximum Impact Parameter
2. Parameter Bank	
Version Number of Monte Carlo code	
Flags specific to Monte Carlo Code	
Status of decayed particles	
Only parents stored	
Only daughters stored	
Both parents and daughters stored	
3. Event Header	
Z_p^{par}	Projectile participant charge
A_p^{par}	Projectile participant mass
Z_t^{par}	Target participant charge
A_t^{par}	Target participant mass
b	Impact parameter for event
N	Total multiplicity of event
4. Particles	
S#	Particle sequence number in event
ID#	Particle identification number
P_x	X- momentum of particle
P_y	Y- momentum of particle
P_z	Z- momentum of particle
M	Mass of particle
τ	Lifetime of particle
D(1)	Decay identifier: Mother or daughter
D(2)	Sequence number of mother, if daughter

DETECTOR SIMULATION

Having replaced an accelerator by an event generator we are now faced with the task of replacing the detector system by a suitable simulation of it. This procedure involves defining detector geometries, materials, and identifying the nature and cross sections of the interactions of the generated particles with the detector. A good framework for doing this is provided within the computer program GEANT[1]. We have chosen to embrace this program as the one of choice owing to its good software support, and extensive use in the relativistic heavy ion community. The particle identification numbers in use in this program differ from those in use in the event generators, but interfaces exist to convert for example the ISAJET format into the GEANT format.[2]

Calorimeters

Shower Parametrization

One of the more time consuming aspects of detector simulation is the simulation of electromagnetic and hadronic showers. A few programs exist that simulate these showers in great detail. In particular, EGS[3] for the simulation of electromagnetic cascades and GHEISHA[4] and CALOR[5] for the simulation of hadronic showers have been particularly successful and widely used. These codes are very CPU intensive. Often one does not need detailed shower simulation in order to understand detector acceptance or response. In this case, one can resort to parametrizations of showers. These energy deposit profiles then replace the detailed hadronic or electromagnetic cascades. An alternative approach is to generate banks of detailed showers as generated by EGS, GHEISHA or CALOR. These can then be retrieved and applied whenever a shower is initiated in a detector. These approaches will perhaps lack in the details of reproducing fluctuations in calorimetry, further fixes for which can be introduced through introduction of fluctuations in the incident energies of particles.

---

[1]R.Brun, F.Bruyant, M.Maire, A.McPherson, GEANT Users Guide, CERN DD/EE 84-1

[2]ISAJET to GEANT interface, T.Throwe, private communication.

[3]W.R.Nelson, H.Hirayama, and D.W.O.Rogers, "The EGS4 code system", Stanford Linear Accelerator Center Report SLAC-265 (1985).

[4]H.Fesefeldt, The Simulation of Hadronic Showers - Physics and Applications, RWTH Aachen PITHA 85/02 (1985).

[5]T.A.Gabriel, K.C.Chandler, Particle Accel. 5, 161 (1973).

Low Energy Response

In the energy region of several 100 MeV, the simulation of hadronic cascades is not well implemented in any of the codes. This is the region of transition between two dominant modes of interaction between hadrons and calorimeters. The lower energy collisional energy loss begins to be influenced by hadronic interactions. A substantial fraction of the incident particle energy is lost in inelastic nuclear collisions. The energy is also only just above the pion production threshold. A fair amount of the energy in RHIC collision is carried by several such soft particles, and their proper simulation requires both computational effort, and complementary test beam studies. Some time has been devoted to such studies by the 814 collaboration[1], and further work is strongly encouraged.

Albedo Particles

Several of the detectors being proposed for RHIC experiments rely on central tracking or vertex detectors surrounded by calorimeters to effect total event characterization. It is well known that some of the energy of particles incident on calorimeters is directed backward in the form of Albedo neutrons, photons and charged particles. These can affect the experiment through the introduction of spurious tracks, and increased measured multiplicities. It is important therefore that the multiplicity, energy and angular distributions of Albedo particles be measured, and such information be incorporated into simulation codes. There has been some effort in this direction[2,3], and further test beam studies are encouraged. There have also been attempts to study the predictions of GHEISHA in this context.[4]

Side Leakage

Some of the proposed detectors use tracking over limited solid angles through ports in calorimeters. It is important to know therefore the number and character of tracks generated in these detectors by particles leaking out of the sides of these calorimeters. An estimate puts the number of these tracks in the case of the external spectrometer in the NA34 experiment at the level of 20%. Such leakage needs further study, and is already included in detailed shower simulations. Some attempt needs to be made to see how well

---

[1]M.Fatyga, E814 note, Brookhaven National Laboratory,1987.
[2]K.Jayananda, W.Cleland, and D.Kraus, E814 Note #34, Feb 1988.
[3]M.Albrow et al., Nucl. Instrum. Meth., **A256**, 23 (1987).
[4]A.Gavron, p169 in in Proceedings of the Second Workshop on Experiments and Detectors for a Relativistic Heavy Ion Collider, H.G.Ritter and A.Shor, editors, LBL 24604, Jan 1988.

these leakage fluxes are predicted by existing codes, and if these numbers can be parametrized is some simple manner.

RADIATION ENVIRONMENT

A good knowledge of the radiation present in the vicinity of RHIC detectors is essential in evaluating the likelihood of detector failure as a consequence of radiation damage. The radiation fluxes can be estimated from a knowledge of luminosities and interaction rates. The expected maximum luminosity at RHIC is 9.2×10^{26} cm^{-2} sec^{-1}. For an Au + Au cross section of 5.13 barns this corresponds to an event rate of 5×10^{3} sec^{-1}. From fig. 5 one notes that the charged particle flux at a distance of 1m from the target is 2×10^{-2} cm^{-2}. For a minimum ionizing energy loss of 2 MeV gm^{-1} cm^{2} this translates to a charged particle flux of 100 sec^{-1} and an energy deposit of 2×10^{12} MeV Kg^{-1} $year^{-1}$. This is equivalent to 32 Rads/yr. or 0.32 Grays/yr. (1 Gray = 1 Joule/Kg). This information is plotted in figure 9. It is interesting to note that these radiation levels are two orders of magnitude below the levels at the SSC.[1]

The beam at RHIC consists of buckets of 10^{9} particles, 100 of which are in the ring at any time. This corresponds to a total energy of 2×10^{18} MeV. If per chance this energy gets dumped into a detector, it can be very damaging. It is at such energy deposits in the calorimeter that the NA38 experiment at CERN has had to replace their scintillators. It is fair to state however that newer and more radiation resistant scintillating materials are becoming available. The concern of radiation damage by direct beam however is still an important consideration for detectors and electronics.

[1]Radiation Levels in the SSC Interaction Regions. D.E.Groom editor. p46, SSC-SR-1033 (1988).

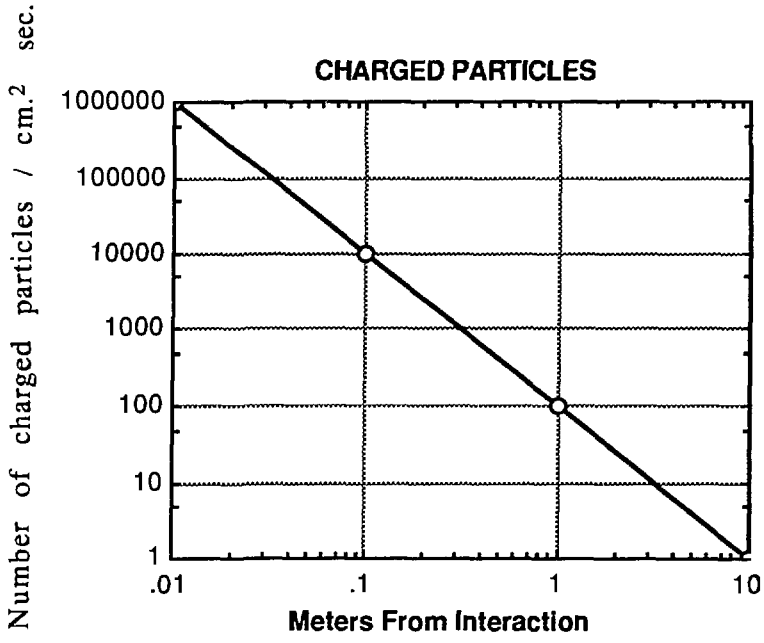

FIGURE 9:

The fluxes of charged particles seen by RHIC detectors plotted as functions of distance from the interaction. The plot is for central collisions.

COMPUTATIONAL POWER

Time

In units of millions of instructions per second (MIPS), the simulation of calorimeter showers takes of the order of 10 seconds/GeV for hadronic showers, and 30 seconds/ GeV for electromagnetic showers. Assuming an event multiplicity of 10^4, for particle energies of 3 GeV, this translates to 10^6 MIPS. seconds per event (10 days). These simulations propagate showers in great detail. Detailed shower simulation is not always essential. One can, for the most part resort to parametrizing showers[1], or work from banks of showers[2], and combined with improved computational efficiency, one can perhaps improve the throughput of calculations by one to two orders of magnitude. Hence in order to achieve reasonable statistics on simulations, and results in a timely fashion, one needs the dedicated use of a 100 MIPS computer. This can be achieved either through use of ACP farms[3] or local networks of VAX[4] or other computers[5].

Manpower

We feel that there is a need to set up a central design group for RHIC to focus on detector issues in the manner of the group that exists for the design of the accelerator. This group should include scientists, engineers and programmers. In the context of detector simulation, there needs to assigned to supporting computational activities. We expect the actual detector simulation will be performed by people associated with the various detector groups. The centralized effort will either support a dedicated RHIC computational effort, or augment existing computational efforts at Brookhaven, with an emphasis on RHIC specific needs. We anticipate that this will occupy four full time persons.

Money

We estimate that first round RHIC computational effort going would require an initial hardware expense of around 0.5 M$. This would allow the purchase of a 100 MIPS equivalent machine. An annual expenditure of 300K$ would be required for salary support .

---

[1] R.Bock et al., Nucl. Instrum. Meth, **186**, 553 (1981)

[2] A.Caldwell et al., Report of the working group on practical Shower algorithms, p270 in the Proceedings of the Workshop on Detector Simulation for the SSC, L.E.Price, Editor, Argonne National Laboratory, August 1987.

[3] I.Gaines and T.Nash, Annual Review of Nuclear and Particle Science, **37**, 177 (1987).

[4] R.Raja, p146 in the Workshop on Detector Simulation for the SSC, L.E.Price, editor, ANL Report, 1988.

[5] N.Carriero and D.Gelernter, Yale Univ. Dept. of Com. Sci. RR-628, May 1988.

100K$/yr would be required for hardware upgrades, and a sum of 50K$ per year should cover operating expenses.

RECOMMENDATIONS

Our primary concern is that there needs to be a centrally supported computational effort to facilitate the simulation of RHIC detectors. Such support should include the maintenance of computational hardware and the updating, documentation and distribution of physics specific software such as the CERN library, event generators, and RHIC detector geometry information Centrally supported software efforts could provide enhancements to existing software, and perhaps direct some effort to writing code to interface CAD/CAM software, as will undoubtedly be used in the design of detectors, with the geometry banks of detector simulation codes such as GEANT. Such code will be effective in providing an invaluable interplay between detector design and simulation.Such effort can be successful only if there is specific allocation of manpower and money.to RHIC detector simulation.

We have only begun to highlight the aspects of detector simulation that we think merit further study in the context of RHIC detectors. Much work remains to be done, and some of it needs to start right away. We share in the eagerness of the other detector techniques groups in looking forward to participating in this work and in an exciting and enriching research program at RHIC.

ACKNOWLEDGEMENTS

We acknowledge gratefully the hospitality of Brookhaven National Laboratory for the duration of the workshop, and for providing us with a stimulating working envirinment. This work was supported in part by the A.W.Wright Nuclear Structure Laboratory, Yale University, under contract #DE-AC0276-ER03074 with the U.S. Department of Energy.

B Physics at RHIC

B Factory at RHIC?[1]

N. S. Lockyer, R. Van Berg, F. M. Newcomer
University of Pennsylvania

K. Foley, W. Morse, F. Paige, V. Polychronakos,
S. Protopopescu, P. Rehak
Brookhaven National Laboratory

R. Sidwell
Ohio State University

E. Mannelli, M. Mannelli
Yale University

Abstract

A dedicated B physics experiment located in the proposed Relativistic Heavy Ion Collider at Brookhaven (RHIC) is considered. The machine may operate in a p-p mode with a luminosity in excess of $10^{32} cm^{-2} sec^{-1}$ at 250×250 GeV. The estimated $B\bar{B}$ cross section at these energies is about 10 $\mu barns$ and a run of $10^7 sec$ would produce roughly 10^{10} $B\bar{B}$ pairs. A comparison to similar ideas proposed for the Fermilab Tevatron Upgrade and the SSC are discussed. The most ambitious physics objective of such an experiment would be the study of CP nonconservation. Particular emphasis at this workshop was given to the self tagging mode $B \rightarrow K^+\pi^-$. Experimental techniques developed during this experiment would be extremely useful for more ambitious projects anticipated at the SSC.

Introduction

The possibility of studying large samples of heavy quarks has been a subject of discussion at Brookhaven since the early 1980's [1]. The proposed Relativistic Heavy Ion Collider (RHIC), operated in a p-p mode, is expected to reach a luminosity in excess of $10^{32} cm^{-2} sec^{-1}$ at an energy of 250×250 GeV. The $B\bar{B}$ cross section is estimated to be [2] 10 $\mu barns$ and could produce a sample of about 10^{10} $B\bar{B}$ pairs per run. The use of a single lepton or stiff track trigger to enhance the ratio of events containing B mesons to total production, a Lorentz boosted B system, manageable interaction rates, and a very large B cross section make the RHIC hadron collider approach very attractive.

There are several considerations to take into account when running at lower than SSC energies in a p-p collider.

1. The $B\bar{B}$ cross section increases with energy and the ratio of $B\bar{B}$ to the total cross section becomes more favorable at higher energy. The $B\bar{B}$ production cross section at RHIC energies is $\sim$ 1000 times that at fixed target energies using hadron beams and nearly 10,000 times that of $e^+e^- \rightarrow \Upsilon(4s)$. Some estimates place the SSC $B\bar{B}$ cross section some 500 times larger than that expected at RHIC energies. The SSC may produce a $B\bar{B}$ pair every 100 collisions. The $B\bar{B}$ cross section at 2 TeV is

[1] B Physics Working Group Summary presented by N. S. Lockyer at the RHIC Workshop held at BNL July (1988)

about 5 times larger than at RHIC energies and an experiment at the Tevatron can expect a $B\bar{B}$ pair every 1000 collisions.

2. At RHIC energies the detector need only cover a fraction of the full solid angle. The rapidity range of produced $B\bar{B}$ pairs and the decay products are limited to ± 2 units of rapidity. This simplifies the detector design . A Tevatron and SSC detector must cover down to 3.5 and 6 units of rapidity respectively.

3. Results from Monte Carlo studies indicate triggering on the number of stiff, >1–1.5 GeV P_t , tracks per event in the RHIC and Tevatron energy range efficiently identifies $B\bar{B}$ events. Requiring several stiff tracks in conjuction with a secondary vertex appears to have sufficient rejection to allow triggering on modes such as $B \rightarrow K^+\pi^-$. This is a so called self tagging mode, the daughter K determines or "tags" whether the parent is particle or anti-particle. These modes are interesting for CP studies. Stiff track techniques are thought to be much less useful at SSC energies because the number of "mini-jets" or the fraction of minimum bias events with a hard scattering component increases with center of mass energy.

4. A factor related to the machine energy is the Lorentz boost. There is a smaller bottom path length at RHIC relative to the SSC and Tevatron. This is because the boost is governed by the kinematics of production and the bottom meson P_t which changes slowly between the two energies.

5. At RHIC energies and above, the production of bottom quarks is dominated by gluon fusion and therefore little difference exists between production rates in p-p and $\bar{p}$-p colliders.

The demands on the experimental design and performance are challenging at a hadron collider and much detector simulation and study is required to demonstrate that the efficiency for reconstructing the $B\bar{B}$ pairs is high enough to be competitive with other ideas. An ambitious goal, including triggering, is to achieve an efficiency of a few percent for reconstructing an all charged, low multiplicity mode. When the CP study requires tagging the other B, the best one can realistically do in a p-p collider is about 10%.

This paper addresses some of the first issues regarding a bottom collider experiment at RHIC. The work here follows from work elsewhere and has raised several interesting ideas and options for people wishing to pursue this physics. The latest round of interest in B colliders followed from two Letters of Intent to build dedicated experiments for intersection region C at the Fermilab Tevatron Collider in March 1987 [3,4]. Since then the High Sensitivity Beauty Workshop at Fermilab (Nov. 1987) began to address many of the issues in a little more detail [5,6,7,8]. This work is being continued by the Bottom Collider Study Group at Fermilab, and other individuals who have participated in various workshops such as the Berkeley SSC Workshop in 1987 [9] the SSC Snowmass '88 Summer Study and at Brookhaven for RHIC related activities. The main issues relevant to a bottom collider experiment discussed here are:

1. Bottom Physics Goals
2. Comparison to Other Machines

3. Machine Issues for RHIC

4. Kinematics

5. The detector

6. Conclusions

1. Bottom Physics Goals

The physics these experiments address is very broad in scope and is reviewed by A. Sanda at this conference [10,11,12,13]. The topics of interest are mixing in both the B_d and B_s systems. The UA1 Experiment CERN has observed evidence for mixing in a study of dimuons. The Argus experiment has observed mixing in the B_d system at the 20% level [14]. Recently, the Cleo experiment at *CESR* has confirmed this result. This large mixing can substantially increase the size of CP violation in the B system, and therefore a more precise measurement of the mixing is important. The observation of a B_s mass peak and the subsequent study of the decay modes and B_s mixing are very important. It has been pointed out that the relative size of the mixing in B_s and B_d is a test of new quark generations [15]. Other important information will derive from the study of production mechanisms, rare decays, forbidden decays, and bottom baryons [16,17]. A thorough study of the charmless decays will be important for understanding the standard model [18,19]. Some of the above will be studied by the existing 'B factories,' *CESR* and *DORIS*, *Z0* factories, and hadron experiments.

The major physics goal is to observe and study CP nonconservation in the neutral and charged bottom system. First consider the neutral B system decaying to a CP eigenstate. The CP asymmetry discussed is the difference in rates for particle and antiparticle into the same final CP eigenstate, for example

$$A = \frac{\Gamma(B \to \psi K_s) - \Gamma(\bar{B} \to \psi K_s)}{\Gamma(B \to \psi K_s) + \Gamma(\bar{B} \to \psi K_s)}$$

The uncertainty in predicting which decay modes give large CP asymmetries suggests that more than one mode should be studied. In particular, an analysis Bjorken suggests [20] would imply that $B \to \psi K_s$ and $B \to \pi^+\pi^-$ gives complimentary information. Consequently, any experiment embarking on a study of CP must be sensitive to as many modes as possible. When studying neutral B mesons, in order to label the B as particle or antiparticle , the other B in the event must be identified or tagged.

A mode of particular interest at the workshop was $B \to K^+\pi^-$. This mode is expected to have a CP asymmetry of about 10% and the particle anti-particle nature of the parent B meson is determined by the K^+ or K^-. The two body decay will produce tracks with a P_t of about 2 GeV/c which are separable from the 300 MeV/c tracks in the underlying event. With good particle identification the combinatorics will be reduced substantially. Some estimates of the experimental factors are the:

- branching ratio, about 10^{-5}.
- trigger efficiency about 33%.

- vertex separation efficiency, about 50%.
- tracking efficiency, about 95%.
- cracks and Z length of beam, about 50%.
- reconstruction efficiency, about 25%.
- geometric acceptance , about 75%
- fraction of B_d mesons, about 40%
- B cross section of 10 μ barns.

We would like to achieve a combined efficiency, not including the branching ratio, of about a few percent. With a sample of 10^{10} $B\bar{B}$ events a CP asymmetry of about 10% could be observed at the 3 σ level. This assumes little background and no mistagged events. Typically, the CP asymmetries are in the 5–30% range [21].

For modes such a $B \to \psi K_s$ it is necessary to tag the other B in order to calculate the CP asymmetry. Tagging efficiencies (of the other B) are estimated to be in the 5%–10% range. Eventually the sources of mistagged events will have to be studied very carefully.

2. Comparison to Other Machines

- e^+e^- machines

The main advantages of the high energy hadron collider are the large cross section and the Lorentz boost of the $B\bar{B}$ pair. The cross section at the $\Upsilon(4s)$ is about 1 nb or $\sim$ 10,000 times less than at RHIC and p-p colliders can be competitive in luminosity with even the next generation e^+e^- machines being discussed. The aid of a vertex constraint on the tracks from the B meson produced at RHIC will be very powerful in reducing combinatoric background and is a technique not fully available at $\Upsilon(4s)$ machines.

The e^+e^- environment is very clean, the ratio of B meson to continuum production is about 1/4, compared to about 2×10^{-4} at the collider. Furthermore, on the $\Upsilon(4s)$ resonance, all charged tracks come from the bottom meson since there is not enough energy to produce extra pions. At RHIC, an average of 30 charged tracks are produced per collision in the bottom events. Again, the vertex constraint will eliminate the spurious tracks in the event.

It is unlikely present day e^+e^- machines will observe CP violation in the B system. The linear collider approach, proposed by U. Amaldi and G. Coignet [22] and by D. Cline [23] have suggested that luminosities of $10^{34} cm^{-2} sec^{-1}$ may be achievable as well as collisions with asymmetric beam energies, thus providing a Lorentz boost to the $\Upsilon(4s)$ system. Other ambitious approaches have been put forward from *SIN, KEK,* and *SLAC* [24,25,26]. More recently, *SLAC* has been studying the option of asymmetric collisions, yielding a boosted $\Upsilon(4s)$ system, by building a small ring to collide with *PEP*.

The higher energy e^+e^- colliders like LEP and SLC have the benefit of a boosted bottom meson allowing the possibility of vertex detection, a reasonably low multiplicity event, and very powerful detectors. However, they will not produce enough events to address CP violation in the neutral B system. Even at 10^7 Z^0's produced per year this is less $B\bar{B}$'s than *CESR* produces now.

• Hadron Machines Fixed Target

If the RHIC B experiment can handle $\sim 10^7$ interactions/sec, it can take full advantage of the larger $B\bar{B}$ cross section at collider energies. It seems likely that at least 10^9–10^{10} $B\bar{B}$ pairs are needed to initiate a study of CP in a hadron machine. The large bottom cross section, $\sim$ 1000 times larger than at hadron beam fixed target energies is an overwhelming advantage for the collider experiment. Furthermore, the ratio of bottom to total cross section, about 500 times larger at the collider, makes triggering and the extraction of a bottom signal easier than in fixed target experiments.

Events containing $\psi's$ may provide a clean trigger and sufficient background rejection to signal bottom production [27]. Alternative approaches to triggering in fixed target experiments are being considered to improve efficiency by including single lepton and multiplicity jump triggers. Other ideas are to pursue only two-body decay modes in very high rate experiments [28]. Considerably more experience is needed in this area. With a few hundred B's in hand in a couple of years, the reach of fixed target experiments may become greater. Recent reviews on this subject are given by J. Bjorken [29] and P. Garbincius [30].

3. Machine Issues for RHIC

The present RHIC ring has 4 developed and 2 undeveloped intersection regions. The layout of the accelerator is shown in fig. 1. A B experiment would need a new collision hall to be developed. The design report calls for an initial luminoisty of $10^{31} cm^{-2} sec^{-1}$ when operated in the p-p mode [31]. The machine design allows a luminosity of at least $2 \times 10^{32} cm^{-2} sec^{-1}$.

A two ring proton collider permits a crossing angle at the collision point which results in a significantly smaller interaction diamond in the beam direction. The nominal RHIC p-p beams collide with a σ_z of about 20 cm. This can be reduced to about 7 cm with a crossing angle of 3 mr, at some loss in luminosity, if there are no problems with beam stability.

The vacuum pipe can be placed within 1 cm of the beam collision point. The expected vacuum is 10^{-10} torr in the collision halls and 10^{-8} in the arcs.

The machine is presently expected to run $\sim$ 38 weeks of the year for heavy ions. This would mean roughly 8-10 weeks are available for high energy physics running. At a peak luminosity of $2 \times 10^{32} cm^{-2} sec^{-1}$ about 10^{10} events would be produced.

The funding profile requested for RHIC is such that if funding is started in $FY90$, then first beams are expected in 1995.

4. Kinematics

The kinematics of bottom production at RHIC are in many ways startling at first observation. The B meson P_t spectrum is very soft, averaging about 4.4 GeV/c. This can be compared to the P_t at the SSC (20 $\times$ 20 TeV), where it is about 6.5 GeV/c, quite similar. The reason is that the large cross section, about 10 μbarns, comes from gluon fusion, which has a pole around a P_t equal to the mass of the heavy quark being produced [32]. The other constraining factor is the rapidity distribution of the tracks from

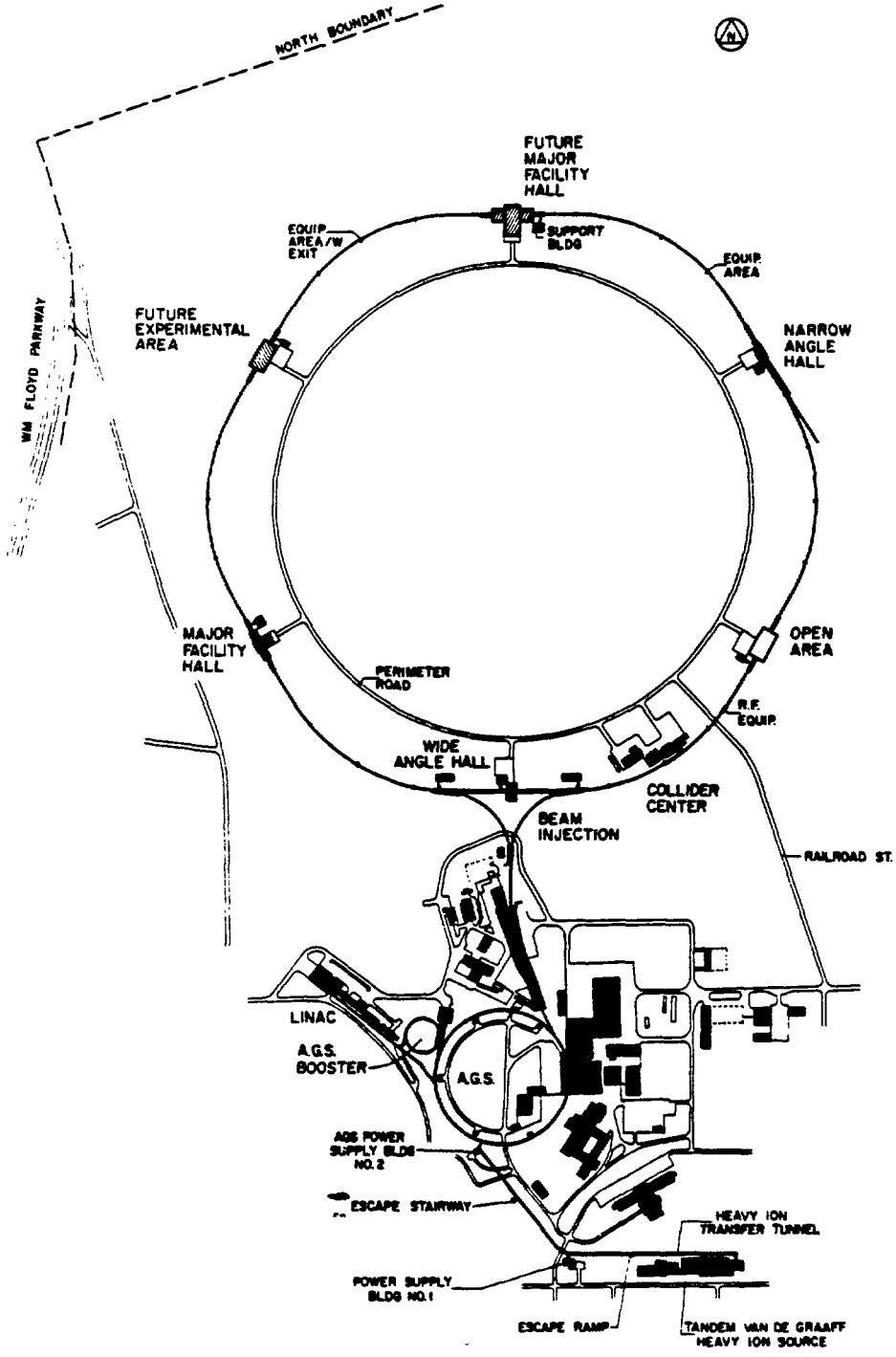

SITE MAP

Figure 1: RHIC storage ring showing the intersection regions. Either one of the two intersection regions marked for future use could be made available for a B Physics experiment.

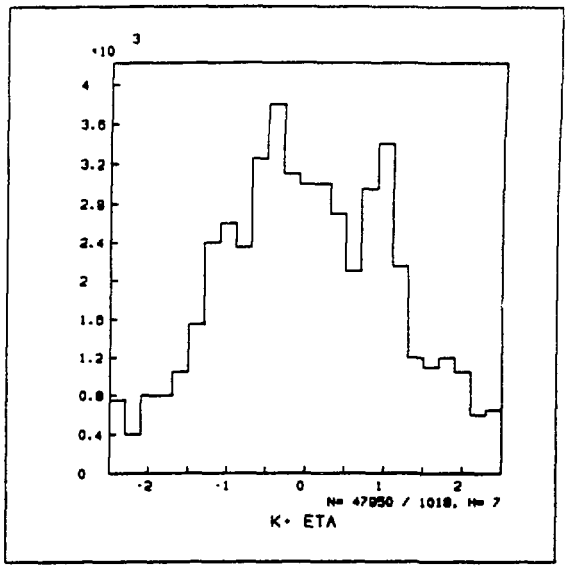

Figure 2: η of K Tracks from $B \rightarrow K^+\pi^-$

both bottom particles. About 90% of the tracks are contained within ± 2 units of rapidity at RHIC. The η spectrum of K's from bottom is shown in fig. 2. At the SSC, most tracks are contained within ± 6 units and this is because the increased particle production is pushed to higher values of rapidity as the energy of the collision is increased.

The average P_t and P of the K from the bottom meson is shown in fig. 3. Here the stiffness of the K relative to a typically 300 MeV/c track in the underlying event is evident. The problems associated with triggering on these "stiff" K's is a challenge for the experimenter.

Another important feature of the kinematics involves the path length l distribution of the B mesons from the collision point. The distribution is shown in fig. 4 for B's and in fig. 5 for D's.

5. Detector

This section describes briefly some of the components of the detector and the required performance. A schematic of the detector is shown in fig. 6. An isometric view of the B Physics detector is shown in fig. 7. All tracking and electromagnetic calorimetry are immersed in a 2.0 meter radius 1.5 tesla solenoidal magnet field. The various systems include: vertex detector, charged particle tracking, transition radiation detectors and calorimetry for electron identification, a muon absorber, particle identification for kaons and no hadron calorimetry since missing E_t is unimportant. These systems cover 90^0 to 20^0 in theta.

• Vertex Detector

The vertex detector must perform well for this experiment to identify a clean B invariant mass peak. The combinatoric background is expected to be reduced substantially

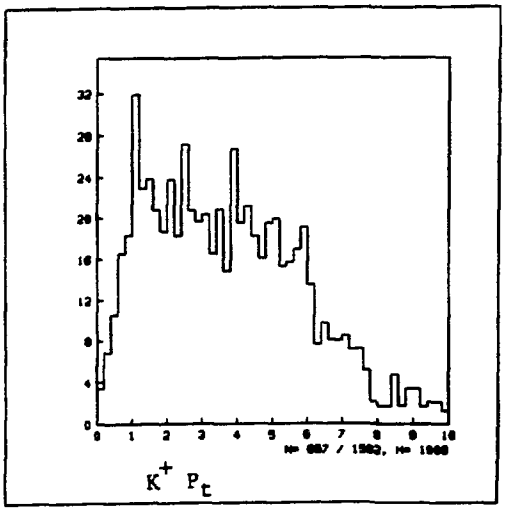

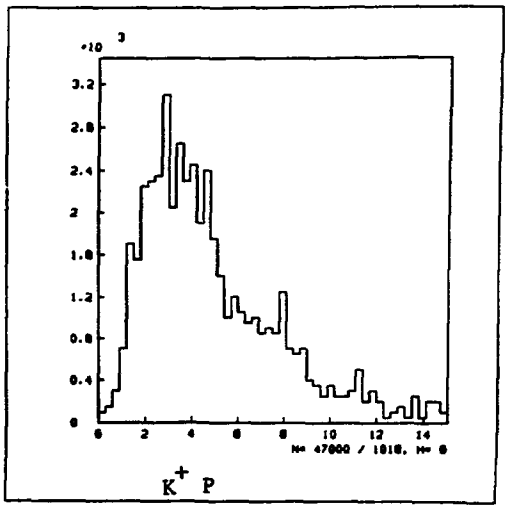

Figure 3: a) P_t , b) P of K from $B \to K^+\pi^-$

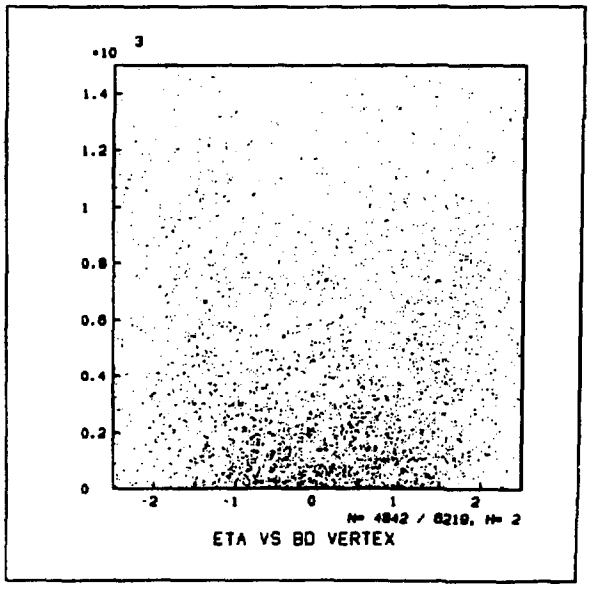

Figure 4: B Path Length (microns) vs. η

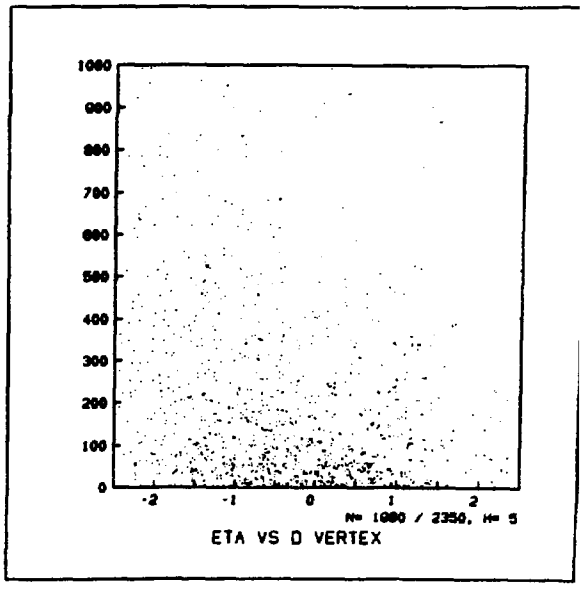

Figure 5: D Path Length (microns) vs. η

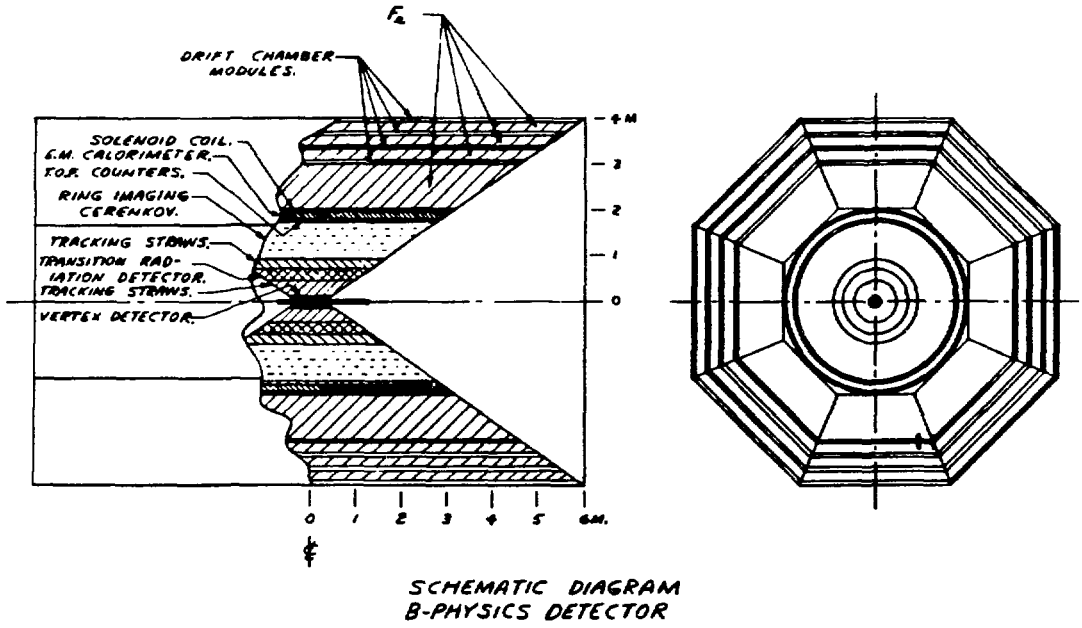

Figure 6: Schematic representation of a B Physics detector showing the various types of devices needed and their likely dimensions.

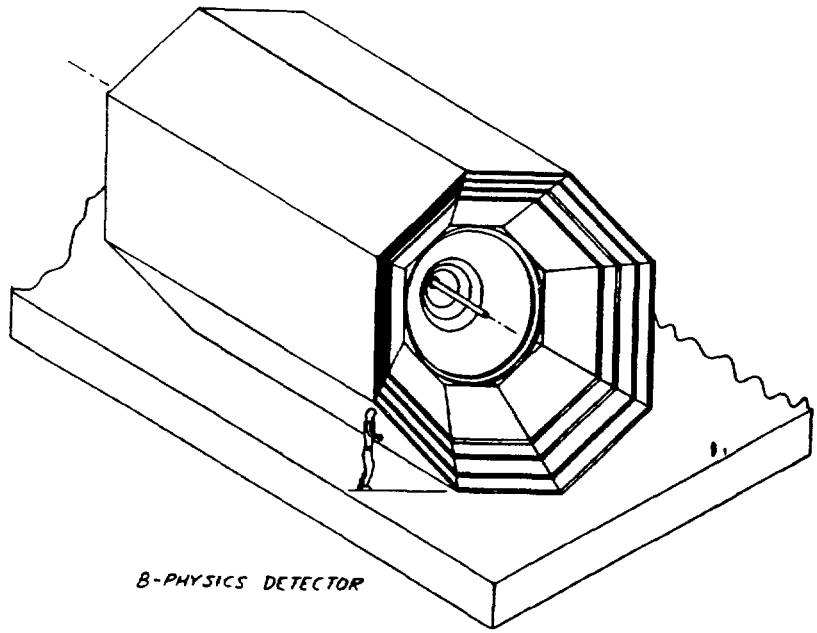

Figure 7: Isometric representation of a B Physics detector

by a path length cut as evidenced by the experience of E-691 at Fermilab. Silicon drift technology is the preferred choice for the vertex detector because of the extra pattern recognition strength of a pixel device over that of projected strips. This detector, developed by E. Gatti and P. Rehak [33], can locate the charged particle trajectory to a 10×10 μ pixel by using drift time information and determining the centroid of the electron cloud. A system of 3 double planes of high resistivity, 280μ thick, silicon positioned at radii $1cm$ $2cm$ and $3cm$ is used. The geometry is that of a polygon that approximates a cylinder. In total, there are 480 $2 \times 2cm^2$ detectors, leading to about 10^5 channels. The drift time is roughly $1\mu sec$ over $2cm$. Recent progress has been made in integrating an amplifier onto high resistivity silicon allowing the next step of placing the amplifier on the same wafer as the detector to take place. This is expected to give an input capacitance of $60fF$ and a noise of about 100 electrons [34]. The detector has been shown to work in principle but now R & D is needed for a system test, including readout, that integrates everything together and demonstrates that the temperature can be held sufficiently stable and that power dissipation from a readout system is low enough for a collider detector.

• Magnet

The solenoid magnetic field will be chosen to achieve the needed mass resolution. The mass resolution needed for separating out B_d and B_s and rejecting combinatoric background is about 25 Mev/c. Gas tracking is needed to minimize the contribution of multiple scattering to the mass resolution. A further challenge is the need for good Z resolution for mass reconstruction and pattern recognition.

• Electromagnetic Calorimeter

The primary function of the Electromagnetic Calorimeter (EC) is electron identification. Because the electrons in the momentum range of interest are relatively soft fairly good momentum resolution can be expected by measuring the electron track and thus good energy resolution is not a primary consideration for the calorimeter, the emphasis must be on shower development and shower localization.

There is lot of activity going on in Electromagnetic and Hadron calorimetry. One of the most promising approaches is the "Spaghetti calorimeter" under construction at CERN by Wigmans and collaborators. It uses scintillating fibers as the sensitive medium and lead as the absorber. The new understanding of the hadron showers and Monte Carlo simulations show that this configuration should achieve full compensation for hadron showers. For EC we have little interest in the compensation mechanism. However, we can use the new technology to produce an EC with the needed electron identification.

The location of EC within the magnetic field makes the use of light for shower detection rather unpractical. A simpler approach may be to use ionization for keeping the lead absorber and stainless steel tubes of the spaghetti calorimeter design and replacing the fiber scintillators with pressurized gas and wires. The pressure should be high enough and the diameter small enough to eliminate δ rays problems. The gas gain can be low enough to avoid any potential problems with the detector aging. The read-out could be essentially projective with small angle stereo in at least 3 projections. Due to the relatively good position resolution of the read-out geometry and the modest density of electromagnetic showers we can get away with projections.

The read-out can be divided in two parts along the beam direction at the symmetry plane of the detector to have the maximum tube length below 2 m. In the radial direction (direction of the shower development) 3 groups (each with 3 stereo directions) would allow use of the longitudinal shower development for identifying electromagnetic showers. The finest division read-out will be at the second group located at the shower maximum. Assuming 2 cm read-out width at this second group (σ = .6 cm) and 4cm width in the remaining 2 groups the number of read-out channels is about 9000. This number could be increased if more detail studies show that a finer division is needed.

• RICH

The ring imaging Cherenkov counters are designed to identify kaons, pions and protons from 1 GeV/c to above 10 GeV/c. The present approach is to use two counters . For the low momenta we use a liquid radiator with proximity focussing ; the preliminary design gives π/K separation up to $\sim$ 5 GeV/c and e/π separation up to $\sim$ 1.5 GeV/c. As a first pass we have chosen a gas radiator, at atmospheric pressure, for higher momenta; this will give π/k separation from $\sim$ 3 GeV/c to well above 10GeV/c, overlapping the range of separation of the liquid counter. This counter will give e/π separation from $\leq$ 1 GeV/c, limited by particle trajectories in the magnetic field, to $\sim$ 10 GeV/c.

A first estimate of the overall length of the counters is 20 cm for the low momentum counter, determined by the free space following the radiator required by proximity focussing, and 50 cm for the higher momentum, determined by the length of radiator required for adequate photoelectron statistics. One should note that if one is prepared to use a high pressure counter the gas counter can be shortened, leading to a more compact detector. Given the difficulties encountered with radiation effects in TMAE we expect to use TEA in the photon detectors. We note that recent measurements on TEA show that, if one is limited by optical dispersion, the two absorbers give comparable performance.

• Muon Detector

Muon identification is achieved by requiring penetration of an amount of iron consistent with the particle's energy. The iron will also serve as a flux return for the solenoidal magnet. The first active element of the muon system is shielded by a one meter thick iron sleeve. Each detector layer consists of two planes of drift tubes orientated at 6 degrees stereo angle. The maximum drift distance will be 5mm. so there will be no overlap with the next beam crossing 100 $nsec$. later. However, the wires could be ganged together to give a spatial resolution consistent with multiple scattering in order to reduce the number of electronics channels. Muons with momentum greater than about 1.4 GeV/c will penetrate one meter of iron. Thus muons with transverse momentum greater than 1.4 GeV/c will penetrate to the first layer. This is followed by three iron sleeves each 33 cm thick interleaved with detector elements. The energy of muons with transverse momentum between 1.4 GeV/c and 2.7 GeV/c will be estimated from range to about 7% $\times$ σ. Range straggling contributes about 6%. Thus the energy will be measured to about 10%. Muons with transverse momentum above 2.7 GeV/c will penetrate through the entire muon identifier.

Hadrons can simulate the muon signal either through decay or punchthrough. About

$2\% \times 1.4$ GeV/P_t of charged pions and $9\% \times 1.4$ GeV/P_t of charged kaons will decay to a muon in the 1.5 m of transverse distance before the electromagnetic calorimeter. The pion/kaon ratio in this pt range is about four to one. The muon momentum varies from $0.57 \times p$ to the full momentum for π decay, and $0.05 \times p$ to the full momentum for K decay. Sometimes the kink in the track can be observed. UA1 rejects 10% of pion decays and 30% of kaon decays by observation of the kink [35]. However, this detector uses high pressure straw chambers with better spatial resolution. When the kink is not detected, the momentum will be mismeasured. It is expected that with the requirement that the energy from range be consistent with momentum, a hadron rejection of better than 100 to 1 can be achieved for $P_t > 1.4$ GeV/c, however more detailed simulation is necessary.

The background from punchthrough is smaller than that due to decays. The probability of a 20 GeV/c hadron punching through two meters of iron is only 0.6% [36]. A negligable number of muons from B decay have transverse momentum this large. The punchthrough background is much less if the particle stops in the iron and the range is required to be consistent with the momentum.

• Trigger

The trigger for the purposes of the workshop was limited to discussing the stiff track trigger and a secondary vertex trigger. The quality of this trigger will determine the physics available to the experiment. Isajet studies indicate that the stiff track trigger will efficiently reject minimum bias events. Shown for $B\bar{B}$ events in fig. 8 is the plot of the number of events per second versus track P_t with the curves indicating the number of events with ≥ 2, ≥ 3, ≥ 4 or more tracks per event above that P_t . A cut requiring the K and π from the B tracks with projected impact parameters of at least 50μ has been applied. Shown in fig. 9 is the same plot for background events, both assuming a luminoisty of $2 \times 10^{32} cm^{-2} sec^{-1}$. Work on the vertex trigger is about to commence.

The lepton trigger presents a major challenge because the leptons are extremely soft in P_t. Shown in fig. 10 is the P_t and p spectrum of e from semi-leptonic B decays. Already it can be seen the electron trigger will require pulse height information from the silicon near the beam pipe, tracking TRD's, online charged track momentum analysis, longitudinal shower information after a couple of radiation lengths from the calorimeter, small tower sizes, and summed energy in the event. Maintaining a high electron efficiency while keeping the rejection high is the major challenge here. The prompt electron rate from all sources is a couple of kilohertz at a luminosity of $10^{32} cm^{-2} sec^{-1}$. The trigger should reduce the electron misidentification background to about this level, about a kilohertz. This emphasizes the need for a high rate data acqusition system and considerable online software event analysis as a further stage in the trigger.

It is this tracking and vertexing trigger requirement that makes a processor based trigger attractive if it can be fast enough. The learning curve for tracking is known to be long and arduous and the system with the greatest flexibility will eventually make the least number of errors.

6. Conclusions

The bottom physics that can be studied at RHIC is broad in scope and potentially very

Fig. 8

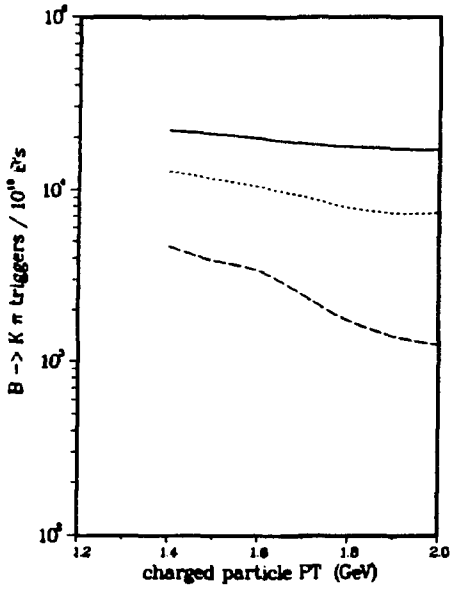

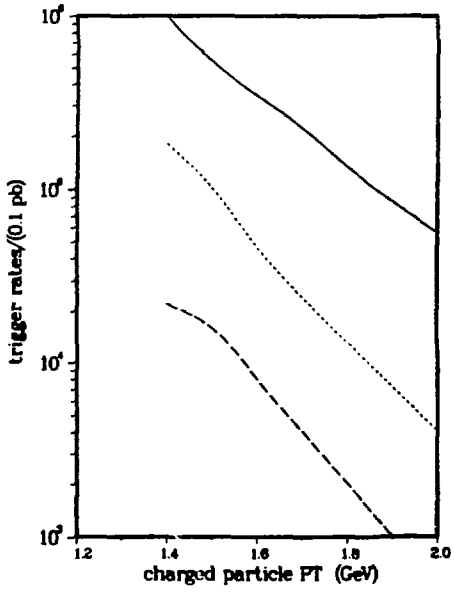

Fig. 9

Figure 8: (number of B's $\rightarrow K\pi$)/($10^{10}B$'s) vs. minimum P_t for each of: 2 charged tracks (solid line), 3 charged tracks (dotted line), 4 charged tracks (dashed line). The K and π from the B have an impact parameter cut of 50 microns

Figure 9: (number of events)/(0.1 pb) vs. minimum P_t for each of: 2 charged tracks (solid line), 3 charged tracks (dotted line), 4 charged tracks (dashed line)

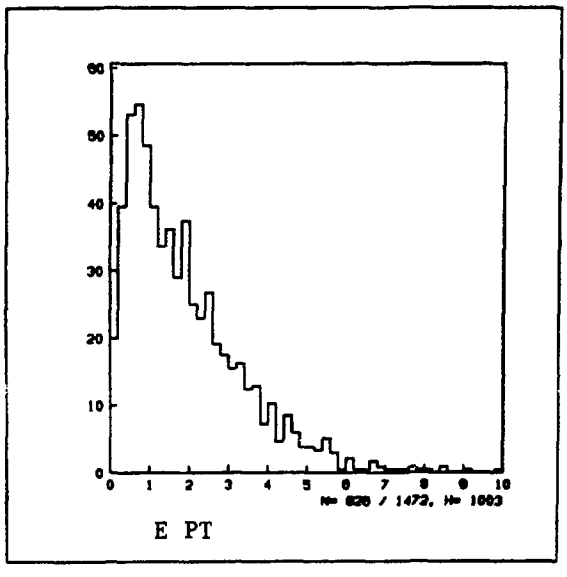

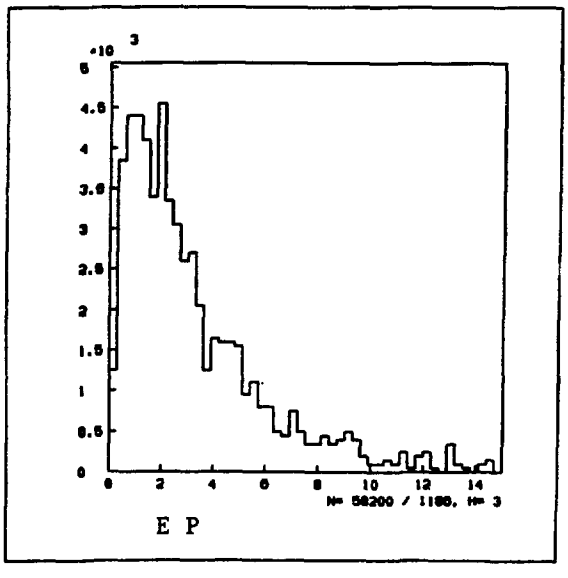

Figure 10: a) P_t , b) P of e from semi-leptonic B decays

exciting. People have begun to study the design issues of a bottom collider detector. It is a lot of work to demonstrate that one can effectively use a sample of 10^9–10^{10} produced bottom events. Though challenging, the group feels strongly the technical goals can be met and the experiment successfully built and operated in the high rate collider environment. The most ambitious physics goal of this experiment would be to make the first observation of CP nonconservation in the bottom system. Studying CP aymmetries at the 10%–20% level in several modes appears attainable for a new experiment designed explicitly for studying the B system. Once observed, it is of great interest to study CP nonconservation in the neutral and charged bottom system in detail. This may require moving to the SSC and taking advantage of the large increase in the $B\bar{B}$ cross section.

Acknowledgements

We thank the organizers, especially T. Ludlam for a pleasant working environment and interesting workshop. N. S. Lockyer also wishes to acknowledge the generous support of the University of Pennsylvania Research Foundation.

References

[1] G. Benenson et al., *Detecting Heavy Quark Jets* Proceedings of the 1983 DPF Workshop on Collider Detectors, Berkeley, Ca. Feb 28 (1983) pages 143-156.

[2] E. Berger, *Benchmark Cross Sections for Bottom Quark Production* Proceedings of the High Sensitivity Beauty Physics Workshop held at Fermilab Nov. (1987); also P. Nason, S. Dawson and K. Ellis, *The total cross-section for the production of heavy quarks in hadronic collisions*Fermilab Preprint PUB-87/222-T.

[3] P. Karchin, N. S. Lockyer et al., *Proposal for a Bottom Collider Detector* **BCD**. March 1987.

[4] N. Reay et al. *Letter of Intent for a Tevatron Beauty Factory* March 1987.

[5] N. S. Lockyer *Issues for a Bottom Collider Detector at Fermilab* Proceedings of the High Sensitivity Beauty Physics Workshop held at Fermilab Nov. (1987) Editors. J. Slaughter, N. S. Lockyer, M. Schmidt.

[6] Neville W. Reay et al. *Summary of the Collider Architecture Working Group* Proceedings of the High Sensitivity Beauty Physics Workshop held at Fermilab Nov. (1987)

[7] A. J. Lankford and M. Johnson et al., *Summary of the Trigger and Data Acquisition Group* Proceedings of the High Sensitivity Beauty Physics Workshop held at Fermilab Nov. (1987)

[8] T. Ludlam *Summary of the Particle Identification Group* Proceedings of the High Sensitivity Beauty Physics Workshop held at Fermilab Nov. (1987)

[9] K. Foley et al., *A Beauty Spectrometer for the SSC* Proceedings of the Workshop on Experiments, Detectors and Experimental Areas for the Supercollider. Berkeley (1987) R. Donaldson and G. Gilchriese editors.

[10] A. Sanda *CP Revisited at BNL* To appear in these proceedings.

[11] F. Gilman *B Physics* To appear in the proceedings of Les Rencontres de Physique de la Vallee d'Aoste, La Thuile, Italy Feb. (1988)

[12] H. Harari *B Physics* To appear in the Proceedings of Les Rencontres de Physique de la Vallee d'Aoste, La Thuile, Italy Feb. (1988) Session.

[13] C. Hamzaoui, J. L. Rosner, A. I. Sanda *B Meson Decay Asymmetry and $B\bar{B}$ Mixing* Proceedings of the High Sensitivity Beauty Physics Workshop held at Fermilab Nov. (1987)

[14] H. Albrecht et al., (Argus Collaboration) Phys. Lett. B. 192, 245 (1987)

[15] A. Ali. *$B\bar{B}$ Mixing - A Reappraisal* Proceedings of the U.C.L.A. Workshop, Linear Collider $B\bar{B}$ Factory Conceptual Design, Editor Donald Stork (Jan. 1987)

[16] A. Soni. and G. Hou *Loop Induced Rare B Decays.* Proceedings of the U.C.L.A. Workshop, Linear Collider $B\bar{B}$ Factory Conceptual Design, Editor Donald Stork (Jan. 1987)

[17] I. Dunietz ,contributed to this workshop *Measurement of the Mass and Lifetime Differences between the Heavy and Light B_s eigenstates.* Proceedings of the High Sensitivity Beauty Physics Workshop held at Fermilab Nov. (1987)

[18] Ling-Lie Chau and Hai-Yang Cheng *In Search of V_{ub} in Nonleptonic Decays from the Quark Diagram Scheme* Physics Letters B, Vol 197, Number 1,2 Oct (1987).

[19] I. I. Bigi and B. Stech *Future Lessons from Two-Prong Two Body decays of Beauty* Proceedings of the High Sensitivity Beauty Physics Workshop held at Fermilab Nov. (1987)

[20] M. Schmidt, J. L. Rosner, A. I. Sanda *Physics Group Summary* Proceedings of the High Sensitivity Beauty Physics Workshop held at Fermilab Nov. (1987)

[21] I. I. Bigi and A. I. Sanda. *CP Violation in Heavy Flavor Decays* Nucl. Phys. B281 (1987) 41-71

[22] U. Amaldi and G. Coignet *Conceptual Design of A Multipurpose Beauty Factory Based on Superconducting Cavities* CERN-EP/86-211 Dec. 16,1986

[23] D. B. Cline *A Conceptual Design for a High Luminosity Linear Collider $B\bar{B}$ Factory.* Proceedings of the U.C.L.A. Workshop, Linear Collider $B\bar{B}$ Factory Conceptual Design, Editor Donald Stork (Jan. 1987)

[24] R. Eichler, T. Nakada, K. R. Schubert, S. Weseler, and K. Wille, *Proposal for a Double Storage Ring* SIN Report PR-86-13 (Nov. 1986)

[25] H. Aihara *B Factory at KEK* Proceedings of the U.C.L.A. Workshop, Linear Collider $B\bar{B}$ Factory Conceptual Design, Editor Donald Stork (Jan. 1987)

[26] E. Bloom *N-PEP $B\bar{B}$ Factory* Proceedings of the U.C.L.A. Workshop, Linear Collider $B\bar{B}$ Factory Conceptual Design, Editor Donald Stork (Jan. 1987)

[27] B. Cox and D. Wagoner, *Physics of the SSC* R. Donaldson and J. Marx editors.

[28] D. M. Kaplan et al., *A Proposal to Measure The Production and Decay into Two-Body Modes of B-Quark Mesons and Baryons*

[29] J. Bjorken *Prospects for Future Fixed-Target B Physics at Fermilab* Proceedings of the High Sensitivity Beauty Physics Workshop held at Fermilab Nov. (1987)

[30] P. Garbincius *Review of Fixed-Target B Physics at Fermilab* Proceedings of the High Sensitivity

[31] *Conceptual Design of the Relativistic Heavy Ion Collider* Brookhaven National Laboratory- 51932, May (1986) Beauty Physics Workshop held at Fermilab Nov. (1987)

[32] F. Paige and S. Protopopescu *Isajet Monte Carlo*

[33] P. Rehak, et al. *Progress in Semiconductor Drift Detectors* Nuclear Instruments and Methods in Physics Research A248, 367 (1986)

[34] V. Radeka et at., *Design of a Charge Sensitive Preamplifier on High Resistivity Silicon* IEEE Transactions on Nuclear Science Vol. 35, No. 1, (1988)

[35] H. Moser PITHA 87-22, Phys. Inst., Aachen, Fr Germany

[36] A. Bodek UR911, Dept. of Physics, Univ. of Rochester

List of Figures

Report Number DOE/ER/40325-47-TASKB

CP VIOLATION REVISITED AT BNL[+]

B Physics at Relativistic Heavy Ion Collider (RHIC)

A.I. Sanda

Physics Dept. Rockefeller University, New York, N.Y. 10021

[+]Invited talk presented at the Workshop on Heavy Ion Colliders held at Brookhaven National Laboratory.

[*]Work supported in part by the U.S. Department of Energy under Contract Grant Number DE-AC02-87ER40325B.000

Just this past May, during the celebration of Bram Pais' 70th birthday held at Rockefeller, I heard about the air of great excitement at Brookhaven surrounding the discovery of CP violation some 25 years ago. Continuing this distinguished tradition, it is quite appropriate for Brookhaven National Laboratory to push forth a program which will result in another major step toward our understanding of CP violation.

Results of all experiments, so far, seem to agree with the prediction of the standard model.[1] This model, however, must be incomplete since it leaves too many questions unanswered - just in the quark and lepton mass matrix, there are 13 parameters. In the standard model, CP violation is parameterized in terms of a phase in the mass matrix. The key to go beyond the standard model must be an understanding of CP violation. With such an understanding, the CP violating parameters in the model can eventually be related to those which cause baryon asymmetry of the universe - a concept which is likely to involve physics beyond the standard model.

With this philosophy in mind, I shall review the recent results in B-$\bar{B}$ mixing, predicted CP asymmetries in B decays and finally discuss the prospects for measuring them.

Mixing

Since b quark decays leptonically in to

$$b \to c e^- \bar{\nu}_e \quad \text{or} \quad c \mu^- \bar{\nu}_\mu ,$$

The $\bar{B}$ meson which is a bound state of $(b\bar{d})$ will leptonic decay with e^- or μ^- in the final state. Then in the absence of B-$\bar{B}$ mixing, we have

$$e^+e^- \rightarrow T(4S) \rightarrow B\bar{B} \rightarrow \ell^+\ell^- + \ldots \qquad (1)$$

where

$$\ell = e \text{ or } \mu.$$

The presence of same sign ee, $\mu\mu$ or μe pair from direct decays of $B\bar{B}$ pair is a signal for B-$\bar{B}$ mixing.

In describing particle-antiparticle mixing, the crucial parameter is

$$x = \frac{\Delta m}{\Gamma}, \qquad (2)$$

the ratio of average life time/mixing time. If the particles were to decay before they had chance to mix, they could not reveal the effects of mixing. Thus for observable mixing,

$$x = 0(1) \qquad (3)$$

must be satisfied.

Indeed, for the K meson system

$$x = \frac{\Delta m}{\frac{1}{2}(\Gamma_L + \Gamma_S)} = .6. \qquad (4)$$

It is well known[2] that the major contribution to the short distance part of M_{12} for the K meson system is given by the box diagram shown in Fig. 1a.

It is quite easy to extend the discussion of particle-antiparticle mixing to other heavy meson mixings: $D\text{-}\bar{D}$, $B_d\text{-}\bar{B}_d$, $B_s\text{-}\bar{B}_s$ and $T_q\text{-}\bar{T}_q$. The diagrams which contribute to mixing of these heavy mesons are shown in Figs. 1b ~ 1d. In describing the contributions from these box diagrams, let us write

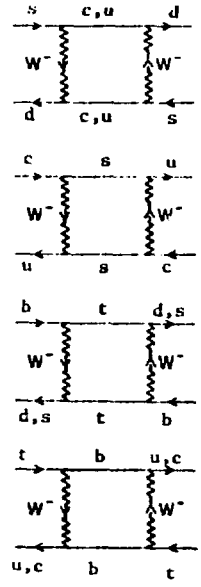

Fig. 1. Box diagrams contributing to K,D,B, T mixing effects, respectively.

$$L=i\frac{g}{\sqrt{2}}\bar{u}_i U_{ij}\gamma_\mu\left(\frac{1-\gamma_5}{2}\right)d_j W^\mu \quad (5)$$

where the KM matrix given in the Wolfenstein representation is

$$U\approx\begin{bmatrix} 1-\lambda^2/2 & \lambda & \lambda^3 A(\rho-i\eta) \\ -\lambda & 1-\lambda^2/2 & \lambda^2 A \\ \lambda^3 A(1-\rho-i\eta) & -\lambda^2 A & 1 \end{bmatrix} \quad (6)$$

Note that the unitarity of the KM matrix

$$\sum_j U_{ij}U_{jk}^*=0 \qquad \text{if} \quad i\neq k \quad (7)$$

leads to a GIM cancellation which implies vanishing contribution of the box diagram if all intermediate quarks were degenerate in mass. A detailed analysis[3] yields expected results shown in Table I.

	M_{12}	Γ	x
K	$G_F^2 M_K (\lambda^2 m_c^2)^2$	$G_F^2 m_s^5 \lambda^2$	$\frac{m_c^4}{m_K^4}\lambda^2$
D	$G_F^2 M_D (\lambda m_s^2 + \lambda^5 m_b^2)^2$	$G_F^2 m_c^5$	$(\lambda m_s^2 + \lambda^5 m_b^2)^2 / m_c^4$
B_d	$G_F^2 M_{B_d} (m_t^2 \lambda^3 ((\rho-1C^2+\eta^2)^2)^2$	$G_F^2 m_b^5 \lambda^4$	$\frac{m_t^4}{m_b^4}\lambda^2((1-\rho)^2+\eta^2)^4$
B_s	$G_F^2 M_{B_S} (m_t^2 \lambda^2)^2$	$G_F^2 m_b^5 \lambda^4$	$\frac{m_t^4}{m_b^4}$
T	$G_F^2 M_T (m_b^2 \lambda^2)^2$	$G_F^2 m_t^5$	$\frac{m_b^4}{m_t^4}\lambda^4$

(8)

Table I. Rough estimates of M_{12}, Γ, and x for K-$\bar{K}$, D-$\bar{D}$, B_d-$\bar{B}_d$, B_s-$\bar{B}_s$, and T-T mixing.

From this rough argument, we conclude that x_D, $x_T \ll x_K$ - we do not expect any mixing effect to be observed in the D or T meson systems. We note that there is a good chance that the B_s system will exhibit large mixing. This

argument does not automatically imply observable B_d-$\bar{B}_d$ mixing - it depends on the size of m_t and U_{td}.

Recent ARGUS observation of mixing[4]

$$\frac{N^{++}+N^{--}}{N^{+-}} = .234\pm.067\pm.031$$

$$= \frac{x^2}{2+x^2} \tag{9}$$

yields

$$x_{B_d} = \frac{\Delta m}{\Gamma} = .78\pm.16. \tag{10}$$

While the uncertainty in evaluating the matrix element of the quark operator between $<B^o|$ and $|\bar{B}^o>$ forbids us to make a definite statement about m_t and U_{td}, large X_{B_d} given in Eq. 10 tends to require[5] large m_t:

$$m_t \gtrsim 50\text{GeV}.$$

From Table I, it can be seen that

$$\frac{x_{B_s}}{x_{B_d}} \sim \frac{1}{\lambda^2((1-\rho)^2+\eta^2)^2} \tag{11}$$

From a phenomenological analysis of the KM matrix, we note that the ratio is larger than 5; the standard model predicts a large mixing effect in the B_s system.

CP Violation

In order to go through a simple argument which brings out the essential physics, let us for a moment use the original representation of the KM matrix

$$U = \begin{bmatrix} c_1 & -s_1c_3 & -s_1s_3 \\ s_1c_2 & c_1c_2c_3-s_2s_3e^{-i\delta} & c_1c_2s_3+s_2c_3e^{i\delta} \\ s_1s_2 & c_1s_2c_3+c_2s_3e^{i\delta} & c_1s_2s_3-c_2c_3e^{i\delta} \end{bmatrix} \tag{12}$$

It can be shown that all CP violating observables are proportional to [6]

$$J \sim s_1^2 s_2 s_3 \sin\delta . \tag{13}$$

Indeed it is quite easy to show that CP violating effects vanish if anyone of s_1, s_2, s_3 or $\sin\delta$ vanishes. To see this consider Fig. 2.

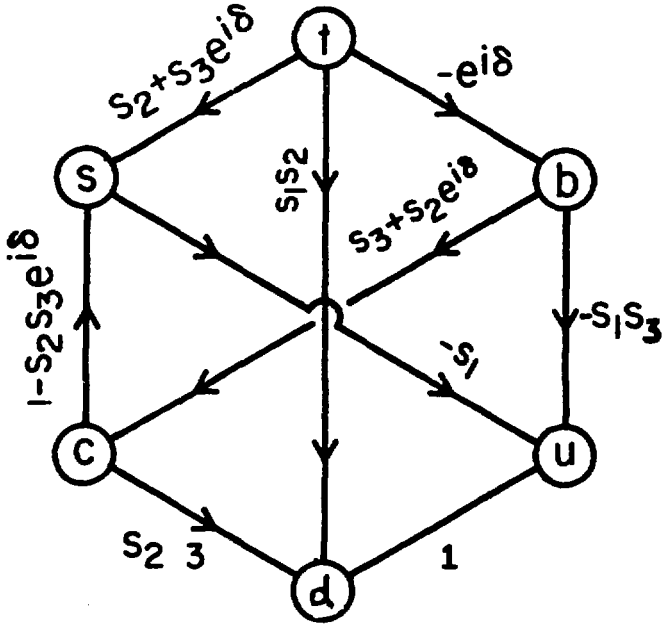

Fig. 2. Diagramatic representation of the KM matrix.

All allowed transitions are shown by lines together with the corresponding KM matrix element. Now set $s_2=0$. We have

$$U_{ts} = s_3 e^{i\delta}$$

$$U_{tb} = -c_3 e^{i\delta}$$

$$U_{td} = 0$$

(14)

and the phase of the t quark can be adjusted in such a way that the phase $e^{i\delta}$ is absorbed absorbed making the KM matrix real. Similarly, the phase of b quark can be readjusted to obtain an orthogonal KM matrix if $s_3=0$. Thus any CP asymmetry, e.g. between some cross sections, must have the numerator

$$\frac{\sigma^+ - \sigma^-}{\sigma^+ + \sigma^-} \sim \frac{s_1^2 s_2 s_3 \sin\delta}{(\qquad)} .$$

(15)

and the crucial issue is to find a process in which the denominator of the ratio is minimized. For K meson decays, the largest suppression factor one obtains is $(\sigma^+ + \sigma^-) \sim s_1^2$ and we have

$$\left(\frac{\sigma^+ - \sigma^-}{\sigma^+ + \sigma^-}\right)_K \sim s_2 s_3 \sin\delta$$

(16)

Calculation of ϵ in K meson system shows that $s_2 s_3 \sin\delta \sim \epsilon = 2\times10^{-3}$. Thus the CP violating effect in the K system is at most $0(10^{-3})$. For B decays the major modes are suppressed: $(\sigma^+ + \sigma^-)_B \sim \Gamma_B \sim |s_2 + e^{i\delta} s_3|^2$, since the b→c decay amplitude is proportional to U_{cb}, this tends to enhance the CP asymmetry for the B meson system over that for the K meson system:

$$\left(\frac{\sigma^+-\sigma^-}{\sigma^++\sigma^-}\right)_B \sim \frac{s_1^2 s_2 s_3 \sin\delta}{|s_2+e^{i\delta}s_3|^2}$$

(17)

In addition, for CP asymmetry which requires B-$\bar{B}$ mixing, we note that, since

$$x \sim 0((s_1 s_3)^2),$$

(18)

x vanishes if s_1 or s_3 vanishes. Asymmetries which involve processes with B-$\bar{B}$ mixing are proportional to x. Here x replaces some of the suppression factors and we have

$$\left(\frac{\sigma^+-\sigma^-}{\sigma^++\sigma^-}\right)_B \sim 0(x\sin\delta)$$

(19)

an expression which satisfies the condition that the numerator vanishes if any of the s_i's vanish.

Now since $x \sim .7$ and $s_2 s_3 \sin\delta = 0(10^{-3})$ implies $\sin\delta$ can be 0(1), we may expect a large asymmetry in B decays.

So far we have been waving hands showing why B meson decay asymmetries may be much larger then familiar ones in K decays. Below, we shall illustrate this effect by a specific example. Consider a final state f such that both B and $\bar{B}$ can decay to f. Then, since there is a nonvanishing B-$\bar{B}$ transition, there are two possible amplitudes:

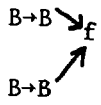

(20)

It can be shown that the interference between the two amplitudes will cause the asymmetry:[7]

$$\frac{\Gamma(B^o(t)\to f)-\Gamma(\tilde{B}^o(t)\to f^{CP})}{\Gamma(B^o(t)\to f)+\Gamma(\tilde{B}^o(t)\to f^{CP})} = \sin(\Delta m t)\,\mathrm{Im}\left(\frac{p}{q}\rho\right)$$

(21)

where

$$|B^o(t)\rangle = g_+(t)|B^o\rangle + \frac{q}{p}g_-(t)|\tilde{B}^o\rangle$$

$$|\tilde{B}^o(t)\rangle = \frac{p}{q}g_-(t)|B^o\rangle - g_+(t)|\tilde{B}^o\rangle$$

$$g_\pm(t) = \exp(-\tfrac{1}{2}\Gamma_1 t)\exp(im_1 t)\left(1\pm\exp(-\tfrac{1}{2}\Delta\Gamma t)\exp(i\Delta m t)\right)/2$$

(22)

and we have used the definitions:

$$\Delta\Gamma=\Gamma_2-\Gamma_1; \quad \Delta m=m_2-m_1;$$

Γ_i and m_i, i=1,2 are the width and mass, respectively, of the two mass eigenstates B_i.

Also,

$$p/q = \frac{1+\epsilon}{1-\epsilon} = \frac{M_{12}-i\Gamma_{12}/2}{M_{12}^*-i\Gamma_{12}^*/2}, \quad \text{and } \rho=\frac{A(B^o\to f)}{A(\tilde{B}^o\to f)}.$$

(23)

t above denotes the proper time measured in the rest frame of the B meson and f^{CP} is the CP conjugate of f. Final states we consider in this note are $f=\psi K_s$, $\pi^+\pi^-$, D^+D^-. Here the emphasis on two body decay channels has to do with the ease of identifying the genuine B decays. Also, as we shall see below, there is a definite advantage in restricting ourselves to the CP eigenstate f which is a common decay channel for B and $\bar{B}$. It should be emphasized that the restriction on f is made purely from above technical constraint. For example,

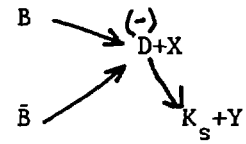

(24)

is an inclusive process for which we expect some asymmetry. Eq. 21 applies for this process also.

For majority of f's, ρ depends on hadronic dynamics and it is not possible to give a firm theoretical prediction. If f is CP eigenstates such that $A(B\to f)$ gets a major contribution from one operator, it can be shown that[7]

$$\rho = \frac{A(B\to f)}{A(\bar{B}\to f)} = e^{i\alpha} \tag{25}$$

where α depends only on the KM matrix element.

Also, for B meson system, it can be shown that[7] $|\Gamma_{12}| << |M_{12}|$ and we have

$$\frac{p}{q} = e^{i\beta}$$

where

$$\beta = \arg(M_{12}). \tag{26}$$

For example take $f=\pi^+\pi^-$. Then Fig. 3 shows that

$$\arg\left(-\frac{p}{q}\rho\right)_{\pi\pi} = \arg(U_{tb}U^*_{td}U^*_{ub}U_{ud})^2$$

and for ψK_s

$$\arg\left(\frac{p}{q}\rho\right)_{\psi K_s} = \arg(U_{tb}U^*_{td}U_{cs}U^*_{cb}U^*_{us}U_{ud})^2 \tag{27}$$

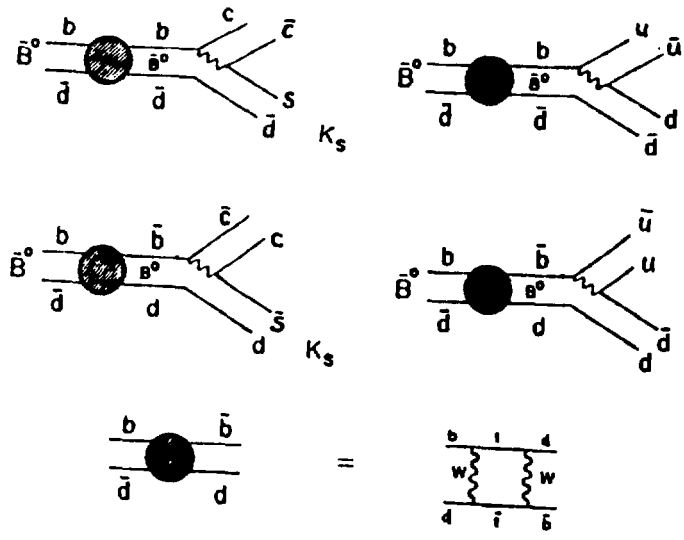

Fig.3 $\beta=\arg(U_{tb}U_{td}^*)^2$, $\alpha)_{\pi\pi}=\arg(U_{ub}^*U_{ud})^2$, $\alpha)_{\psi K_s}=\arg(U_{cb}^*U_{cs}U_{us}^*U_{ud})^2$ where $\arg(U_{us}^*U_{ud})$ is the phase associated with the definition of the K_s state.

Unitarity Triangle[8]

We shall now give a simple interpretation of the asymmetry in terms of the unitarity triangle.

In the Wolfenstein representation, it is a good approximation to set $U_{tb}=U_{ud}=1$; $U_{cs}=1$, $U_{us}^*=\lambda$, so that

$$\mathrm{Im}\left(\frac{p}{q}\rho\right)_{\pi\pi} = -\sin 2\phi_2$$

$$\mathrm{Im}\left(\frac{p}{q}\rho\right)_{\psi K_s} = -\sin 2\phi_3 \tag{28}$$

where $\phi_3=\arg(U^*_{td}U^*_{ub})$; $\phi_2=\arg(U_{td}U_{cb})$. Consider a unitarity relation

$$U_{td}U^*_{tb}+U_{cd}U^*_{cb}+U_{ud}U^*_{ub}=0 \tag{29}$$

with an approximation on the KM matrix element mentioned above and $U_{cd}=-\lambda$, we obtain[5]

$$U_{td}+U^*_{ub}= \lambda U_{cb} \tag{30}$$

which leads to a representation of the approximate unitarity relation by a triangle shown in Fig. 4.

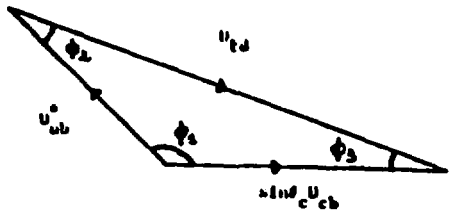

Fig. 4. Unitarity triangle representing Eq. 30.

Now if we divide the sides of the triangle by λU_{bc}, we can imbed the triangle on the ρ-η plane shown in Fig. 5. In this figure we have shown restriction on ρ and η obtained from various experimental information.[8]

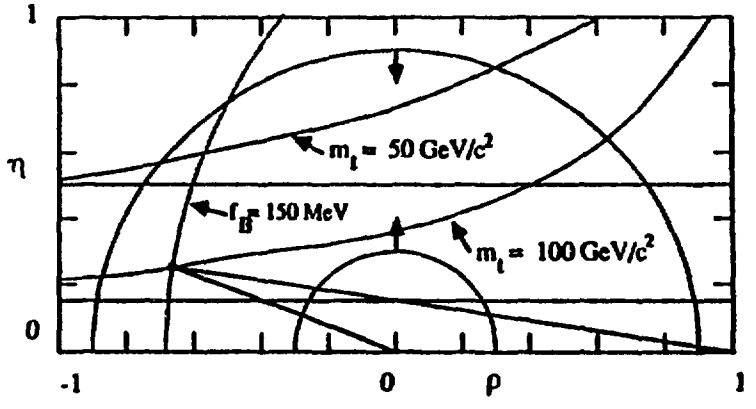

Fig. 5. Constraints on the parameters η and ρ from various observables in kaon and B systems. Solid curves labeled by m_t: ϵ(CP violating parameter in the kaon system), for B=0.7. Horizontal unshaded band: ϵ'/ϵ. Solid semicircles: upper and lower bounds on $|V_{ub}/V_{cb}|$. Light semicircle B-$\bar{B}$ mixing. Here we have taken the illustrative values U_{cd}=0.0484, f_B=150MeV, m_t=100GeV.c^2, B_B=1.

From Fig. 5, we obtain a rough estimate:

$$.1<\sin 2\phi_3$$

This implies very large CP asymmetries in B decays. If t quark is found, the knowledge of m_t will greatly constrain the triangle. Furthermore, knowledge of $|U_{cb}|$, $|U_{ub}|/U_{cb}|$ and one CP asymmetry, e.g. ϕ_3 will predict

the other CP asymmetry as well as $|U_{td}|$. Thus the experimental study of the triangle will lead to a critical test of the KM model.

Prospects

At present several groups are interested in detecting the large CP violating asymmetries in B meson decays. Efforts are directed toward e^+e^- colliders as well as pp and $\bar{p}p$ colliders. For example, table II shows the number of $B\bar{B}$ events needed at SSC in order to observe these asymmetries.

Class	Modes	Branching Ratio	Asymmetry	# $B\bar{B}$ Events Required
I. Charge Asymmetry in Same Sign Dileptons	$B_d\bar{B}_d \to \ell^\pm\ell^\pm + X$	0.01	10^{-3}	6×10^{9}
	$B_s\bar{B}_s \to \ell^\pm\ell^\pm + X$	0.02	10^{-4}	2×10^{12}
II. Mixing with Decay to a CP Eigenstate	$B \to \psi K_s$	5×10^{-4}	$0.05 - 0.3$	$(1 - 34) \times 10^{6}$
	$B \to \psi K_s X$	2×10^{-3}	$0.05 - 0.3$	$(2 - 85) \times 10^{7}$
	$B \to D\bar{D}K_s$	5×10^{-3}	$0.05 - 0.3$	$(3 - 100) \times 10^{7}$
	$B \to \pi^+\pi^-$	5×10^{-5}	$0.05 - 0.5$	$(0.3 - 32) \times 10^{9}$
	$B \to D^{+*}D^-, D^+D^-, D^*D^*$	3×10^{-3}	$0.05 - 0.3$	$(0.7 - 26) \times 10^{8}$
III. Mixing with Decay to a CP Non-Eigenstate	$B_d \to D^+\pi^-$	6×10^{-3}	0.001	3×10^{11}
	$B_d \to D^0K_s$	6×10^{-5}	0.01	7×10^{11}
	$B_s \to D_s^+K^-$	3×10^{-4}	0.5 ?	5×10^{7}
IV. Cascade Decays to the Same Final State	$B^- \to D^0K^- + X$ ↳ $K_s + Y$	10^{-5}	0.1 ?	9×10^{8}
V. Interference of Spectator and Annihilation Graphs	$B^- \to D^{0*}\bar{D}^-$	3×10^{-3}	0.01	2×10^{9}
VI. Interference of Spectator and Penguin Graphs	$B^- \to K^-\rho^0$	$\sim 10^{-5}$	·0.1	1×10^{8}
	$\bar{B}_d \to K^-\pi^+$	$\sim 10^{-5}$	0.1	1×10^{8}

***The specific channels considered here for each class of asymmetry are illustrative and not exhaustive. At this time we need to keep an open mind as to which channels will be best suited for CP violation studies. In this spirit we have included among the modes illustrating Class II asymmetries $\psi K_s X$ and $D\bar{D}K_s$, which are not necessarily CP eigenstates. There is some danger of a cancellation between the asymmetries produced by sub-channels with opposite CP quantum numbers, but a total cancellation is unlikely.**

Table II. Estimation of the number of $B\bar{B}$ events required for CP violation studies at the SSC.

Due to the complicated final state of B meson decays, experimental detection of these asymmetries is not easy.

Since the unitarity triangle gives relations between various observables, it offers an opportunity to test the standard model unambiguously.

Possibility of detecting effects beyond the three generation through violation of these relationships makes the challenge worth while.

It is my belief that further advances in track reconstruction techniques are necessary in order to detect the asymmetries discussed here. For example, if reconstruction efficiency for the D meson is increased, we may not restrict ourselves to specific two body final state such as ψK_s and $\pi^+\pi^-$. This will greatly reduce the number of B mesons necessary to observe the CP violating effects.

Above is the physics and the competition. The remaining task is to show that RHIC can compete with other efforts towards the same goal, and win.

References

1. See for example P. Langacker's review talk on the status of electroweak interaction, given at XXIV Int. Conf. on High Energy Physics, Munich, Germany, 1988.
2. M.K. Gaillard and B.W. Lee, Phys. Rev. D10, 897 (1976).
3. J. Ellis, J.S. Hagelin and S. Rudaz, Phys. Lett. B192, 201 (1987); I.I. Bigi and A.I. Sanda, Phys. Lett. B194, 307 (1987); F.J. Gilman invited talk at the International Symposium on the Fourth Family

of Quarks and Leptons, Santa Monica, February 26-28, 1987 and SLAC-PUB-4315, 1987 (unpublished); G. Altarelli and P.J. Franzini, Z. Phys. C37, 271 (1988); V.A. Khoze and N.G. Uraltsev, Leningrad preprint, 1987 (unpublished); L.L. Chau and W.Y. Keung, Phys. Rev. Ltt. 59, 958 (1987); J.F. Donoghue et al., B195, 285 (1987); A. Ali, DESY preprint DESY-87/083, 1987 (unpublished); J.R. Cudell et al., Phys. Lett. B196, 227 (1987); A. Datta et al., Phys. Lett. B196, 376 (1987); D. Du and Z. Zhao, Phys. Rev. Lett. 59, 1072 (1987); H. Harari and Y. Nir, Phys. Lett. B195, 586 (1987); J. Maalampi and M. Roos, Phys. Lett. B195, 489 (1987); V. Barger et al., Phys. Lett. B194, 312 (1987); L. Angellini et al., Phys. Lett. Phys. Lett. B195, 469 (1987).

4. H. Albrecht et al. Phys. Lett. 192B, 245 (1987).

5. See the first two references in Ref. 3.

6. C. Jarlskog, Phys. Rev. Lett. 55, 1839 (1985); O.W. Greenberg, Phys. Phys. Rev. D32, 1841 (1985); D.-d. Wu, Phys. Rev. D 33, 860 (1986); I. Dunietz, O.W. Greenberg and D.-d. Wu, Phys. Rev. Lett. 55, 2935 1985; C. Hamzaoui and A. Barroso, Phys. Lett. 154B, 202 (1985); C. Hamzaoui, Ph.D. thesis, University of Sussex, 1987 (unpublished).

7. For the most recent review see I.I. Bigi, V.A. Khoze, N.G. Uraltsev and A.I. Sanda, SLAC-PUB-4476. To appear in Review of CP Violation editor C. Jarlskog (1987). This article gives references to original articles.

8. C. Hamzaoui, J.L. Rosner, and A.I. Sanda, Proceeding of Fermilab Workshop on High Sensitivity Physics, Fermilab, Batavia, IL. Nov. 11-14 (1987) and references therein.